

Vulnérabilité des milieux urbanisés face aux impacts physiques des écoulements volcaniques, des lahars et des crues associées : le cas de la ville d'Arequipa (sud du Pérou)

Rapport final – octobre 2011



Le volcan Misti et la ville d'Arequipa, Pérou – Septembre 2008

Mlle **Kim M. MARTELLI**

Encadrant : Professeur Jean-Claude THOURET

Fondation MAIF
Agence Nationale de la Recherche ANR RiskNat, Projet « Laharisk »
Centre National de la Recherche Scientifique
PRES Clermont, Université Blaise Pascal
Laboratoire Magmas et Volcans UMR 6524 CNRS et IRD, OPGC



Résumé

Les écoulements volcaniques (lahars, écoulements hyperconcentrés) et les crues soudaines représentent des phénomènes destructeurs et dangereux. Malgré leur pouvoir destructeur (cf. Armero, Colombie, 1985), les effets des lahars en zone urbaine sont peu étudiés, alors qu'ils représentent une menace réelle pour de nombreuses villes, comme Arequipa au Pérou. Cette ville rassemble presque 1 million d'habitants à 17 km au sud-est du volcan El Misti. La dernière éruption majeure du Misti remonte à 550 ans (1440-1460 après J.C.) et de plus petites éruptions sont survenues au 18 et 19^e siècle. Des lahars dont les volumes sont compris entre $0,01 \times 10^6$ et 11×10^6 m³ se sont déclenchés et des inondations empruntent les vallées vers la ville tous les 5 à 10 ans en moyenne. Suite à l'augmentation de la population d'Arequipa, la zone urbanisée s'étend maintenant à seulement 9 km du sommet sur les flancs du volcan. En réponse à cette croissance rapide et apparemment incontrôlée, il était essentiel d'évaluer la vulnérabilité des modes d'utilisation des sols, du bâti et des infrastructures face aux impacts des lahars et des crues éclair.

Des scénarios d'aléas ont été développés à partir d'études géologiques réactualisées, de cartes géomorphologiques des dépôts volcaniques et torrentiels, des modèles de simulation numérique (tels que Titan2D), d'analyses statistiques du mode d'utilisation des sols, des types de bâtiments et d'infrastructures, et enfin des caractéristiques géotechniques des matériaux de construction. Trois scénarios de référence ont été utilisés, depuis celui d'une crue quinquennale à décennale jusqu'à celui d'une éruption Plinienne (VEI >3, récurrence de 10 000 à 20 000 ans). Les zones inondables ont été délimitées à partir des résultats des simulations issues du code numérique Titan2D couplées au zonage des aléas et à l'analyse du couple magnitude et fréquence des écoulements. Un MNT plus précis (10 m de résolution) calculé sur la base de données GPS différentiel et ASTER, a permis de modéliser les écoulements de lahar avec Titan2D. Les résultats montrent que les écoulements atteindraient des distances plus longues que celles proposées dans les études précédentes (par ex. Vargas *et al.*, 2010)

L'étude de terrain a permis de classer le mode d'utilisation des sols selon 19 catégories et le bâti et les infrastructures selon 10 catégories. Par exemple, les bâtiments ont été classés et ordonnés selon la nature du matériau principal, l'âge, le nombre d'étages et d'ouvertures, etc. De la même manière, la classification de l'utilisation des sols et des types d'infrastructures a été opérée selon différents critères comme le taux d'occupation, l'importance des évacuations d'urgence etc. Les effets mécaniques des écoulements sur les immeubles et les infrastructures ont été inventoriés dans le but d'évaluer leur fragilité. Cette étude a révélé que les bâtiments et certains types d'utilisation des sols sur le cône alluvial de la Quebrada Huarangal sont particulièrement vulnérables et exposés au risque, même lors d'un écoulement de faible magnitude. Ceci est essentiellement dû à la très faible qualité des constructions. Au contraire, le risque est relativement plus faible dans la vallée du Rio Chili, sauf dans le canyon à 8 km à l'amont de la ville, qui compte déjà cinq usines hydro-électriques et un lac de barrage. Le niveau de risque inhérent au système d'alimentation électrique et aux réserves d'eau potable s'avère très préoccupant pour la ville, notamment durant une crise volcanique, une inondation décennale et à la suite d'un séisme.

Cette étude a mis en évidence les capacités d'intégration des données grâce à un SIG, qui aide à produire de nouvelles informations via la combinaison de scénarios d'aléas et d'éléments de vulnérabilité. Cette méthode semble être prometteuse car une mise à jour constante de la base de données pourrait aider à gérer de manière efficace une possible crise volcanique ou hydrologique en assistant en temps réel les opérations de réduction des risques.

Mots-clés : El Misti, volcan, aléa, risque, vulnérabilité, lahar, crue éclair, système d'information géographique, Titan2D, environnement urbain, Arequipa, Pérou.

Remerciements

Je remercie la Fondation MAIF pour le soutien qu'elle m'a prodigué durant près de 3 ans à Clermont. Nos remerciements vont également au Laboratoire LMV, au Projet « Laharisk » de l'ANR RiskNat qui m'a soutenue en 2010, à l'Ambassade de France en Nouvelle-Zélande, et au réseau franco-péruvien R. Porrás Barrenechea qui m'a aidée durant deux séjours au Pérou en 2007 et 2008. Je n'oublie pas mes camarades doctorants et mon encadrant pour leur soutien. Je suis reconnaissante envers les membres du jury de thèse et notamment les deux rapporteurs, M. Michael F. Sheridan (University at Buffalo, NY) et M. Cees Van Westen (ITC, University of Twente, Pays-Bas). Je remercie enfin ma famille qui, malgré la distance, a su préserver ma motivation durant mon long séjour en France.

Abstract

Volcanic mass flows (lahars, hyperconcentrated flows) and flash floods represent destructive and dangerous phenomena. Given evidence concerning the destructive nature of lahars (e.g. Armero, Colombia, 1985) there appears to be a lack of studies into the effect of lahars in dense urban environments; a very real threat for many cities worldwide including the Arequipa, Peru. Arequipa, with nearly one million inhabitants, is located 17 km SW of El Misti Volcano. El Misti's last major eruption occurred 550 years ago (1460AD), with smaller eruptions occurring in the 18 and 19th Centuries. Lahars with volumes ranging from $0.01 \times 10^6 \text{ m}^3$ to $11 \times 10^6 \text{ m}^3$ have occurred, and flash floods have swept down valleys every 5 to 10 years. Population growth has resulted in urban sprawl to within 9 km of El Misti's summit. It is this rapid and seemingly uncontrolled expansion which warrants the assessment of building, land use and infrastructure within a vulnerability framework.

Hazard scenarios were developed from former and current geological studies; conventional and computer-aided (e.g. Titan2D numerical modelling) mapping of volcanoclastic and fluvial deposits; field surveys of land use, buildings and infrastructure; statistical analysis (including multivariate analysis); and geotechnical characteristics of building materials. Three reference scenarios were used from a flash flood scenario (recurrence interval of 5 to 10 years) to a (sub)Plinian eruption (VEI >3, recurrence interval of 5000 to 20,000 years). Inundation zones were defined using simulation code results coupled with geological mapping and magnitude/frequency analysis. The results of Titan2D modelling feature a longer flow runout than in previous studies (e.g. Vargas et al., 2010) due to the creation of an enhanced 10 m DEM, constructed from DGPS surveys and ASTER data.

Land-use, building and infrastructure surveys identified nineteen different land-use patterns, ten main building types and many key infrastructures. Building types were classified and ranked according to a number of components, such as the dominant building material, number of floors etc. Similarly land use and infrastructure were ranked according to a number of different elements such as occupancy rate, emergency importance etc. The mechanical effects of the flows on buildings and infrastructure were then investigated to elaborate vulnerability functions. The vulnerability and risk assessment have indicated that building, land use and infrastructure on the Quebrada Huarangal fan are particularly vulnerable and at risk even during the smallest magnitude flow. This is primarily due to very poor quality construction in high hazard areas on the Quebrada Huarangal fan. In contrast the risk posed in the Río Chili Valley is in general much less. The level of risk posed to the hydroelectric power scheme and the potable water supply is concern for the city, especially during a volcanic crisis.

Data integration abilities of GIS in generating risk information by combining hazard scenarios with vulnerability elements have been highlighted in this research and offer promising prospects in the field of volcanic risk assessment and management. In addition, an updated database could help to efficiently handle possible volcanic crisis in real-time, and more importantly assist the risk reduction tasks.

Keywords: El Misti Volcano, hazards, risks, physical vulnerability, lahars, GIS, Titan2D, urban environment, Arequipa, Peru.

Sommaire

Résumé.....	2
Résumé anglais.....	4
Sommaire	5
Résumé étendu en français	7
Introduction	17
1.1 Cadre : les grandes villes exposées aux aléas volcaniques	17
1.2 Evaluer l'aléa volcanique, la vulnérabilité et le risque encouru par les communautés	18
1.3 Objectifs du projet.....	20
1.3.1 Arequipa au sud du Pérou – une grand cité à l'ombre du volcan actif El Misti.....	21
1.4	23
2.0 Méthodes	24
2.1 Introduction	24
2.2 Zones étudiées	25
3.0 Aléas liés aux écoulements volcaniques issus du volcan Misti	27
3.1 Introduction – type, magnitude et fréquence.....	27
3.2 Détermination des scénarios d'aléas pour les lahars, ruptures de barrage et crues éclair	28
3.3 Cartes de zonage de l'aléa	29
3.4 Résumé	31
4.0 Modéliser les lahars avec le code de simulation Titan2D.....	31
4.1 Introduction	31
4.2 Nouvelles simulations Titan2D entreprises sur le volcan El Misti	32
4.2.1 Paramètres d'entrée.....	33
4.2.2 Implication de différents DEMs sur les simulations avec Titan2D	33
4.3 Carte d'aléa de lahar utilisant les simulations Titan2D.....	36
4.4 Résumé	38
5.0..... Eléments exposés au risque : utilisation du sol, le bâti et les infrastructures à Arequipa	38
5.1 Introduction	38
5.2 Classification de l'utilisation du sol	39
5.3 Classification du bâti.....	41
5.4 Susceptibilité des types de bâtiments et de l'utilisation du sol	46
5.5 Classification des infrastructures	48
5.6 Résumé	50
6.0 Le risque posé à la ville d'Arequipa.....	51
6.1 Introduction	50
6.2 Evaluer le risque lié au bâti	50
6.3 Evaluer le risque lié aux types d'utilisation du sol.....	52
6.4 Combiner les deux types de risque.....	53
6.5 Le risque liés aux infrastructures	55
6.6 Résumé.....	58
7.0 Conclusions et application de la recherche	59
Références	61

Table of content

Résumé	2
Abstract	4
Extended Abstract in French	7
1. Introduction	17
1.1 Scope: Large cities exposed to volcanoes	17
1.2 Evaluer l'aléa volcanique, la vulnérabilité et le risque encouru par les communautés	18
1.3 Objectifs du projet	20
1.3.1 Arequipa in south Peru – a large city in the shadow of the active El Misti volcano ..	20
1.4 Summary	23
2.0 Methods	24
2.1 Introduction	24
2.2 Study areas	25
3.0 Mass flow hazards from El Misti	27
3.1 Introduction – type, magnitude and frequency	27
3.2 Determination of hazard scenarios for lahars, dam-break and flash floods	28
3.3 Hazard zone maps	29
3.4 Summary	31
4.0 Modelling lahars using Titan2D	31
4.1 Introduction	31
4.2 New Titan2D simulations undertaken on El Misti Volcano	32
4.2.1 Input parameters	33
4.2.2 Implication of differing DEMs on Titan2D simulations	36
4.3 Titan2D-derived lahar hazard map	36
4.4 Summary	38
5.0 Elements at risk: land, building stock and infrastructure in Arequipa	38
5.1 Introduction	38
5.2 Land-use classification	39
5.3 Building stock classification	41
5.4 Susceptibility of building types and land use in Arequipa	46
5.5 Infrastructure classification	48
5.6 Summary	50
6.0 The risk facing the city of Arequipa	51
6.1 Introduction	51
6.2 Building risk	51
6.3 Land use risk	52
6.4 Combining building and land use risk	53
6.5 Infrastructure risk	55
6.6 Summary	58
7.0 Concluding remarks and application of the research	59
References	61

Résumé français étendu

La thèse de Kim Martelli a pour objectif de **définir la vulnérabilité physique d'une grande ville** (en l'occurrence Arequipa au Pérou) **face aux lahars** (coulées de débris volcaniques) **et aux crues éclair**. La vulnérabilité physique est celle du bâti et des infrastructures urbaines : systèmes de transport et tous types de réseaux, communications et ressources de la ville, dans son environnement régional.

La thèse de K. Martelli propose une évaluation qualitative et semi-quantitative de l'aléa et du risque, qui s'appuie sur des études traditionnelles (géologie, géomorphologie, hydrologie) et sur des méthodes modernes (mesures GPS, analyse de MNT, modélisation des écoulements grâce au code de simulation numérique Titan2D). L'outil principal destiné à convoier l'information au lecteur et aux autorités ainsi qu'aux populations de la ville d'Arequipa est un SIG « urbain ». L'évaluation de l'aléa et du risque volcanique et hydrologique et la contribution à la prévention dans le périmètre urbanisé résultent de la combinaison de méthodes usuelles et novatrices. Faisant l'objet de développement actuel, certains outils comme Titan2D sont à l'origine de certaines limites constatées dans les résultats obtenus.

Cette thèse ne traite pas de la vulnérabilité sociale et économique, ni d'autres aspects qui fondent également l'analyse du risque comme l'estimation financière des dommages potentiels. Ceci fera partie du projet ANR RiskNat « Laharisk » (2010-2012) dont cette thèse est l'un des premiers résultats. L'objectif de la thèse, auprès de la Fondation MAIF, était la mise en œuvre d'une méthode inter-disciplinaire visant à évaluer la vulnérabilité, afin de contribuer à la délimitation du risque dans les secteurs d'une grande ville d'un pays en développement les plus exposés au risque des lahars et des crues éclair. La thèse contribuera finalement au transfert de l'information obtenue au profit des autorités civiles et des populations menacées. Ce transfert a déjà été opéré en partie à la suite des crises survenues pendant la période d'investigation (2011), tandis que des exercices de prévention (simulacres d'évacuation) ont été conduits dans un quartier exposé de la ville avec nos partenaires (*Ingemmet* – Institut de Géologie et *Defensa Civil* – Protection civile) en 2010.

1. Cadre général et portée de l'étude

Tilling (2005) a estimé que 500 millions de personnes (environ 9% de la population mondiale) vivaient à moins de 100 km d'un volcan actif en 2000. A présent, plus de 200 millions vivent dans des métropoles comptant plus d'un million d'habitants près de volcans actifs ; de grandes villes comme Tokyo, Mexico, Naples et Arequipa sont toutes dans ce cas (Tilling, 2005 ; Chester *et al.*, 2001). Pendant le 20^e siècle plus de 90 000 personnes ont été tuées et plus de 5 millions ont été blessés par les effets des éruptions volcaniques (Witham, 2005). Le registre des désastres volcaniques récents est dominé par les catastrophes de la Montagne Pelée en Martinique (1902) et du Nevado del Ruiz en Colombie (1985), qui à elles seules comptent pour 50% du total des victimes.

Les écoulements volcaniques (lahars, comprenant les coulées de débris et les écoulements hyperconcentrés selon la concentration en solide) et les crues éclair représentent des phénomènes dangereux et destructeurs qui exigent une investigation complémentaire dans le domaine de la vulnérabilité physique. A ce jour, très peu d'études (par ex. Zanchetta *et al.*, 2004) ont été consacrées aux effets des lahars sur l'environnement urbain, qui représente pourtant une menace réelle pour de nombreuses villes situées près d'un volcan actif. En outre, cet impact est plus grand dans les pays en développement à cause de l'habitat plus fragile dans des zones densément peuplées, notamment près des vallées et ravines ou sur des cônes

de déjection en milieu urbanisé. Cet impact est aussi accru par les facteurs de vulnérabilité liés au type de bâti, aux matériaux de construction, à l'utilisation du sol, aux ségrégations sociales à l'intérieur de la ville et à d'autres caractéristiques politiques. Les pertes humaines et des biens imputables aux dommages provoqués par les lahars et les crues éclair peuvent être réduites si les autorités et les populations exposées comprennent et gèrent les risques au quotidien dans la ville. C'est pourquoi ce rapport final fournit une liste de recommandations quant à la prévention des impacts sur le bâti, les infrastructures de la ville et la population.

2. Objectifs de la thèse

Le principal but de cette thèse est de proposer une méthode d'étude de la vulnérabilité physique et des risques dus aux lahars et aux crues éclair dans un environnement urbain, à partir du cas extraordinaire de la ville d'Arequipa au sud du Pérou (Figure 1). Arequipa est en effet, avec Naples, l'une des grandes villes (presqu'un million d'habitants en 2008) les plus exposées dans le monde aux risques volcaniques et aux crues associées.

En premier lieu, les caractéristiques de l'aléa géologique, identifiés d'après les travaux géologiques publiés (Thouret et al. 1999, 2001), sont suivis par le diagnostic de l'histoire éruptive visant à définir la magnitude et la fréquence des types d'éruptions. L'information obtenue, ainsi que les données de la modélisation, servent ensuite à caractériser trois scénarios d'éruptions et à cartographier les zones d'Arequipa potentiellement affectées par les aléas volcaniques et hydrologiques. L'identification des éléments exposés aux risques vient au cœur du projet de recherche. Celle-ci a été accomplie par la cartographie et l'analyse de tous les éléments susceptibles d'être affectés par les impacts des lahars et des crues. Ces éléments englobent par exemple l'habitat, les négoce, les églises, les clubs de sport et stades, les stations électriques et les ponts dans le centre de la ville, le long de la vallée du Rio Chili et dans le district de Huarangal au NE de la ville. La répartition des éléments exposés est ensuite combinée dans un SIG à l'aléa (aire d'impact et hauteur de crue attendue) et aux scénarios. Les impacts physiques des écoulements sur le bâti et les infrastructures sont délimités au sein du SIG, et à leur tour utilisés pour évaluer la vulnérabilité et le risque à Arequipa.

2.1. Arequipa au Sud du Pérou : une grande ville à 17 km du volcan actif El Misti

Arequipa, la seconde ville du Pérou avec plus de 860 000 habitants (en 2008), évoque le cas de Naples en Italie, où plus de 600 000 habitants sont exposés à l'activité éruptive du Vésuve. À Arequipa les habitants vivent à 17 km au SW du Misti et les faubourgs du nord s'étendent à moins de 9 km du volcan (Fig. 1). La ville a connu une croissance démographique importante après 1940, qui s'est accélérée après 1970, la population étant multipliée par 5 (Fig. 3). Depuis 1970 la surface urbanisée s'est accrue à cause de l'exode rural dans la Cordillère combinée à l'agitation sociale dans le pays. En 45 ans (1970-2005) la surface construite a augmenté de 13 à 60 km² : l'espace urbanisé aujourd'hui est 400% plus vaste que celui de 1960. Des quartiers populaires se sont maintenant étalés sur le flanc sud-ouest du volcan, sur les terrasses du Río Chili et sur celles de ses affluents jusqu'à 9 km du sommet. Il s'agit en outre de la seconde destination touristique majeure au Pérou (après Cusco), qui réunit des monuments d'architecture coloniale classés au patrimoine de l'UNESCO : plus d'un million de touristes ont visité Arequipa en 2008 (INEI, 2008). À 20 km à l'est s'ajoute les 3000 habitants de la ville de Chiguata sur le flanc sud et à 11 km du Misti.

Le développement de la ville dans l'oasis et au pied du volcan a pour conséquence d'augmenter le nombre de personnes face aux futures éruptions et aux écoulements. L'identification des écoulements volcaniques et hydrologiques est donc primordiale. La dernière éruption importante du Misti eut lieu il y a 550 ans mais de petits événements phréatiques se sont produits depuis, y compris au 17^e et 18^e siècle. En sus des lahars dont le volume estimé est de $0.1 \times 10^6 \text{ m}^3$ à $11 \times 10^6 \text{ m}^3$, des inondations sont survenues une à deux fois tous les 10 ans en moyenne dans la période historique récente le long du Río Chili et de ses affluents, le plus souvent des oueds, appelés *quebradas* (=Qda.) (Thouret *et al.*, 2001). Thouret *et al.* (2001), Delaite *et al.* (2005), Stinton *et al.* (2004) et Vargas *et al.* (2010) avaient déjà indiqué qu'une éruption du Misti, si modeste soit-elle, poserait une menace sérieuse à la ville.

Sur la base des études livrées par les auteurs précédents au sujet de l'histoire éruptive et des aléas posés par la présence du Misti (Delaite *et al.*, 2005; Stinton *et al.*, 2004; Thouret *et al.*, 1999, 2001; Vargas *et al.*, 2010), il s'agit de délimiter les zones potentiellement affectées, puis de cartographier et définir l'impact des écoulements sur les éléments exposés. Un autre besoin vital est de communiquer les résultats de cette évaluation auprès des autorités afin de contribuer à la prise de décisions en matière de prévention des risques et à l'élaboration de plans de contingence en cas de crise. Le cas d'étude et la méthode sont enfin applicables aux grandes villes exposées aux effets de volcans actifs, comme Kagoshima au Japon, Quito en Equateur, Yogyakarta en Indonésie et Naples en Italie.

2.2. Diversité des méthodes mises en œuvre dans la thèse

Les méthodes sont résumées à la Figure 4, qui montre également la démarche de recherche entreprise, visant à évaluer la vulnérabilité physique du bâti, des modes d'utilisation du sol et des infrastructures urbaines d'une grande ville, dans un pays en voie de développement très exposé aux effets des aléas naturels. Ces méthodes englobent les études géologiques traditionnelles et la cartographie assistée des résultats des modèles pour les dépôts volcaniques et torrentiels ; la modélisation numérique des lahars à l'aide du code Titan2D ; des enquêtes et l'analyse statistiques du type et de la qualité du bâti et des infrastructures ; la création d'un SIG urbain et d'une base de données, et enfin les tests géotechniques des matériaux utilisés de construction.

Trois zones pilotes dans et autour d'Arequipa ont été choisies dans cette étude (Fig. 5) : (1) un secteur autour de l'usine hydroélectrique de Charcani Grande dans l'amont du canyon du Río Chili ; (2) la vallée du Río Chili depuis la sortie du canyon dans l'oasis cultivée à 8 km à l'amont de la ville jusqu'à la limite méridionale d'Arequipa à 25 km du Misti, et (3) le cône alluvial et la ravine de la Qda. Huarangal à l'est de la ville et sur le flanc du volcan Misti.

Les méthodes employées dans ce projet nous ont permis de conduire une recherche pluridisciplinaire qui met notamment en lumière les capacités, ainsi que les limites, des outils de diagnostic comme le SIG et Titan2D appliqués à l'évaluation des aléas, de la vulnérabilité et du risque en milieu urbanisé.

3. Les résultats appartiennent à quatre domaines essentiels

3.1. Aléas des écoulements volcaniques du Misti : type, magnitude, fréquence et scénarios

Le type, la magnitude et la fréquence des écoulements produits par le volcan El Misti sont issus de l'interprétation des dépôts datés (Thouret *et al.*, 1999, 2001). On a déterminé les principaux groupes de dépôts attribués à chaque stade d'édification du Misti avec leur âge, épaisseur et étendue, le type d'activité prédominant, la magnitude (IEV) et une estimation de la fréquence. L'analyse des données a montré que les écoulements, surtout pyroclastiques, ont été fréquents, au moins 10 fois dans l'histoire éruptive depuis 50 000 ans (Thouret *et al.*, 2001). Les lahars syn- et post-éruptifs se sont formés durant et après la dernière éruption du Misti au 15e siècle (AD 1440-1460) lorsqu'une éruption volcanienne a produit une retombée qui a recouvert la zone de la ville de 5 à 10 cm d'épaisseur (Thouret *et al.*, 2001). Des lahars dont le volume est compris entre 1.5 et 3 million m³ se sont déposés dans la vallée du Rio Chili et dans les Qda. San Lazaro et Huarangal il y a approximativement 1000 ans BP, 500 ans BP et durant le 17e siècle (Thouret *et al.*, 2001).

Les archives géologiques et l'histoire récente fournissent la base de plusieurs scénarios possibles de génération d'écoulements volcaniques durant et après une éruption du Misti. Des dépôts éruptifs volumineux notamment les retombées de ponces pliniennes (épais de 3 m et datés à 21 000-20 000 ans BP à 13 km au SE du Misti) sont des sources de débris mobilisables par les lahars, longtemps après ou même sans éruption. Les scénarios éruptifs proposés par Thouret *et al.* (2001), Delaite *et al.* (2005) et Vargas *et al.* (2010) couvrent toute la gamme des lahars produits par les pluies ou la fusion de la neige. Vargas *et al.* (2010) ont proposé trois scénarios : 1) des lahars non éruptifs de petit volume (<1.5 million m³) et assez fréquents (2 à 10 ans); 2) des lahars plus volumineux (1.5-4 million m³) et moins fréquents (300 à 1000 ans) en cas d'éruption, même modeste comme celle du 15e siècle, et 3) des lahars volumineux (4-11 million m³) mais rares (1000 à 5000 ans) durant ou après une éruption de grande magnitude (VEI>3). Des lahars peuvent se déclencher sans éruption après un orage intense, la fusion de la neige au sommet du volcan, un séisme important ou un glissement de terrain sur le flanc WNW du Misti dominant le canyon du Rio Chili. La neige n'est plus permanente sur le sommet du Misti Cependant, le manteau neigeux peut recouvrir une surface de 7 km² en hiver (Août) et persister entre décembre et juillet, avec un volume estimé à 2.5 million m³ (Delaite *et al.*, 2005). La saison des pluies s'étend de novembre à avril mais les précipitations ne dépassent pas 150 mm/an à Arequipa. Les orages sur le Misti déclenchent pourtant des pluies fortes de décembre à mars (particulièrement en février), dont l'intensité peut dépasser 10 mm/h. Ces abats d'eau engendrent des crues éclair et des écoulements hyperconcentrés au moins 2 fois par décennie depuis 70 ans.

Un autre scénario doit être considéré car des dépôts lacustres existent à la base d'une haute terrasse de 15 m d'épaisseur à Charcani Grande dans le canyon du Rio Chili à 20 km à l'amont du centre ville : une crue et un lahar peuvent être déclenchés par la rupture d'un barrage dû à un glissement de terrain en cas d'éruption ou de séisme. Une faille active est localisée sur le flanc WNW du Misti là où une sismicité faible mais superficielle est enregistrée depuis 2005. La récurrence et le volume des débâcles de ce type sont peu connus mais le processus est discuté dans cette thèse, car la menace vis à vis d'Arequipa et des 5 usines hydroélectriques construites dans le canyon posent un grave problème de gestion du risque.

Un zonage des aléas a été réalisé dans la vallée du Rio Chili et sur le cône torrentiel et volcanique de la Qda. Huarangal à partir de l'histoire géologique, du système de terrasses et des scénarios d'aléas de lahars et inondations (Fig. 6 et 7). Le degré maximum de l'aléa a été attribué aux terrasses t0 à t1' formées par les dépôts des écoulements fréquents (1-10 ans) mais de faible magnitude (scénario 1). Logiquement, les hautes terrasses 3 formées par les

dépôts d'écoulements volumineux et rares représentent les zones de très faible aléa. Même si ces écoulements ont une magnitude exceptionnelle (4-11 million m³), leur récurrence excédant 1000 ans rend ces événements moins dangereux pour les populations, si l'on retient le principe d'une période de retour décennale à centennale pour notre évaluation des risques. Les résultats montrent clairement que les crues éclair et les lahars, ayant des origines diverses, vont affecter Arequipa même si leur magnitude est faible. En effet, les populations les plus vulnérables habitent dans les zones les plus exposées le long des oueds et dans les faubourgs proches du volcan, d'autant plus que l'expansion urbaine récente, l'exode rural et le coût élevé de la terre contribuent à accroître le nombre d'habitants dans ces zones soumises au risque. A cela s'ajoute la localisation des infrastructures essentielles (par ex. les 5 barrages et usines hydroélectriques dans le canyon à une distance de 8 à 20 km du centre ville), dont l'endommagement entraînerait des conséquences désastreuses dans toute l'agglomération, telle la rupture de l'alimentation en électricité et en eau potable.

3.2. *La modélisation des écoulements de lahar*

La modélisation numérique des écoulements volcaniques est devenue un outil incontournable pour évaluer les aléas (Sheridan *et al.*, 2005). Les simulations fondées sur des codes numériques aident à estimer la distance parcourue au-delà de la rupture de pente du cône volcanique, à délimiter les zones potentiellement inondables et rétroactivement à examiner le comportement des écoulements. Plusieurs modèles (Flow2D, DAN, Flo-2D, VolcFLOW) ont été exploités, avec des degrés de succès divers, pour délimiter les aléas autour des volcans actifs dans le monde. Les zones potentiellement inondées par les lahars ont été mieux délimitées sur les flancs et le piémont du Misti et dans la ville d'Arequipa grâce à la modélisation semi-empirique ou numérique. Le code semi-empirique LaharZ (Schilling, 1998) a été utilisé par Toyos (2000), Van Gorp (2002), Delaite (2003) et Delaite *et al.*, (2005) afin d'identifier les zones potentiellement affectées par les lahars dans la vallée du Río Chili et dans celles des Qda. San Lazaro, Huarangal et Agua Salada. Stinton *et al.* (2004a) ont comparé les simulations issues de LaharZ (Delaite, 2003) avec celles réalisées à l'aide de la version monophasique du code numérique Titan2D (Patra *et al.*, 2005). Vargas *et al.* (2010a) ont poursuivi cette recherche en utilisant la version biphasique du code Titan2D (Pitman and Le, 2005) afin de simuler les lahars, en les comparant à nouveau avec les résultats obtenus par Delaite *et al.* (2005).

La modélisation a d'abord été effectuée en utilisant un MNT de 30 m de résolution, obtenu à partir de cartes topographiques 1/25 000 digitalisées et de l'interférométrie radar (Delaite, 2003). Les simulations de lahars ont été conduites avec des scénarios d'écoulement dont les volumes compris entre 0.01×10^6 m³ et 11×10^6 m³ se propagent dans la vallée du Río Chili et la Qda. Huarangal. De nombreuses simulations utilisant Titan2D ont été effectuées en faisant varier les paramètres d'entrée suivants : point de départ, angles de friction interne et basal, et fraction solide, afin de reproduire des écoulements « réalistes ». Ces paramètres ont donc été calibrés d'après les arguments de terrain des lahars récents, les données de la littérature et des expériences in situ, et d'après l'examen des impacts de ces écoulements (Tab. 3). Une fois le modèle établi, les simulations des lahars plus ou moins volumineux ont été conduites sur un MNT plus précis (résolution de 10 m) calculé à partir des mesures effectuées avec un GPS différentiel et un MNT ASTER à 30 m de résolution. Le but est d'évaluer la distance dite de « *runout* », c'est-à-dire celle parcourue par un lahar au delà de la rupture de pente du volcan : cette distance a aidé à délimiter les zones potentiellement inondées, notamment dans la vallée du Río Chili (Fig. 11) et sur le cône de la Qda. Huarangal (Fig. 12). Les quatre catégories de volumes entre 0.5×10^6 m³ et 11×10^6 m³, correspondant aux scénarios déjà identifiés

précédemment, ont servi à modéliser, sur le MNT de 10 m, les lahars ayant un ratio solide/fluide de 0.40 et dont le matériau a un angle de friction interne de 30° et basale de 12°. La délimitation des contours des zones inondées coïncide avec l'épaisseur d'un lahar simulé supérieure à 0.1 m. La zone inondable la plus dangereuse correspond à celle des lahars de petit volume mais fréquents, tandis que la zone inondée la moins dangereuse est celle des écoulements plus volumineux mais rares (cf. valeurs p. 10).

Les zones inondées d'après les simulations utilisant Titan2D dans la vallée du Río Chili et sur le cône de la Qda. Huarangal sont plus larges et plus longues que celles montrées préalablement par Stinton *et al.* (2004a) et Vargas *et al.* (2010a) : la distance atteinte par le plus long lahar avec un volume de $11 \times 10^6 \text{ m}^3$ dans le Río Chili est de 12 km plus longue que les précédentes. Pour le même volume, la distance atteinte par le lahar sur le cône de la Qda. Huarangal est plus longue de 2.5 km dans notre étude. Cependant et à l'instar des travaux de Stinton *et al.* (2004a) et Vargas *et al.* (2010a), les distances de "runout" issues des simulations utilisant Titan2D s'avèrent encore plus courtes de 9,5 km dans le Río Chili et de 4,8 km sur le cône de la Qda. Huarangal que celles obtenues par Delaite *et al.* (2005) avec LaharZ. En outre, la carte des zones inondées par les lahars d'après les simulations produites avec Titan2D n'est pas comparable avec celle fondée sur des arguments géologiques et géomorphologiques. L'utilisation du MNT amélioré à 10 m de résolution au lieu de 30 m a permis de résoudre certains problèmes rencontrés lors des simulations préalables. Par exemple sur le MNT initial, les écoulements modélisés stoppaient là où la direction des rivières changeait brutalement, ce qui entraînait le raccourcissement des distances de propagation. Ces distances augmentent lorsque les écoulements sont modélisés sur le MNT amélioré parce que leur mobilité est accrue grâce à la morphologie plus « réaliste » du chenal représenté.

En dépit des différences notables entre les cartes issues des travaux de terrain et celles issues des simulations utilisant les codes, les résultats obtenus en utilisant Titan2D ont des implications importantes sur le zonage de l'aléa dans la vallée du Río Chili et du cône de la Qda. Huarangal. Les différences visibles dans les résultats des simulations sont aussi dues au contenu et aux objectifs différents entre le code semi-empirique LaharZ et le code numérique Titan2D. Les paramètres d'entrée dans la simulation et les conditions au moment de l'initiation peuvent être responsables des différences observées entre les modèles et les dépôts. Une autre caractéristique très importante dont il faut tenir compte dans le domaine de l'évaluation des aléas est la grande variabilité des lahars. Un lahar comprend en effet plusieurs phases distinctes durant un écoulement et en conséquence ses propriétés et son impact varient considérablement dans l'espace et le temps (Procter, 2010; Dumaisnil *et al.*, 2010). Ceci limite l'utilisation du code Titan2D lorsqu'on modélise les lahars : il est en effet incapable de prendre en compte l'entraînement des sédiments et le cycle incorporation/dilution montré par les lahars, qui peuvent être influencés par la moindre variation topographique du chenal et par la moindre modification de la dynamique de l'écoulement. En dépit des limites d'utilisation du code que le chercheur doit considérer, les simulations sont des outils très valables pour délimiter les zones inondables et l'intensité de l'aléa et in fine pour approcher le comportement des écoulements. Les résultats de la modélisation et les cartes des zones inondables par les lahars et crues éclair constituent la base de l'évaluation de la vulnérabilité de la ville.

3.3. Vulnérabilité des éléments exposés : bâti, utilisation du sol et infrastructures urbaines

Les trois classifications des modes d'utilisation du sol, du bâti et des infrastructures urbaines sont cruciales si l'on veut définir la vulnérabilité des éléments exposés aux risques, parce que l'endommagement potentiel dépend de l'occupation des bâtiments par les habitants. En définissant leur utilisation, on peut identifier les structures dont la survivance est vitale durant une crise et devrait se prolonger après la catastrophe. Ces structures essentielles sont par exemple les services médicaux, le réseau de distribution d'énergie et les centres de commandement. Sur la base des enquêtes conduites à Arequipa en 2007 et 2008, vingt modes d'utilisation ont été identifiés (Tab. 4, Fig. 13), depuis les zones agricoles non construites jusqu'aux zones urbaines densément construites.

En suivant les méthodes promues par Chevillot (2000) et d'autres (Pomonis *et al.*, 1999 ; Kelman, 2002 ; Spence *et al.*, 2004a,b ; Baxter *et al.*, 2005) les enquêtes du bâti ont été réalisées dans les deux secteurs pilotes de la ville à l'échelle du pâté de maisons et dans les propriétés lorsqu'elles étaient accessibles. Neuf types de constructions ont été identifiés (Tab. 6, Fig. 14) et classés selon leur résistance à l'impact, qui tient compte du matériau dominant, du nombre d'étages, du type et angle de toit, du nombre et type d'ouvertures, des réparations et de l'intégrité structurale du bâtiment. À Arequipa, la plupart des infrastructures urbaines essentielles (ponts, usines électriques et lignes de haute tension, conduites d'eau) sont concentrées le long du Río Chili et également en centre ville. Les services d'urgence et les infrastructures névralgiques en cas de crise (ouvrages de protection, centres de décision, stades ou clubs pour le tri des blessés, réseaux vitaux de transport, énergie, communication et alimentations) ont été classés parmi les modes d'utilisation du sol et hiérarchisés.

Après avoir analysé la vulnérabilité du bâti et des modes d'utilisation du sol, celle des infrastructures urbaines a été mesurée. Des coefficients, de 0 (faible *enjeu*) à 1 (*enjeu élevé*), ont été attribués à différentes catégories (telles les répercussions économiques, l'exposition de la population et la valeur en cas de perte) pour chaque type d'infrastructure (la méthode d'attribution des coefficients est discutée dans le chapitre 1). Les valeurs des coefficients ont été additionnées et pondérées afin de livrer un résultat final compris entre 0 et 1 qui exprime l'enjeu représenté par chaque infrastructure et par conséquent la vulnérabilité durant une crise (Tab. 7). Les enquêtes ont révélé l'hétérogénéité des types de bâti et des infrastructures à une échelle aussi grande que celle du pâté de maisons. On pourrait donc attribuer la vulnérabilité du bâti à sa localisation puisque les constructions les plus fragiles sont sans surprise situées dans ou près du lit majeur des rivières et sur le cône formé par la Qda. Huarangal. En fait, l'exercice de pondération montre que le bâti est davantage menacé à cause du type de construction et du mode d'utilisation du sol.

La ville dépend du Río Chili pour son électricité, son eau et son alimentation, et dans l'hypothèse d'un lahar ou d'une crue, ces services vitaux sont situés ou produits dans les zones les plus vulnérables. Le réseau de transport est vital durant une crise alors que l'analyse des infrastructures révèle que les ponts unissant les deux rives de la vallée du Río Chili près du centre ville sont les plus vulnérables. En outre, les réseaux d'alimentation en eau, en électricité et des télécommunications sont souvent localisés près des ponts, donc très exposés. Le réseau d'électricité provenant de la centrale thermique d'Egasa située sur une terrasse moyenne (t1') et des barrages hydro-électriques dans le canyon est très vulnérable. Leur rupture provoquerait un effet domino dans la ville et aggraverait la situation des hôpitaux et des centres de santé.

3.4. Le SIG urbain : combinaison des évaluations et définition des zones exposées au risque

Le risque a été déterminé en combinant la vulnérabilité du bâti, des infrastructures et du mode d'utilisation du sol avec les zones d'aléas dans le cadre des trois scénarios pris comme références. Sur la base du troisième scénario, le niveau d'aléa dans la vallée du Rio Chili est cartographié pour des lahars volumineux ($4 \text{ à } 11 \times 10^6 \text{ m}^3$) mais assez rares (>1000 ans) à la Figure 19. L'aléa d'inondation par les lahars varie de *très faible à fort* (Fig. 19 A). La quasi totalité de la zone inondable par ces écoulements, d'après la simulation effectuée avec Titan2D, présente un risque très faible sauf le cas du restaurant La Chocita près de Chilina (Fig. 19 B) ; ce secteur encourt un risque d'endommagement élevé car il coïncide avec la position d'un front de lahar volumineux simulé avec Titan2D.

Le risque d'endommagement au bâti est plus élevé à proximité du lit du Rio Chili et sur les terrasses basses à moyennes t_0 à t_2 seulement si les lahars fréquents (<100 ans) ou volumineux ($4-11 \times 10^6 \text{ m}^3$) sont pris en compte. Dans cette vallée, le mode d'utilisation du sol résulte d'un mélange entre habitat, centres commerciaux, clubs de sport, usines et terrains agricoles. Le type de constructions dans le Rio Chili est beaucoup moins hétérogène que celui de la zone de la Qda. Huarangal. En revanche, la carte montre un risque modéré à très élevé pour la majorité des terrasses et du cône de la Qda. Huarangal (t_0 to t_2). L'hétérogénéité du bâti dans cette zone explique la variété du niveau de risque, qui reste élevé en général. Ce contraste entre les deux zones est dû aux grandes variations de qualité du bâti, au mode d'utilisation du sol, à la localisation des bâtiments et à la forme encaissée de la vallée (Rio Chili) par rapport à la faible épaisseur du cône de déjection (Qda. Huarangal).

En revanche, le risque posé au réseau de voies de communication traversant le Rio Chili est très élevé en cas de crise, car tous les ponts peuvent être endommagés, le Pont colonial Grau étant encore le plus résistant. Les implications sont sévères quant à l'évacuation des populations et la planification des secours. Dans le cas du cône de la Qda. Huarangal, le risque posé aux voies de communications est élevé car les routes traversant le lit majeur et surtout les terrasses t_0 à t_2 au sud du cône pourront être inondées par le débordement probable de la rivière. L'évacuation des secteurs SE et S du cône de la Qda. Huarangal, très peuplés, sera probablement difficile vers l'est et peu recommandable vers l'ouest, le centre de la ville déjà engorgé. Toutes les routes croisant les secteurs SE et S sont situées en zone de risque élevé et celle croisant la Quebrada au sud est en zone de risque très élevé.

4. Conclusions

Cette recherche a rassemblé plusieurs techniques visant à définir la vulnérabilité physique. Les zones vulnérables ont été identifiées sur la base des éléments suivants : les études géologiques et la cartographie des dépôts, soit traditionnelle soit fondée sur les simulations issues de codes ; l'emploi d'un SIG urbain ; la modélisation des écoulements avec le code Titan2D ; les enquêtes et l'analyse statistique de la nature et de la qualité du bâti et des infrastructures ; enfin les caractéristiques géotechniques des matériaux de construction à partir de tests mécaniques. L'objectif principal a été atteint, à savoir la combinaison de méthodes visant à déterminer la vulnérabilité physique et le risque dans une zone urbaine à proximité d'un volcan actif.

Des recommandations visant à réduire le risque dans les zones exposées à Arequipa ont aussi été formulées. Cette étude met en lumière les zones que l'on devrait protéger en priorité : la vallée du Rio Chili à l'amont et au centre de la ville, ainsi que les ravines et cônes façonnés par les Qdas. San Lazaro et Huarangal, afin que les autorités civiles protègent les populations et les centres décisionnels en cas de lahar et de crue. L'élaboration d'un plan d'utilisation du

sol opposable au tiers a été lancée à Arequipa (et les premières mesures annoncées en 2010) mais son application reste à démontrer aujourd'hui : il faudrait pouvoir interdire la constructions dans les zones exposées à un risque majeur et définies sur la carte des aléas et risques volcaniques (Vargas et al., 2010) et dans le zonage effectué dans cette thèse. Les constructions ont gagné les pentes du volcan au NE de la ville depuis une décennie et dans les lits majeurs des oueds et ravines qui traversent la ville. Certains lotissements appelés « quartiers d'invasion » semblent "illégaux" vis-à-vis du plan municipal d'urbanisation mais la population qui envahit les lotissements exige ensuite l'installation des services vitaux par la municipalité, ce qui obère une planification de prévention efficace dans ces quartiers. Certes, le principe de l'interdiction des constructions a été retenu en 2011 par la municipalité d'Arequipa dans les zones les plus dangereuses, notamment sur les flancs du volcan depuis quelques années. Cette zone d'interdiction est fondée sur la carte de zonage des aléas volcaniques publiée en 2007. Bien qu'il s'agisse d'un pas décisif vers la mitigation des risques, l'application de la loi n'est pas garantie à ce jour.

5. Recommandations

Notre étude a mis en lumière la vulnérabilité du bâti à Arequipa, tandis que les réseaux urbains (électricité, eau et transport), cruciaux en cas de crise, s'avèrent très vulnérables face aux lahars et surtout aux crues éclair, plus fréquentes.

1. Un plan stratégique de prévention des risques doit être entrepris par les autorités locales afin de montrer et réduire la vulnérabilité des infrastructures et les réseaux en cas de cas de crise. Les constructions doivent être interdites dans et à proximité du lit majeur de toutes les rivières ou ravines parcourant Arequipa. Des plans de contingence doivent être élaborés afin de prévoir les impacts, les pertes, ainsi que les évacuations. A titre d'exemple, existe-t-il un plan d'acheminement de l'eau si celle-ci était contaminée ? Quels seront les effets de la pénurie en eau sur les services de secours ? Si les ponts enjambant l'artère principale dans le centre ville étaient détruits, prévoit-on une voie de contournement afin de transporter les biens nécessaires ? Si l'électricité venait à manquer, quelle énergie prendrait le relais dans la ville ? Combien de temps le réseau d'hôpitaux pourrait-il fonctionner ? Comment serait-il alimenté sans le réseau routier principal ? Les patients pourraient-ils être évacués ? En effet, le réseau électrique est, avec celui de l'eau, le plus menacé car les usines électriques sont toutes situées dans le fond de vallée de la rivière principale. Des réponses concrètes à ces questions devraient être fournies par de nouveaux plans de prévention afin de rechercher un consensus auprès de la population au sujet du risque acceptable. Les sources d'eau et d'énergie alternatives doivent être inventoriées dans le but de couvrir les besoins de la ville durant les 72 premières heures après la catastrophe, qui précèdent l'arrivée des secours gouvernementaux ou internationaux. Si l'on veut durablement réduire le risque, un plan d'évacuation efficace doit être proposé, discuté et testé selon les scénarios proposés ici.

2. Une analyse approfondie du risque encouru par toutes les infrastructures est recommandée afin de mettre en lumière les obstacles ou les faiblesses dans le cas d'une crise. Un réseau routier en bon état et alternatif est impératif en cas d'urgence afin de pouvoir coordonner les opérations de secours des blessés et sinistrés. Des mesures de protection des bâtiments essentiels comme des barrages à l'amont et des ouvrages de déflexion sur la structure elle-même peuvent minimiser l'impact des lahars et des crues éclair et peuvent donner du temps pour évacuer et reloger les habitants sinistrés. D'autres mesures de protection proactive englobent l'interdiction de construction dans les zones inondables, l'obligation de surélever le rez-de-chaussée des bâtiments situés sur les terrasses basses et moyennes (au moins jusqu'à

t1') et la construction ou l'amélioration des digues de protection le long de toutes les Quebradas. Il faut réhabiliter les ponts bas ou étroits et l'ex-pont ferroviaire et rehausser leur tablier afin qu'ils puissent absorber des crues de 4 m de hauteur (260 m³) au minimum dans le cas du lit majeur du Rio Chili. Dans le cas des oueds affluents, il s'agit de 2 à 4 m de hauteur selon la morphologie de la ravine, à condition que celle-ci soit nettoyée des immondices.

3. Un programme d'éducation et de prise de conscience de la population vivant dans les zones exposées le long des vallées est crucial. En 2008, les enquêtes auprès des résidents du faubourg de San Jeronimo à proximité du lit mineur de la Qda. Huarangal, a révélé qu'ils n'avaient pas conscience du degré de risque lié aux lahars et crues éclair. Ils avaient le sentiment d'une fausse sécurité, prétendument mal diffusée et peu comprise, de la part des autorités locales. Or, ils ont été gravement sinistrés le 11 février 2011 lorsque 22 maisons ont été détruites dans ce quartier populaire. La population résidente, surtout si elle est récemment migrante, ainsi que les autorités locales, doivent recevoir une éducation en termes de risques : un simulacre d'évacuation a été conduite en 2010 grâce à l'action de L. Macedo (Ingemmet), de la Protection civile et de la municipalité. A son tour, le programme d'éducation doit être testé et vérifié postérieurement par des professionnels dans le domaine des risques, de l'éducation, de la santé et de la psychologie.

4. Les refuges et les voies d'évacuation doivent être clairement indiqués avant, puis communiqués et renforcés pendant la crise. Les plans de contingence élaborés lors de la crise de l'Ubinas (Rivera *et al.*, 2010) offrent une référence dans la région. Aucun refuge, aucune voie n'est actuellement signalée à Arequipa. Vargas *et al.* (2010) ont déjà indiqué que les routes dirigées vers l'ouest et le nord étaient dangereuses en cas de crise. La route principale vers le SW, la Panaméricaine, devrait être portée 4 voies et doublée par la route alternative de la Mine Cerro Verde. Vers le SE de l'oasis conduisant au sanctuaire de Chapi devrait être agrandie et prolongée de 30 km vers le Rio Tambo, qu'un nouveau pont devrait franchir afin de rejoindre la route Panaméricaine vers le sud (Vargas *et al.*, 2010). L'avantage de cette alternative vers le SE est d'éloigner la population vers une zone qui ne devrait pas être atteinte par les écoulements ni même les retombées de cendres, si l'éruption ne dépasse pas l'indice VEI 3. Vargas *et al.* (2010) ont indiqué que des refuges pouvaient être facilement construits dans les zones planes disponibles au SE de l'oasis près des villages de Yarabamba and Quequeña. D'autres refuges pourraient l'être vers l'ouest mais au-delà de Yura, afin d'éviter les retombées épaisses en cas d'éruption plinienne.

5. Enfin, nous recommandons l'emploi d'une plate-forme géomatique (incluant un SIG) qui a la capacité de réunir et traiter toutes les informations relatives à l'aléa, à la vulnérabilité et au risque grâce à une banque de données interrogeable à distance. Une banque de données et de nouvelles couches d'informations ont été ajoutées, comme les scénarios optimisés d'éruptions et des lahars ou crues. Des calculs entrepris dans le SIG ont permis de montrer la répartition spatiale des éléments exposés au risque, qui s'avère un outil de communication attractif à l'intention des décideurs et des communautés. L'avantage de la banque de données évolutive est de donner la possibilité pour les autorités civiles de mettre à jour en temps quasi réel les données urbaines au fur et à mesure de la crise. La diffusion par internet et téléphone mobile dans une ville comme Arequipa rend la technologie associée au SIG disponible et un outil d'éducation aux mains des instituteurs et au profit de la population exposée. La diffusion des résultats sous une forme interactive auprès des jeunes sera une priorité. La majorité de ces recommandations (planification adéquate de l'utilisation du sol, analyse de risque des réseaux vitaux, éducation et prise de conscience parmi la population la plus fragile, construction de

routes d'évacuation et de refuges) est applicable aux grandes villes du monde exposées aux risques des volcans actifs.

1. Introduction

1.1 Scope: Large cities exposed to active volcanoes

Urbanisation has led to an ever-increasing global exposure to a multiplicity of natural hazards as an estimated 50% of the world's population lives in urban areas (Chester et al., 2001). More people are being placed at risk as cities become overcrowded, forcing populations to live on the outskirts where land may be hazardous or unsuited for residential development, such as along drainage channels in cities. Furthermore, urbanisation in developing countries is increasing considerably - 17 out of 20 of the world's largest cities are now located in the developing world (Small and Naunmann, 2001). Alarming, volcanically active areas in developing countries are home to some of the densest populations including Yogyakarta (Indonesia), Quito (Ecuador), Mexico City (Mexico) and Guatemala City (Guatemala) (Chester et al., 2001).

It has been estimated that 500 million people worldwide (~9% of the world's population) live in volcanic zones that are at risk from future eruptions (e.g., Tilling, 2005). In addition, over 200 million people now live in large cities (with greater than 1 million inhabitants) near volcanoes; cities such as Tokyo, Mexico, Naples and Arequipa are all located within the shadow of an active volcano (Tilling, 2005; Chester et al., 2001). During the 20th Century alone over 90,000 people were killed and over 5 million affected by volcanic phenomena (Witham, 2005). The volcanic disaster death toll is dominated by the disasters at Mt Pelée, Martinique (1902) and Nevado del Ruiz, Columbia (1985), which together account for 50% of deaths.

Witham's (2005) database for volcanic disasters not only takes into consideration deaths but also those people injured, made homeless, evacuated and affected. Nevado del Ruiz also accounts for approximately 28% of the total number of injuries resulting from lahars generated by a small eruption (0.02 km³) that melted part of the snow and ice on the volcano. Lahars killed approximately 22,000 people and caused widespread devastation (Voight, 1990). The catastrophe is the worst volcanic disaster since the 1902 eruption of Mt. Pelée, which resulted in the deaths of around 29,000 people when pyroclastic density currents destroyed the town of St. Pierre (Blong, 1984).

The immediate effects of the 1991 Pinatubo (Philippines) eruption and the subsequent and protracted impacts on the region from lahars more than ten years after the eruption rank highly in the homeless and evacuated or affected fields (accounting for 26% of people made homeless and 33% of those evacuated or affected in the 20th Century; Witham, 2005). Merapi, Indonesia, also ranks in the top ten volcanoes for deaths, injuries and homelessness; and of the 1.1 million people living on the flanks of the active Merapi volcano, 440,000 are living in areas prone to pyroclastic flows, surges, and lahars (Thouret et al., 2000).

The volcanic disaster databases have all revealed that pyroclastic flows were the main cause of death, followed by lahars, which were also the principal cause of injuries. The major hazard to human and animal life from lahars is from burial or impact by boulders and other debris; burns can also result from lahars which carry hot debris. Damage to buildings and

infrastructure can include burial, foundation failure, transportation, excessive wall or roof loads, collapse, undermining, and corrosion (Rodolfo, 2000). Historic eruptions at Vesuvius (AD 79 and 1631), Kelud (1919), Casita (1988) and Soufrière Hills Volcano (1997) have produced lahars which have caused death, injury and/or damage (Spence et al., 2004b, Scott et al., 2008).

Loss of life and property damage from lahars can be reduced if officials and at-risk populations understand and manage the risks associated with living and working in these areas. In order for public policies to be developed which minimise the losses due to lahars, methods are needed to evaluate the vulnerability, exposure, and risk to the community. This research project presents an insight in the effects and impacts of lahars on housing and infrastructure and the physical vulnerability of such structures from a lahar impact.

1.2 Assessing the volcanic hazard, vulnerability and risk of communities

Research in identifying volcanic risk usually focuses on a combination of two major components: 1) the range of volcanic hazards that an area is exposed to, and 2) the identification of elements that are vulnerable. Volcanic hazard assessment has traditionally been conducted using a deterministic approach – based on geological and geomorphological investigations, determining the magnitude and frequency of eruptions, and using these to define a maximum impacted area (e.g. Blong, 2000; Scott, 1989). One disadvantage of this method of hazard assessment is that the distribution of deposits and age dating are typically incomplete and may be biased. For example, very significant volcanic hazards (such as ash-surge clouds and volcanic blasts) are not well-preserved in the geological record.

Newer methods developed since the 1990's such as geophysical data obtained from volcanic eruptions and analogue or digital modelling have provided more quantitative parameters to estimate the spatial distribution and properties of tephra, pyroclastic flows and lahars (e.g. Vesuvius, Italy, Spence, et al 2004a; Colima, Mexico, Saucedo et al., 2005). Advances in information technology has also permitted the use of numerical codes coupled with GIS and recently, with viewing platforms (Sheridan et al, 2005).

The second stage of identifying volcanic risk is defining the vulnerability. The study of vulnerability related to natural disasters has been the focus of many different investigations and hence, of several definitions. Westgate and O'Keefe (1976) defined vulnerability as “the degree to which a community is at risk from the occurrence of extreme physical or natural phenomena”, where risk refers to the probability of occurrence and the degree to which socio-economic and socio-political factors affect the community's capacity to absorb and recover from extreme phenomena. However, it is the definition of Blaike et al. (1994), which considers different factors affecting or producing the vulnerability of individuals or groups, which is most relevant. These authors identified vulnerability as “the characteristics of a person or group in terms of their capacity to anticipate, cope with, resist, and recover from the impact of a natural hazard. It involves a combination of factors that determine the degree to which someone's life and livelihood is put at risk by a discrete and identifiable event in nature or society.”

Within the last decade, and particularly in the last five years, research into the impact of volcanic eruptions within the urban environment has become much more advanced. A summary of some of the key studies are presented in Table 1.

City	Hazard	Tools and methods	Results	References
Auckland, New Zealand	<ul style="list-style-type: none"> • Base surge • Lava fountain • Lava flow • Tephra 	<ul style="list-style-type: none"> • Probabilistic tephra dispersal: ASHFALL computer model • Geologic, meteorological and historic observations • Probabilistic Assessment of vent locations (cluster model and various statistics) 	<ul style="list-style-type: none"> • Isomass maps showing tephra fall dispersal and suggested hazards • Probable vent location • Preliminary geological and statistical assessment of risk 	Johnston (1998); Newnham et al. (1999), Wilson & Stirling (2002), Magill & Blong (2005a,b)
Naples, Italy	<ul style="list-style-type: none"> • Tephra • Pyroclastic flows • Tsunamis • Volcanic earthquakes 	<ul style="list-style-type: none"> • Building stock field survey • Analytical and experimental tests • Computer model for simulation runs 	<ul style="list-style-type: none"> • Physical impact of explosive eruptions on urban setting • Human casualty rate and building vulnerability • Structural resistance of buildings 	Spence et al., (2004a,b), Baxter et al., (2008), Neri et al. (2008)
Sao Miguel, the Azores	<ul style="list-style-type: none"> • Tephra • Volcanic earthquakes • Bombs • Pyroclastic-surges/flows 	<ul style="list-style-type: none"> • Field survey: type, condition and damage • Calculations on force on buildings except for lahars • Vulnerability analysis of hazards 	<ul style="list-style-type: none"> • Effects of hazards on buildings/people (casualties) • Risk map of island from effects of hazard on building • Methods to reduce the hazard impact 	Baxter et al. (1999), Pomonis et al. (1999)
Rabaul, Papa New Guinea	<ul style="list-style-type: none"> • Tephra 	<ul style="list-style-type: none"> • Building stock survey • Calculations on tephra loads and strengths of buildings 	<ul style="list-style-type: none"> • Index and categorization of building damage from tephra loads 	Blong, (1994), Blong et al., (2003)
Douala, Buea, Goma, and Limbe, Cameroon	<ul style="list-style-type: none"> • Tephra • Pyroclastic flows • Lava flows • Lahar (small part) • Landslides • Tsunamis 	<ul style="list-style-type: none"> • Identify different hazard components • Elaborate threat matrix by crossing intensity and frequency indices • Mapping the hazards and exposed elements • Vulnerability and risk analysis 	<ul style="list-style-type: none"> • Geological hazard zoning • Qualitative and quantitative inventory of elements at risk • Five risk zoning maps – population, elements at risk, buildings, agriculture, and native environment 	Thierry et al., (2007)

Table 1: Summary of key vulnerability and risk assessments undertaken at volcanoes world-wide. The table highlights the fact that most of the studies have concentrated on the effects of tephra and pyroclastic flows within an urban environment.

Given the evidence from the literature concerning the destructive nature of lahars and evidence of these impacts such as at Herculaneum (Italy, AD79) and Armero (Colombia, 1985), the consequences for buildings and infrastructure from lahars appears not to have been

rigorously examined. Furthermore, good data sets detailing building damage following lahars have not been collected. This lack of information stands in stark contrast to the wealth of data on building damage due to earthquake ground shaking (e.g. Leger and Tremblay, 2009) and the substantial volumes of data on flood (e.g. Kelman and Spence, 2004) and coastal damage (e.g. Reese and Markau, 2002).

Volcanic mass flows (lahars or debris flows and hyperconcentrated flows, flash floods) represent destructive and dangerous phenomena which warrant further study in a vulnerability framework. At present, there is lack of studies into the effect of lahars in dense urban environments - a very real threat for many cities worldwide situated in the vicinity of an active volcano. Furthermore, this impact is greater in developing countries due to the geographical location of urban areas in zones highly susceptible to natural hazards (natural vulnerability), but also due to the various types of economic, social, political and cultural vulnerabilities that exist. As a result of this significant gap in current research an encompassing research project is presented, which has taken into account the physical impacts of lahars on the built environment within a developing country.

1.3 Project aims and specific objectives

The main aim of this research project was to develop a method for assessing hazards and risks from volcanic mass flows (lahars or debris flows and hyperconcentrated streamflows, and flash floods) within an urban environment, using the case study of Arequipa and El Misti volcano in Southern Peru (Fig. 1).

Firstly, the geological hazard components are identified using geological studies (Thouret et al. 1999, 2001), followed by establishment of the eruptive history including magnitude and frequency relationships. The resulting information, along with flow modelling data, is used to characterise volcanic hazard scenarios and to map the volcanic and non-volcanic hazards that potentially affect Arequipa. Identification of the elements at risk was a key part of the research. It was achieved by mapping and identifying everything which is susceptible to the effects of volcanic and non-volcanic mass flows. This includes dwellings, businesses, churches, power stations and bridges etc. within the city centre, along the Rio Chili valley and within the Huarangal district. Distribution of elements at risk combined with geological flow data (expected depth and area), hazard scenarios, and the physical effects of flows on structures form the basis for the GIS maps, which in turn are used to form a risk and vulnerability assessment of Arequipa.

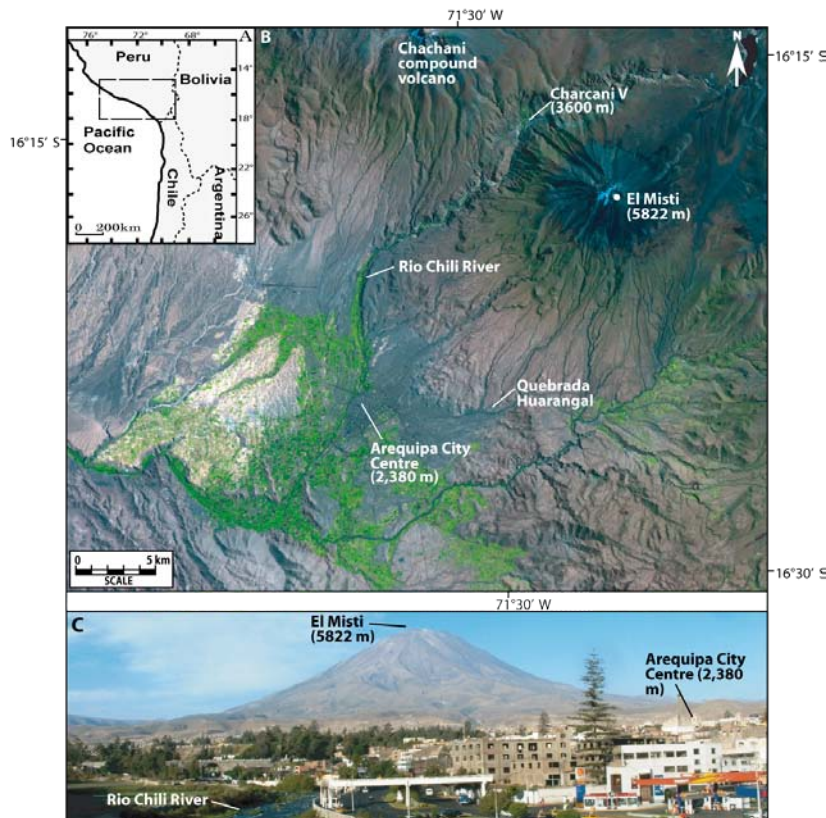


Figure 1 (A): The locality of the study area in South America and in southern Peru. **(B)** Arequipa is situated approximately 17 km the SW of the active El Misti volcano. Increasing population growth has resulted in urban sprawl on the flanks of the volcano and in radial valleys. **(C)** El Misti as viewed from the city centre area of Arequipa adjacent to the Río Chili.

1.3.1 Case study: Arequipa in south Peru – a large city in the shadow of the active El Misti volcano

Much like the city of Naples is to Mt. Vesuvius, Arequipa (southern Peru), with a population of nearly 1 million, is located approximately 17 km SW of El Misti Volcano with suburbs extending as close as 9 km to the volcano (Fig. 1). El Misti's last major eruption occurred 550 years ago, with smaller eruptions occurring during recent and historic times. In addition to geological studies identifying lahar volumes ranging from $0.1 \times 10^6 \text{ m}^3$ to $11 \times 10^6 \text{ m}^3$, floods have occurred historically (at least every 10 years) in the Río Chili and Quebradas (Thouret et al., 2001). Previous workers (e.g., Thouret et al., 2001, Delaite et al., 2005; Stinton et al., 2004; Vargas et al., 2010) have indicated that any volcanic crisis at El Misti volcano will pose a serious threat to the city of Arequipa. Continued development places ever increasing numbers of the city's population at great risk from explosive activity and mass flows. It is therefore imperative that the risk to Arequipa City from volcanic mass flows is identified.

El Misti Volcano

El Misti is one of the eight active volcanoes within the Central Volcanic Zone (CVZ) (Fig. 2); the summit (5824 m amsl.) of which is located 3500 m higher than, and at a distance of only 17 km from the city of Arequipa. El Misti belongs to a group of three volcanoes (with Chachani to the West and Pichu Pichu to the East) which surround the area of Arequipa and its suburbs to the SW as well as Chiguata to the S. The eruptive history of El Misti volcano has been studied by several authors (e.g. Delaite et al., 2005; Thouret et al., 1999, 2001). The stratigraphy of the deposits and maps of erupted products have shown that tephra falls, lahars, pyroclastic flows and debris avalanches underlie the entire city area. It can be inferred therefore, that similar hazards would almost certainly affect Arequipa during future eruptions.

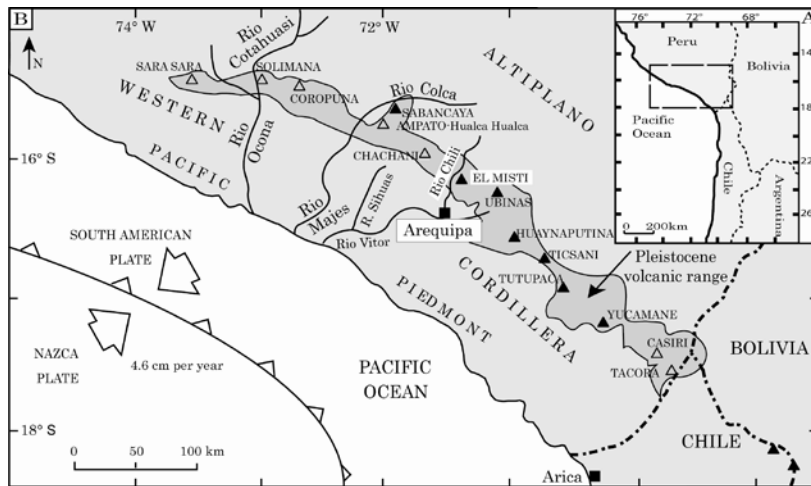


Figure 2 (A): The locality of the study area in South America and in southern Peru. **(B)** Geological setting of the study area highlighting the plate boundary to the west of the Peruvian coastline and the resulting Plio-Quaternary volcanic chain – active volcanoes are shown with black triangles. Adapted from Thouret et al., (2001).

El Misti's eruptive behaviour has been established from the eruptive history of the volcano and from the statistical analysis of dated deposits. A ca. 833,000 year-long evolution of the composite edifice in four stages termed Misti 1 through 4 has been recognised (Thouret et al. 2001). Primary (eruption triggered) and secondary (rain-triggered) lahars have frequently occurred during the Holocene and historical time, even without eruption. The volume of meltwater produced this way may be $\sim 2.5 \times 10^6 \text{ m}^3$ and the volume of the channelled debris flows varies from $\sim 5 \times 10^6 \text{ m}^3$ to a maximum of $11 \times 10^6 \text{ m}^3$.

Hyperconcentrated streamflows also sweep down the five tributaries which cross the city of Arequipa on a 2 to 10-year return interval (Nagata, 1999). These narrow ravines are known locally as quebrada and remain dry for 6 to 9 months a year, but feature occasional torrential streams. On 25 February 1997 flash floods triggered by 33.4 mm of rainfall during a three-hour period, transformed into hyperconcentrated streamflows and claimed three victims in the Quebrada Mariano Melgar.

Arequipa City

Arequipa is the second largest city in Peru, with a population exceeding 860,000, and resembles the city of Naples in Italy, where more than 600,000 people are exposed to Vesuvius volcanic activity. Arequipa has experienced rapid population growth since the 1940s, after which population multiplied by a factor of 5 (Fig. 3). From 1970 onwards the urban area grew due to social unrest and related migration from poor rural areas. In 45 years (1970–2005) the built up area grew from 13 km² to roughly 60 km². The current extension of the city's built up area is 400% larger than it was in the 1960's. Settlements have now expanded onto the southwest flank of the volcano, the Río Chili Valley terraces and on terraces or fans adjacent to tributaries within 9 km of El Misti summit. The small town of Chiguata is located on the Southern flank of the volcano, where 3,000 people live at 11 km from the summit.

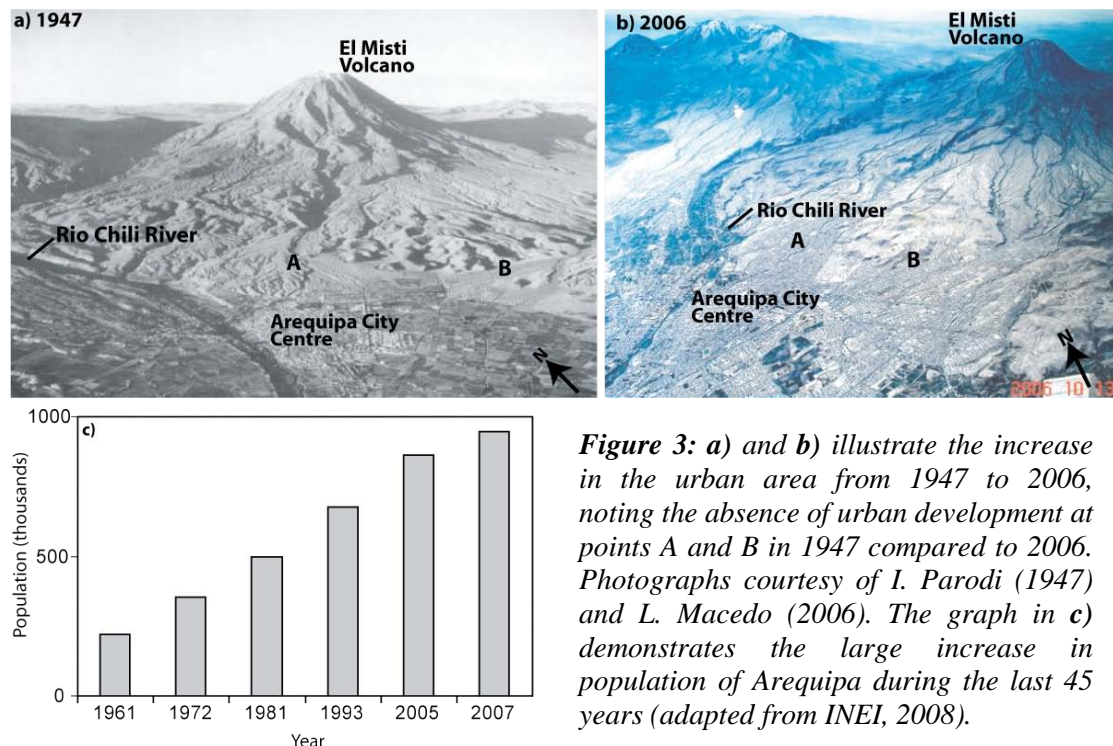


Figure 3: a) and b) illustrate the increase in the urban area from 1947 to 2006, noting the absence of urban development at points A and B in 1947 compared to 2006. Photographs courtesy of I. Parodi (1947) and L. Macedo (2006). The graph in c) demonstrates the large increase in population of Arequipa during the last 45 years (adapted from INEI, 2008).

With the city expanding into more hazardous prone areas it is necessary to assess the vulnerability of buildings and infrastructure in response to the threat posed from volcanic mass flows. On the basis of geological and geomorphological studies, Thouret et al. (2001) pointed out that the urban areas most likely to be struck by pyroclastic flows and lahars are located along the Río Chili as well as two main drainage systems that originate on the upper slopes of the volcano and cross the centre of the city: Quebrada San Lázaro and Quebrada Huarangal.

1.4 Summary

The information above highlights the significant hazards, particularly of volcanic mass flows posed to Arequipa – a major tourist destination in the Peruvian Andes featuring monuments and colonial architecture classified with UNESCO World Heritage status (more than 1 million people visited Arequipa in 2008 alone; INEI, 2008). Previous authors have studied the eruptive history of El Misti, defined the volcanic hazards and made progress towards a vulnerability and risk assessment of the city (e.g. Delaite et al. 2005; Stinton et al. 2004; Thouret et al. 1999, 2001; Vargas et al. 2010). However, further research is necessary, and undertaken within this research project, to precisely delineate areas that could be affected, to map the elements at risk, and define the impact magnitude upon the elements at risk. Another vital need is to evaluate the risks in Arequipa from volcanic mass flows in order to assist the authorities in managing urban development and to make decisions on prevention and elaborate emergency plans in case of disaster. This case-study of Arequipa presents an opportunity to research the effects of mass flows in the urban environment – something that is being faced in large cities at volcanoes world-wide (e.g. Kagoshima, Japan; Quito, Ecuador; and Naples, Italy).

2. Methods

2.1 Introduction

This research combined a number of techniques in order to define the physical vulnerability, namely of buildings and infrastructure, in urban areas threatened by lahars and flash floods. The following flow chart (Fig. 4) shows the approaches undertaken in this research project to establish the risk from lahars in a dense urban environment.

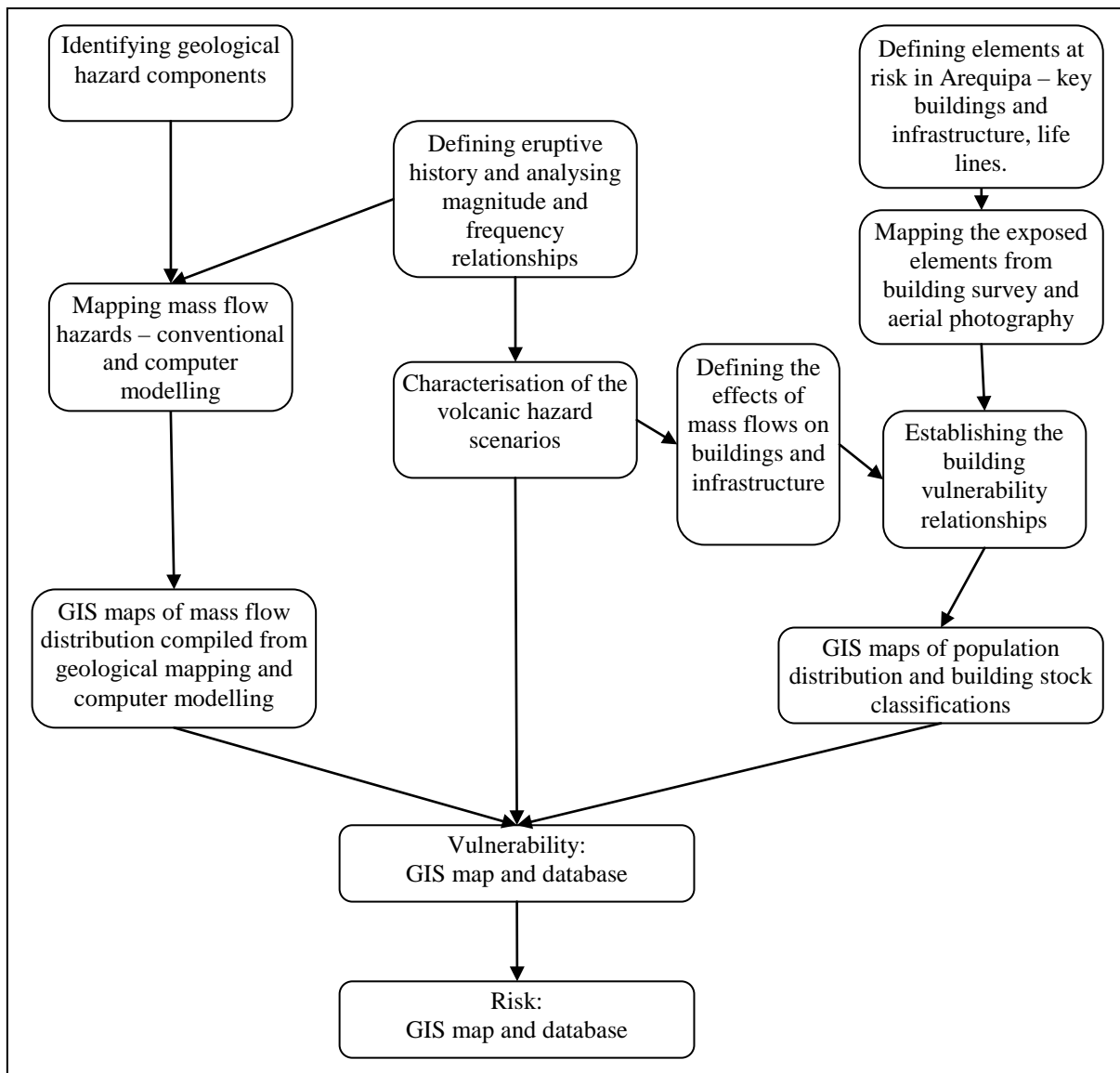


Figure 4: An outline of the processes undertaken to construct a quantitative vulnerability and risk assessment of the city of Arequipa facing volcanic and non-volcanic mass flow hazards.

Using the case study of Arequipa, Peru, vulnerable areas were identified from former and current geological studies; conventional and computer-aided mapping of volcanoclastic and fluvial deposits; numerical flow modelling (Titan2D); field surveys of buildings and infrastructure; statistical analysis including multivariate analysis for the building and infrastructure surveys; GIS; and geotechnical characteristics of building materials (including mechanical tests). These methods are discussed further in their relevant subject areas (i.e. 3.0

Mass flow hazards from El Misti, 4.0 Modelling lahars using Titan2D) with reference to the presented results.

2.2 Study areas

Three areas in and around Arequipa were chosen for this study (Fig. 5): 1) the area around Charcani V hydroelectric power station in the upper Río Chili Canyon, 2) the Río Chili Canyon from the opening of the canyon into cultivated terraces, to the southern boundary of the city and 3) the Quebrada Huarangal fan to the east of the city centre.

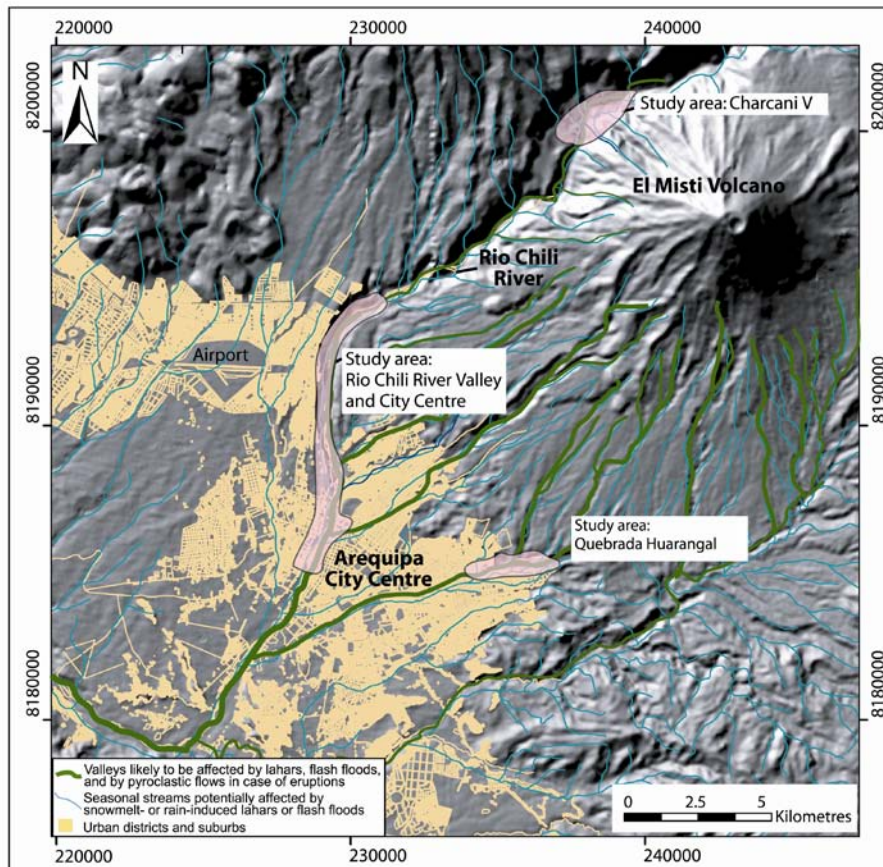


Figure 5: *El Misti mass flow hazard-zone map showing areas likely to be affected by lahars and flash floods during eruptions, and seasonal streams potentially affected by snowmelt- or rainfall-induced lahars or flash floods (based on Thouret et al., 2001 and Delaite et al., 2005). Areas chosen for this project are highlighted.*

The area of Charcani Quinto in the Río Chili canyon

This area is located approximately 19 km upstream of Arequipa City centre and approximately 5.8 km from El Misti's vent, at an elevation of 2990 m (UTM location 238113, 8200820) (Fig. 5). Within this locality is Charcani Quinto, one of six EGASA hydroelectric stations built on the Río Chili to supply power to the national grid and to supply most of the potable water to the city. An exclusive military school, which controls access in and out of the area, is situated on a middle terrace on the western side of the river. The lower terraces on both sides of the river have been cultivated for agriculture, while rural housing and agricultural storage facilities also exist within the area.

An extensive lacustrine deposit of approximately 6-8 m in thickness outcrops on the eastern side of the river; just to the south of the Military school. The extensive and thick lacustrine deposits provide evidence that a large body of water existed here for some time. Pyroclastic and debris flows deposits within this locality provide evidence that these eruptive deposits

could have dammed the Río Chili. Also, non-eruption related mass movements from the very steep and actively eroding NWN flanks of El Misti could have dammed the Río Chili to form a lake. Although no evidence of dam-break flood deposits have been discovered downstream, a mud-line and flood cobbles visible at least 10 m high above the channel can be seen at the entrance of the canyon. While this is not related to the flood event, it is an indication of how powerful floods can get within this narrow (<0.5 km) and deep (0.5 – 1 km) canyon. The occurrence of the lacustrine deposit at Charcani Quinto presents an interesting and potentially devastating scenario for future hazards from El Misti. A dam-break flood scenario is important to consider when assessing the vulnerability of the city of Arequipa to mass flows.

Alluvial valley of the Río Chili

From the southern entrance of the Río Chili canyon (232116, 8194785) to the southern boundary of the city centre (229410, 8187365), approximately 9.5 km in length and covering an area of 7 km², is the site of this study area (Figure 5). At the entrance of the Río Chili Canyon, the river is no longer confined by sheer ignimbrite cliffs but by the valley walls extending into a series of terraces bordering the river – a valley width of 500 m to 1500 m (Fig. 1.2). The point at which the flow is no longer confined by the canyon walls is important in terms of flow behaviour and thus is of interest for simulations presented in this study and future volcanic flow hazards in this locality.

From this point the valley becomes wider, encompassing many heavily cultivated terraces of valuable arable crops. Further south, the agricultural land disappears to make way for urbanisation in the form of houses, commerce, industries (e.g. Egasa main power station), sports clubs, infrastructure and churches etc. The prominent land-use type from the north of the study area to the south changes dramatically and represents a diverse cross-section of the Arequipeño lifestyle. There are three main motives to study this valley (Fig. 5): 1) previous geologic and geomorphological studies of Holocene and historic lahar, hyperconcentrated flow and flash flood deposits and processes along this channel and terraces, 2) the proximity of the city with respect to the river channel, and including buildings, infrastructure, economic centres, farmland and people, and 3) the importance of the Río Chili for Arequipa, by providing water and power generation, irrigation for agricultural land and tourism.

Quebrada Huarangal volcaniclastic fan

The Quebrada Huarangal volcaniclastic fan, with an area of approximately 3.5 km², is represented by dense, low income housing – some of which are constructed within the channel itself (UTM: 235916, 8185133; Fig. 5). The area is of particular interest because overbanking was observed in this locality in previous Titan2D flow simulations (Stinton et al., 2004a). Previous work has also identified this area as one of the main drainage and fan systems, along with Quebrada San Lazaro, that could be affected by a lahar (Thouret et al. 2001).

The study area included the channel and terraces of the Quebrada Huarangal fan starting from a quarry upstream and ending at the downstream bridge of ‘8 de Octubre’. The channel geometry changes and becomes narrower downstream due to channel incision into hard rock, ignimbrite or lava flow. This contrasts with the wider channel upstream which is cut into alluvial and volcaniclastic deposits. To the north of the channel hummocks are formed in subdued debris-avalanche deposits. Where the wide channel (varying from 100-500 m across) becomes confined to a very narrow artificial channel (less than 10 m across), floods and lahars may become constricted and overtop the banks. Furthermore, flow here will

accelerate causing an associated increase in its erosive power. Observed overbanking in the Titan2D simulations was also due to the low (<4 m) bank margin of the Huarangal valley near the fan, and to the south.

Discarded household and industrial waste, vegetation, building materials, and the mining of alluvial material within the channel itself, will be a source of bulking for potential flows. In addition, Quebrada Huarangal represents a much poorer socio-economic group than that of the Río Chili Valley. Houses are of poorer quality and those with the lowest quality have been built within the Quebrada channel itself. The Quebrada Huarangal fan study area provides an interesting land-form upon which to model volcanic flows. The quality, density and location of housing are in contrast to those in the Río Chili Valley, and will provide an interesting comparison of the effects, vulnerability and risk of different areas within Arequipa to volcanic mass flows.

The methods used in this research have allowed for a multi-faceted study which in particular highlights the capabilities and limitations of diagnostic tools such as GIS and Titan2D in the application to the assessment of volcanic hazards, vulnerability and risk.

3. Mass flow hazards from El Misti

3.1 Introduction – type, magnitude and frequency

The type, magnitude and frequency of mass flows generated from El Misti were compiled from the literature (e.g. Thouret et al., 1999, 2001) and from dated deposits. The main depositional units in each Misti stage along with the date, thickness and extent, dominant type of activity at the time of eruption, the corresponding VEI rank and an estimate of the eruptive frequency, were determined. The analysis of the data showed that mass flows have featured fairly frequently in the geological history of this volcano. Eruptive and post-eruptive lahars/mass flows were formed during the last significant eruption of El Misti in the fifteenth century (AD 1440-1460) when a Vulcanian eruption resulted in tephra 5-10 cm thick blanketing the city (Thouret et al., 2001). Furthermore, debris flows with an estimated volume of 1.5 to 3 million m³ were deposited in the Rio Chili valley and Quebrada San Lazaro. Additionally, lahars have swept down the Rio Chili valley and tributaries approximately 1,000 yr BP, 500 yr BP and as recently as the 1700s (Thouret et al., 2001).

Lahars were formed during and following the major Plinian eruption of c.2030 yr BP. The collapse of a c.21 km-high eruption column produced lithic and pumice-rich pyroclastic flows 1.1 km³ in volume (Thouret et al., 2001; Cobenas et al., 2011). Pyroclastic-flow and debris-avalanche deposits were transformed into lahars which flowed in the Rio Chili valley and in quebradas surrounding the volcano (e.g. 2030 yrs BP-old debris-flow deposits in the Río Chili valley and Quebrada San Lazaro). Dome growth and subsequent collapse during Misti stage 3 led to the formation of block-and-ash and pyroclastic flows, depositing sediment several metres thick down many valleys surrounding the volcano (e.g. Misti 3-3, ca. 21,000 to 20,000 yrs BP and Misti 3-2, ca. 30,000 to 25,000 yrs BP). Volcaniclastic sediment and melt water from ice fields that capped Misti during the second glacial maximum (ca. 25,000-20,000 yrs BP) also generated mass flows (Thouret et al., 2001). Reworked tephra, debris flow and stream flow deposits (>14,000 yrs BP) are several metres thick in upper radial valleys of Quebradas Huarangal and San Lazaro.

The volcano has also experienced some particularly large events; ignimbrites deposits (e.g. 34,000 yrs BP, 25,000 yrs BP and 14,000 yrs BP) can be found at least 15 km from the crater, and pyroclastic-surge deposits up to 11 km to the south (Thouret et al., 2001). Calderas were formed between 50,000 to 40,000 yrs BP depositing ignimbrites with a volume of 3-5 km³ to the south-east, south and south-west of the volcano. It was during this time period that hydromagmatic interactions occurred, generating lahars.

Debris avalanches feature in the geological history of this volcano (e.g. during Misti stages 1 and 4). A frightening scenario is the formation of a lake due to waterway blocking by debris avalanche. The result of this could lead to sudden dam bursts where voluminous mass flows could be generated. While no evidence of dam-break flood deposits have been discovered as yet, lake deposits are present in the upper Rio Chili canyon presenting the possibility of dam-break flood generation. Mass flows can also be generated from debris-avalanche deposits, given sufficient water availability.

The voluminous eruptive deposits (e.g. Plinian pumice-fall deposit, ca. 21-20,000 yrs, up to 3 m thick 13 km from the vent) provide evidence for an adequate debris source for mass flow formation, not only during the eruptive period but also many years or decades later. Snow meltwater or rainstorms can bulk loose volcanoclastic sediment on the slope of the volcano or in channels generating mass flows. Generation is dependent on water availability however, snow cover is not permanent at El Misti and rain storms only occur from December to March. Nevertheless, the snowfield can cover an area of up to 7 km² in August or between December and May, with an estimated volume of 2.5 million m³ (Delaite et al., 2005). Furthermore, rainstorms with intensities greater than 10 mm per hour are common between December and March and can trigger flash floods and hyperconcentrated stream flows.

This geological and recent history provides many credible scenarios for mass flow generation during a future eruption of El Misti.

3.2 Determination of hazard scenarios for lahars, dam-break and flash floods

The hazard scenarios proposed by Thouret et al. (2001), Delaite et al. (2005) and Vargas et al. (2010) cover the range of mass flows generated by eruptive processes and rainstorms/snowmelt. Vargas et al. (2010) proposed three scenarios which directly related to lahar generation: 1) non volcanic, small to moderate size and frequent (2 to 10 years); 2) moderate and probable (300 to 1000 years), even if a small eruption; and 3) large but infrequent (1000 to 5000), with a large eruption. However, given the lacustrine deposit present in the upper Rio Chili canyon, a scenario for a dam-break flood must be considered – triggered by an eruption, an earthquake or a landslide. Little is known about the recurrence interval for these events but as discussed in previous sections Arequipa is threatened by lake breakouts originating in the upper Río Chili canyon.

The volumes and recurrence intervals of the scenarios proposed by the other authors have been validated against the data gathered, compiled and analysed for this research project. In addition the scenario for a dam-break flood has been added. The scenarios for lahars and floods are presented in Table 2.

Scenario for mass flow generation		Minimum volume (x 10 ⁶ m ³)	Maximum volume (x 10 ⁶ m ³)	Recurrence interval (years)
Eruption triggered	Non eruption triggered			

1	Small to moderate size frequent floods	0.01 to 0.1	0.1 to 0.5	1.2 times/10 years	
2	Moderate size lahars, probable during small eruption	Moderate to very large size, infrequent floods	0.5 to 1.5	1.5 to 4.0	>50 to 300
	Large but infrequent lahars, generated by large eruption		4 to 9.0	9 to 11	>100 to 2 000
4	Very large lahars but very infrequent generated by large eruption		11 to 15	15 to 30	5,000 to >10,000

Table 2: The scenarios for lahar and flash flood generation in Arequipa. Scenarios 2-4 also consider the formation of a flow from a dam-break flood scenario. Adapted from Vargus et al. (2010).

Scenario 1 relates to small to moderate volume frequent floods, which are generated by heavy rainfall and/or snowmelt, such as the floods in 1989, 1997 and 2011. For the generation of moderate to very large floods, *scenario 2* would involve exceptional rainfall. Scenario 2 also relates to moderate sized lahars produced during a small eruption, such as the AD 1440-1470 vulcanian events where the VEI is 2. *Scenario 3* accounts large lahars that are produced during a moderate magnitude eruption (i.e. VEI 3) such as the ca. 2030 yr BP-old sub-Plinian explosive episode; and *Scenario 4* lahars are very large and generated based on an eruption resembling the 34,000-30,000 year-old or the 13,000-11,000 year-old ignimbrite-forming eruptive episodes (VEI >3).

The dam-break flood is more likely to correspond with the flow volumes of scenarios 2 to 4 – 4 to 47 x 10⁶m³. The recurrence interval is harder to define due to the lack of knowledge of these events at El Misti, but is likely to occur because of a 1) a deep and narrow canyon; 2) active faults and 3) debris-avalanche deposits are present at El Misti.

3.3 Hazard-zone maps

Hazard zone maps were created for the Rio Chili valley and the Quebrada Huarangal fan based upon the geological and historical history, terrace maps and developed hazard scenarios for floods and lahars (Figs. 6 and 7). A high hazard class was assigned to the terraces where deposits from frequent and low magnitude events (i.e. Scenario 1) were mapped. Similarly very large and very infrequent events, representing the upper terraces, were given a very low hazard class. Even though the events of a very low hazard class are of an exceptional magnitude, they are very infrequent (5,000 to 10,000 years) and thus are less hazardous to the population at a smaller time-scale, when compared to much more frequent (2 to 10 years) smaller magnitude events.

Figure 6: Mass flow hazard map for the Rio Chili valley based upon field mapping, geological and historical data, and terrace maps. Image from Google Earth.

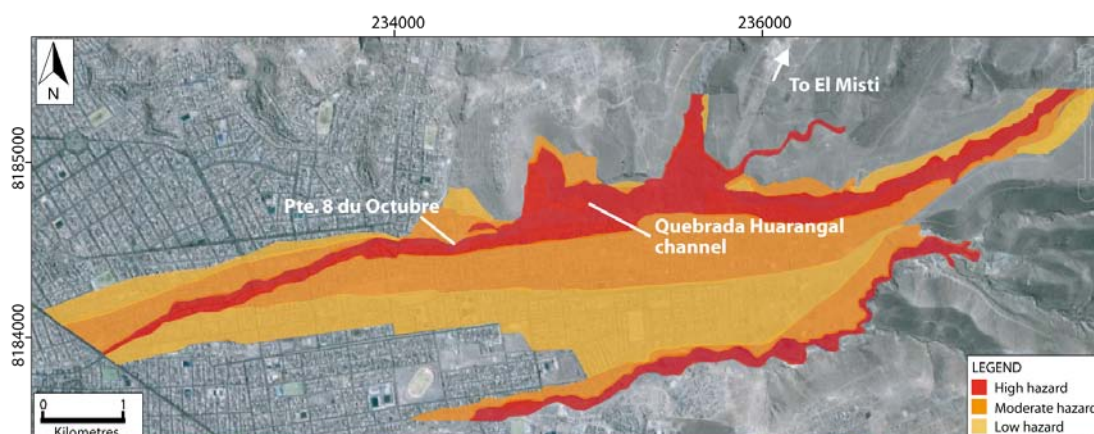
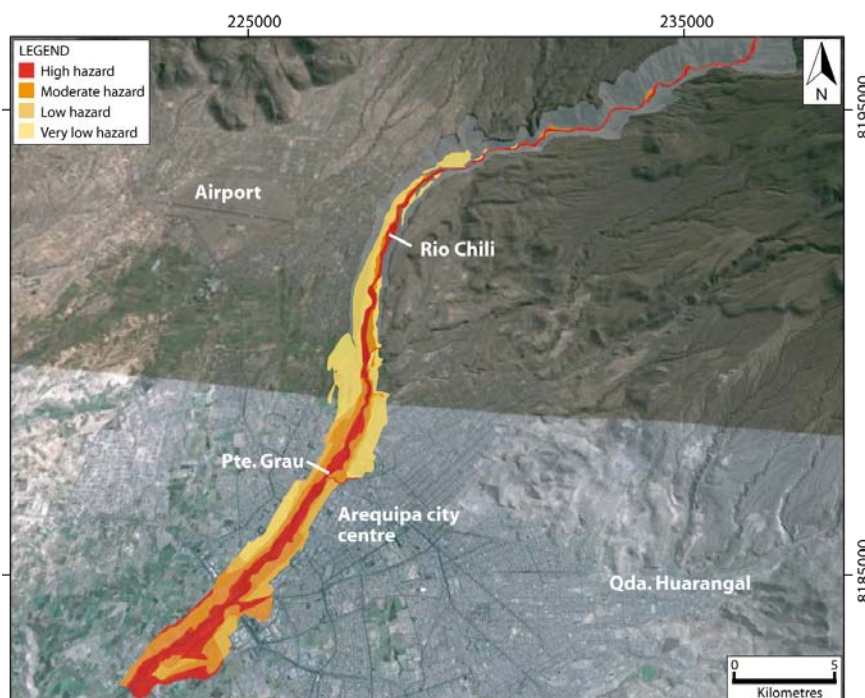


Figure 7: Mass flow hazard map for the Quebrada Huarangal fan based upon field mapping, geological and historical data, and terrace maps. Image from Google Earth.

The hazard zone map for the Rio Chili Valley highlights greater *high hazard* areas to the south of the city centre than higher up in the fluvial system. The gradient in this region has decreased sufficiently for deposition, 2.5% slope gradient across the most populated area, and the topography is more subdued. This has considerable implications in that the areas of highest hazard are confined to the most populated areas along the Rio Chili. Historical accounts of smaller magnitude ($0.01-0.5 \times 10^6 \text{ m}^3$) but frequent (2 to 10 years) mass flows in the Rio Chili have described flooding to be more pronounced in the city centre where banks are overtopped and retaining walls fail, but also where flatter, widespread farmland is located at the southern extremity of the city. In the upper river the flows are more confined and therefore by nature less hazardous.

The highest hazard on the Quebrada Huarangal fan represents frequent low magnitude mass flows (e.g. flash floods of 1997 and 2011) which inundate the modified channel bed and the lowermost terraces t0 to t1. Of deep concern is that the poorest quality and most vulnerable housing occupy the highly hazardous channel bed itself. Wide flat terraces (t0 – t1') which

represent moderate and low hazard classes occupy the land to the south of the channel bed; these areas are the most densely populated in the area. However, in general, the quality of building is superior to that located within the channel bed.

3.4 Summary

Based upon geological and historical evidence mass flows will be generated from El Misti regardless of an eruption (e.g. during an eruption, seismic crisis, and/or no unrest) if a sufficient rainfall threshold (>15 mm/hr) and/or snowmelt conditions are reached. In addition, a dam-break flood scenario is plausible as suggested by dammed-lake deposits forming a 15 m-high terrace in the upper Rio Chili canyon. Debris avalanches and rockslides occurring on the steep slopes of the WNW flank of El Misti's cone, where an active fault is located and new seismic activity has been recorded at a shallow depth since 2005, are capable of blocking the narrow canyon, leading to lake formation.

The results clearly highlight that floods and lahars, even if moderate in magnitude will affect Arequipa. The most vulnerable populations are located within the most hazardous zones, with urban expansion leading to an increasing number of people inhabiting the highly hazardous areas. In addition essential infrastructure (e.g. the hydroelectric power system of five dams located in the upper Rio Chili canyon) is located within the canyon and the failure of such could have dire consequences to the population of Arequipa (e.g. no electricity or clean drinkable water supply).

4. Modelling lahars using Titan2D

4.1 Introduction

The computational modelling of mass flows has become an important tool in volcanic hazard assessment; numerical simulations help to assess quantitatively the rheological behaviour of flows, improve estimations of run-out distances, and to delineate expected inundation zones (Sheridan et al., 2005). Many different flow models exist (e.g. Flow2D, DAN, Flo-2D, VolcFLOW) and have been used with varying degrees of success to delineate hazard zones at volcanoes throughout the world. El Misti volcano is no exception; mass flow inundation zones have been further refined on El Misti's flanks, ring plain, and in the city of Arequipa with the aid of computational modelling. LaharZ (Schilling, 1998) was used by Toyos (2000), Van Gorp (2002), Delaite (2003) and Delaite et al., (2005) to identify areas prone to lahar inundation in the Río Chili Valley, and the Quebradas San Lazaro, Huarangal and Agua Salada. Stinton et al., (2004a) compared the LaharZ results obtained by Delaite (2003) with Titan2D single phase (Patra et al., 2005) simulations. Vargas et al., (2010a) took the research further by using the two-phase Titan2D model (Pitman and Le, 2005) to simulate lahars and compare the results with LaharZ simulations obtained by Delaite (2003).

Stinton et al., (2004a) and Vargas et al., (2010a) noted several differences between the results from the two models including: 1) LaharZ run-out distances were consistently longer than those achieved in Titan2D simulations, for example even the largest volume Titan2D flows ($11.0 \times 10^6 \text{ m}^3$) did not extend further than the smallest volume ($1.5 \times 10^6 \text{ m}^3$) LaharZ simulated flows; 2) common flow features that are present in reality, such as superelevation on river bends, overbanking on low relief fans and flow divergence and convergence around

hills or terraces, were observed in Titan2D simulations but not with LaharZ; and 3) Titan2D simulations reacted to the underlying topography, for example where changes in the slope and channel occurred, more faithful to topographic variations than did the LaharZ simulations. The discrepancies in the results are due to the underlying differences between the two models – LaharZ is a statistical and semi-empirical code, whereas Titan2D takes into account the physical aspects of lahar flow.

Little research has been conducted at El Misti using the Titan2D “two-phase” model; based on recognised and accepted flow physics and successful in modelling other two-phase flows such as lahars at Mt. Ruapehu, New Zealand (e.g. Procter et al., 2010a) and Cotopaxi Volcano, Ecuador (Williams et al., 2008). Consequently, this research utilised the Titan2D “two-phase” model for the delineation of lahar hazard zones at El Misti, and also to investigate the effect of DEM resolution on the simulations. Titan2D is a depth-averaged model for an incompressible Coulomb continuum, a “shallow-water” granular flow suitable for simulating a variety of geophysical mass flows. Conservation equations for mass and momentum are solved with a Coulomb-type friction term for the interactions between the grains and between the granular material and the basal surface. For a more detailed description of the model relationships the reader is referred to Patra et al., (2005) and Pitman and Le, (2005).

4.2 New Titan2D simulations undertaken on El Misti Volcano

Simulations were performed on a 30 m DEM, based upon digitised 1:25,000 scale topographic maps and on radar interferometry (Delaite, 2003) using expected flow scenario volumes ranging from $0.01 \times 10^6 \text{ m}^3$ to $11 \times 10^6 \text{ m}^3$, down the Río Chili Valley and Quebrada Huarangal. Successive runs of Titan2D were conducted varying the input parameters (e.g. starting point, internal and bed friction angles, and solid fraction) in order to constrain the simulations. The input parameters were calibrated against historic and geologic evidence of past events, and by examining the impact of flow features.

Once the model had been constrained successive runs of different volume flows were made on an enhanced resampled 10 m DEM, based upon DGPS points and an 30 m ASTER DEM, in order to define run-out zones for typical flows. These run-out zones then in-turn define areas that are most likely to be inundated during future mass flow events. A summary of input parameters is shown in Table 3.

Input parameter	Value
Internal friction angle (°)	20-30
Basal friction angle (°)	8-25
Solid ratio	0.4-0.7
Volume ($\times 10^6 \text{ m}^3$)	0.5, 1.5, 4, 9, 11

Table 3: Input parameters used in Titan2D two-phase. Basal and internal friction values were chosen based on previous work using Titan2D simulations (Sheridan et al. 2005) and from the literature (e.g. Pierson, 2005). In addition, the basal friction angles are within range of values often used for glacial and fluvial deposits (Stinton et al. 2004a). Solid fraction covers the range of values that define hyperconcentrated flows (e.g. Pierson, 2005).

4.2.1 Input parameters

Starting point

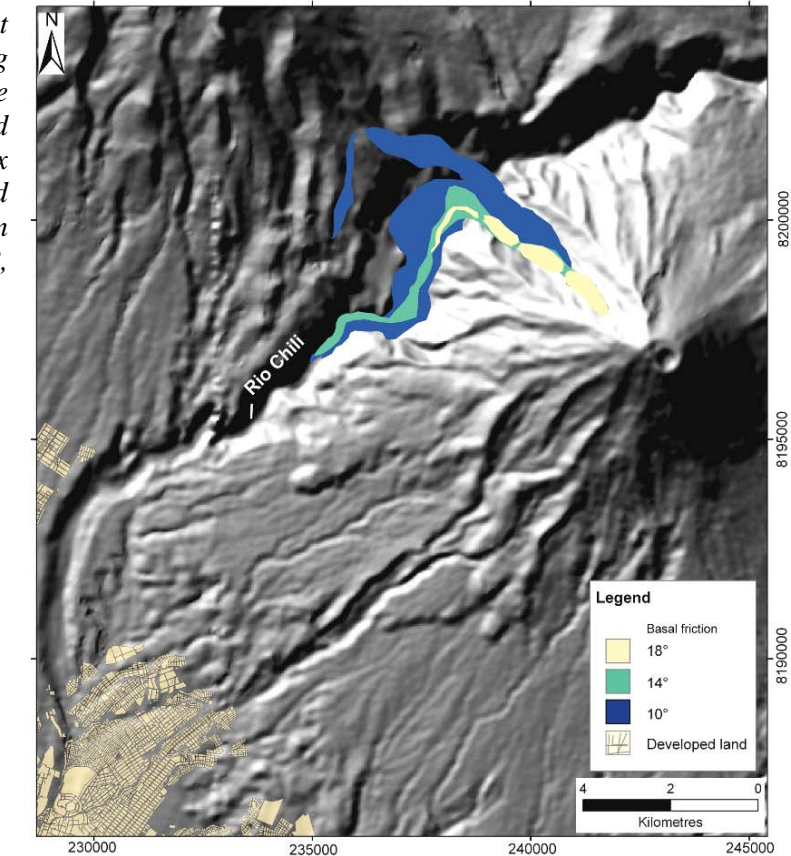
The starting point is where the central point of the initial material pile is located. The starting point can be selected either by applying the energy cone relationship (e.g. Delaite et al., 2005), or by taking into consideration the dimensions and dynamics of the drainage channel and local slope conditions that could lead to the initiation of a volcanic mass flow (e.g. Stinton et al., 2004a). For this study a catchment analysis was performed using ArcGIS (e.g. Procter et al., 2009) where catchments were identified based on channel morphology and the slopes angle. Two points were identified for each catchment; the centre point, which corresponds to the break in slope, and the upper point which is the top of the catchment. The upper and central starting locations for both channels were explored in Titan2D; however the centre point, or the break in slope, was considered more likely to be the point at which flows would initiate. This is because above the break in slope, the slope is too steep for the significant accumulation of loose material.

Friction angles

Friction angles (internal and basal friction) are one of the more important input parameters in Titan2D modelling because they control the acceleration and velocity of the moving mass and also allow a subtle control on the lateral spread. Approximately 200 simulations were run using a constant initial volume and location with every possible combination of internal and basal friction parameters (where appropriate) at intervals of 2° (Table 3). The best results were obtained using internal friction angles between 25°-33°. This is close to the angle of repose of typical El Misti Volcano debris flow sediment (gravel – coarse sand) on the cone, and is consistent with values used by other authors (e.g. Stinton et al. 2004b; Procter, 2009) in a variety of volcanic settings for debris flows and pyroclastic flows.

The simulations are highly sensitive to the basal friction value (Fig. 8). The best results were found using angles between 8-12°. Extremely low basal friction values (<8°) resulted in flows that accelerated rapidly and unrealistically down slope. In addition, low basal friction values resulted in the simulated flow 'unrealistically' flowing up the canyon wall near the military school. While debris flows have deposited within this locality, they have not flowed this far up the canyon wall. Debris avalanches worldwide also show that the lower the basal friction angle the further the distance travelled (Hayashi and Self, 1991). At the opposite end of the spectrum basal friction values of greater than 18° resulted in flow run-outs less than 1 km from the initial starting location. As a result of the repeated simulations, varying the basal friction angle, a basal friction angle of 12° was used in the final simulations on an enhanced 10 m DEM of the region. The range of basal friction values determined in this study are consistent with angles used by other authors (e.g. Williams et al., 2008; Procter et al., 2009) for lahars.

Figure 8: Simulations carried out with Titan2D on a 30 m DEM using the Río Chili flow scenario. The basal friction value was varied using a constant flow volume of $4 \times 10^6 \text{ m}^3$, internal friction of 25° and solid ratio of 0.4. The basal friction angles that were used are 10° , 14° , and 18° .



While the range of basal friction values determined for this study correlate well with previous studies and with aspects of the topography, one value cannot be viewed as representative of the changes in basal friction experienced along a flow path. The addition of a material map, derived from geotechnical and geological maps of the region, would be highly recommended for further research into Titan2D simulations at El Misti.

Solid ratio

Sediment concentration plays an elementary role in flow behaviour and mechanics (Iverson, 1997; Pierson, 2005), and is an important parameter in the Titan2D “two-phase” model. Water floods normally transport mostly fine sediment and in relatively small quantities – containing generally less than 4% by volume (vol.%) or 10% by weight (wt.%) suspended sediment (Pierson, 2005). In contrast, high-discharge debris flows (and/or mudflows) may transport more sediment than water with sediment concentrations in excess of 60 vol.% (80 wt.%) (Pierson and Costa, 1987). A hyperconcentrated flow is often applied to intermediate flows. However these values cannot be regarded as definitive because the solid concentration is highly variable even within one debris flow event and along the path of the propagating flow, other criteria such as grain size and the physical characteristics of the material play a part (Dumaisnil et al. 2010). This is one aspect, a varying sediment concentration, which cannot be altered in Titan2D.

The appropriate solid fraction for El Misti lahars was determined from a literature review and from geological and historical evidence. Field studies at El Misti suggest that lahars are characterised more as hyperconcentrated flows and therefore represent the lower to middle end of the debris-flow scale (e.g. Thouret et al., 2001; and Vargas et al., 2010a). It was found that a solid fraction of between 0.4 and 0.5 was adequate for modelling of lahars at El Misti.

Flow volume

The volume of material used in this study corresponds to flow volumes derived from geological studies, and from volcanic events and hazard scenarios described for El Misti volcano based on the magnitude and frequency of events (Thouret et al. 1999; Stinton et al., 2004a; Delaite et al. 2005; Vargas et al., 2010a; and this study).

DEMs

Previous studies have shown the importance of DEM resolution on computational routines for reconstructing different paths, velocities and extents of various flows, and for correctly estimating the areas and levels of hazards associated with future volcanic activity (e.g., Stevens et al. 2002; Pitman et al. 2003). Prior DEMs used at El Misti were of low resolution which could be a factor in the subsequent ‘unrealistic’ results. To investigate the effect of DEM accuracy on simulated results an enhanced DEM was computed using Differential GPS and ASTER data and compared to a pre-existing 30 m DEM (Delaite et al., 2005) (Fig. 9).

Detailed topographical data was acquired during a DGPS survey of an area of ~12 km² in 2007 and 2008. After post-processing the DGPS points, a DEM was created by interpolating (kriging) ASTER 30 m data with ~50,000 DGPS points. This was then resampled at 10 m to create an enhanced DEM for Arequipa. Merging the DGPS data with the ASTER data was a necessary step for two reasons. Firstly the DGPS data did not cover the entire study area and secondly, the ASTER data does not accurately represent river channels and terraces due to poor resolution in the 30 m DEM. Merging the data allowed for potentially more accurate simulations. The decision to use the ASTER DEM over other DEMs is twofold, 1) the ASTER DEM represents the best resolution publically accessible DEM, and 2) it is more accurate than the 30 m DEM of Delaite (2003) (Fig. 9).

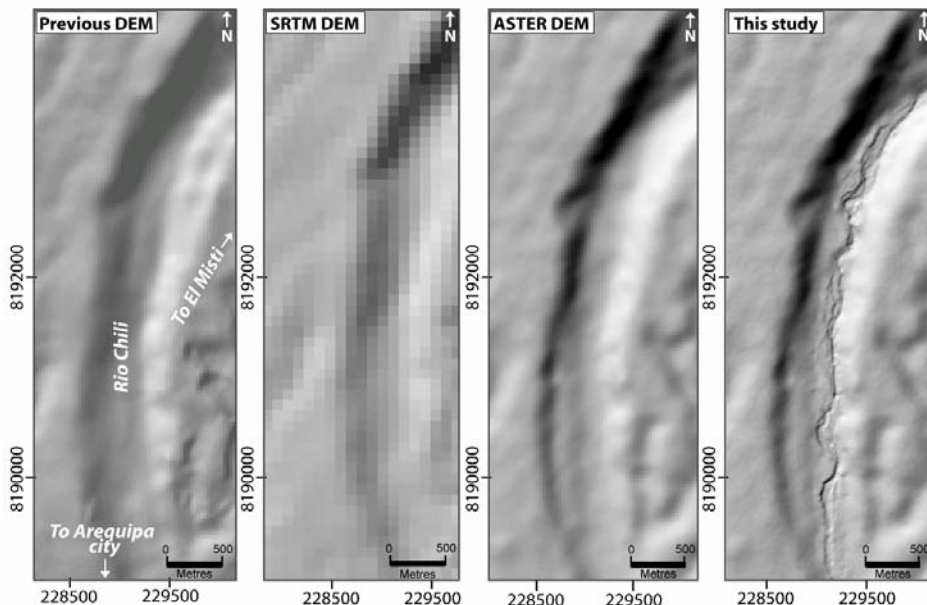


Figure 9: Comparison of DEMs using a subset of the Rio Chili Valley. The previous DEM was used for earlier Titan2D simulations and is similar in resolution and detail to the ASTER DEM. The 90m SRTM DEM has a very coarse resolution. The new enhanced DEM can be seen clearly as an improvement over other DEMs of this region.

4.2.2 Implication of different DEMs on Titan2D simulations

Comparisons of simulations using the differing DEMs are shown in Figure 10. Simulations using constant input parameters (internal friction angle of 25° , a basal friction angle of 12° , a solid ratio of 0.40 and volume of $11 \times 10^6 \text{ m}^3$) were undertaken on the previous 30 m and the enhanced 10 m DEMs. Topography differences clearly affect the run-out and inundation area of simulated flows – simulations undertaken on the 10 m DEM feature longer run-out than those of the 30 m DEM. Furthermore, the 10 m DEM resolves earlier issues encountered with the 30 m DEM where flows tended to pond in the Río Chili upper canyon, a location where the width of the channel is confined by sheer cliffs (at least 500 m high). The increased resolution of the 10 m DEM has allowed simulated flows to move through the canyon featuring less unrealistic ponding, resulting in longer run-out lengths.

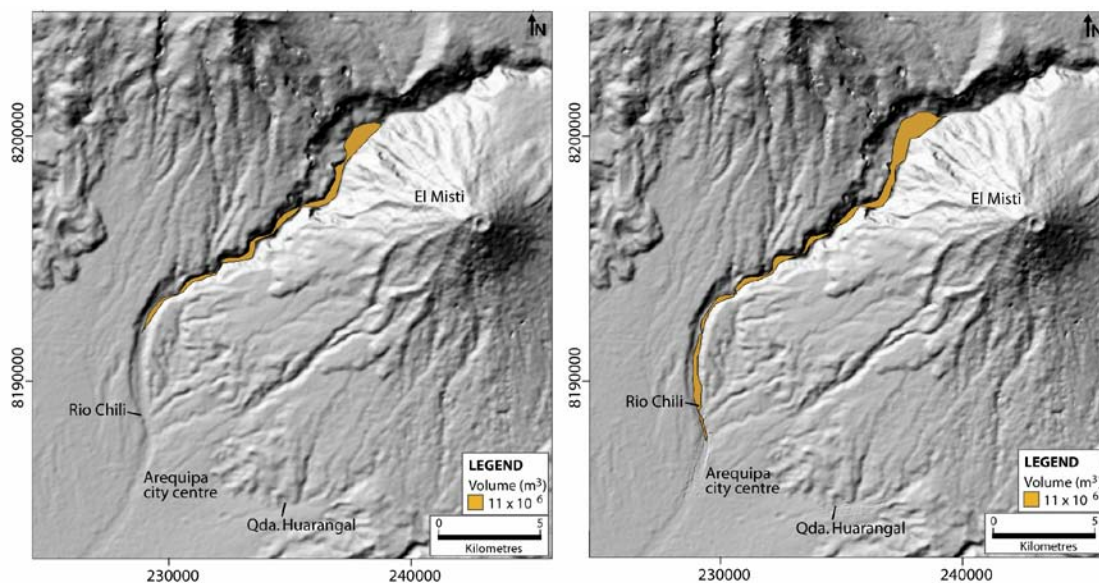


Figure 10: The results of a Titan2D simulation in the Río Chili River using the 30m DEM (left) and the 10m DEM (right). The flow is $11 \times 10^6 \text{ m}^3$ in volume simulated with an internal friction angle of 25° , a basal friction angle of 12° and a solid ratio of 0.40. The map illustrates that the largest volume flow reaches the city with the new DEM, whereas the flow is ~ 5 km from the city with the 30 m DEM.

As with the studies of Stinton et al. (2004a) Delaite et al. (2005), and Vargas et al. (2010a) the run-out and inundation of the simulated flows in this study, even on the new enhanced DEM, do not conform to the previous deposits in the Río Chili Valley. This could be due to the inadequate DEM resolution of the Río Chili canyon – DEMs used cannot sufficiently represent the narrow (<10 m to 60 m across) and deep Río Chili Canyon bed which funnels flows to the middle and lower valley, 20 m to >500 m in width. Another reason for the shorter run-out of Titan2D simulated flows could be related to the Titan2D modelling program itself; such as whether or not Titan2D can adequately simulate geophysical flows. The addition of a GIS-based surficial material map, an optional Titan2D input to define the zones in the region where changes in the surface morphology results in a change in the basal friction angle, may aid in the better simulation of lahars and other flows at El Misti.

4.3 Titan2D-derived lahar hazard map

Zones susceptible to lahar inundation were identified in Titan2D simulations undertaken in the Río Chili valley (Fig. 11) and on the Quebrada Huarangal fan (Fig. 12). Volumes from 0.5

$x 10^6 m^3$ to $11 x 10^6 m^3$, corresponding to the previously identified hazard scenarios, were modelled using an internal friction angle of 30° , a basal friction angle of 12° and a solid ratio of 0.40 on the enhanced 10 m DEM. Inundation outlines were delineated based upon a stopped simulated flow where the pile height is greater than 0.1 m. The *high hazard* corresponds to the low volume but frequent lahars, *moderate hazard* to the moderate volume and frequency lahars and the *low hazard* for the large volume but infrequent events.

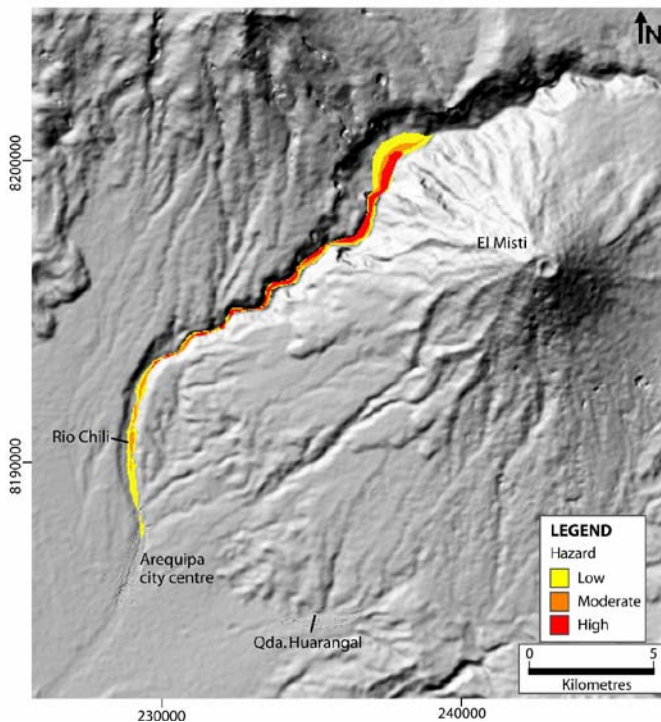


Figure 11: Hazard map for the Río Chili derived from Titan2D simulations on a 10 m DEM. Volumes from $0.5 x 10^6 m^3$ to $11 x 10^6 m^3$ were modelled using an internal friction angle of 30° , a basal friction angle of 12° and a solid ratio of 0.40.

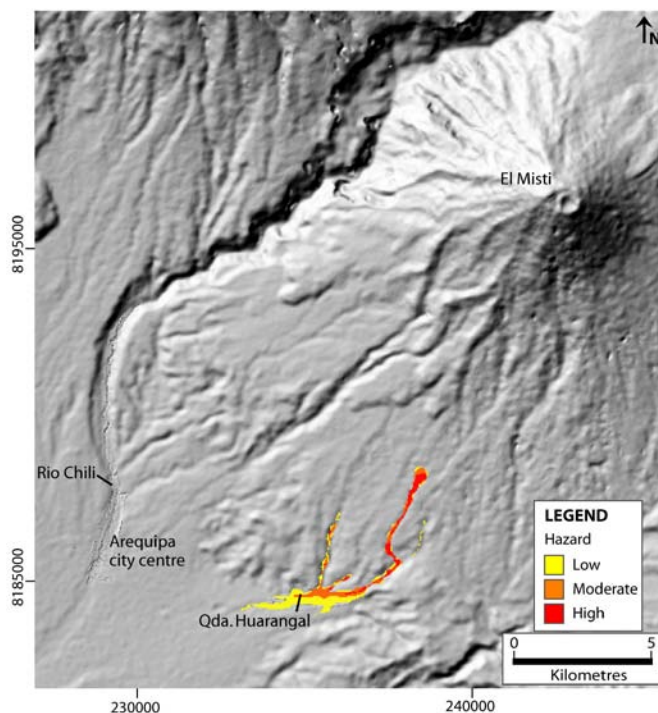


Figure 12: Hazard map for the Quebrada Huarangal fan derived from Titan2D simulations on a 10 m DEM. Volumes from $0.5 x 10^6 m^3$ to $11 x 10^6 m^3$ were modelled using an internal friction angle of 30° , a basal friction angle of 12° and a solid ratio of 0.40.

Titan2D flow inundation in the Río Chili Valley and on the Quebrada Huarangal fan are both larger in extent and run out than previous Titan2D studies by Stinton et al., (2004a) and

Vargas et al., (2010a). For example, the largest flow of $11 \times 10^6 \text{ m}^3$ in the Río Chili reaches approximately 12 km further downstream than in previous simulations. Similarly for the same volume flow on the Quebrada Huarangal fan the simulated run out length is 2.5 km longer for this study. However, as with studies of Stinton et al., (2004a) and Vargas et al., (2010a), the Titan2D simulations are still shorter in run-out length than the LaharZ run-outs of Delaite et al., (2005). The Titan2D simulation run-out for the largest volume flow in the Río Chili is 9.5 km shorter than LaharZ simulation run-out, and on the Quebrada Huarangal fan the Titan2D simulation run-out is 4.8 km shorter. Also, the lahar inundation map generated by Titan2D does not compare with the lahar and flash flood inundation map created from geological and geomorphological evidence. Despite the differences between the Titan2D and LaharZ inundation areas, and the inundation areas derived from mapped deposits, this Titan2D derived lahar inundation map still has significant implications for the Río Chili Valley and Quebrada Huarangal fan.

4.4 Summary

Some of the problems encountered using a 30 m DEM for Titan2D “two-phase” modelling at Arequipa were overcome using an enhanced 10 m DEM. For example, at abrupt changes in channel direction the modelled flows temporarily cease to move on the 30 m DEM, resulting in shorter run out lengths than expected. Conversely, simulations on the enhanced DEM feature longer flow run out lengths because simulated flows can move more easily through the channels due to the better definition in the 10 m DEM. Despite this, the run out lengths of Titan2D simulations are still much shorter than LaharZ simulations and the mapped deposits. This has significant implications for a hazard assessment because the resulting lahar inundation areas differ. The discrepancies in the results are due to the underlying differences between the models. LaharZ is a statistical and semi-empirical code, whereas the experimental Titan2D model takes into account the physical aspects of lahar flow.

The physical parameters used for the simulation, or the conditions at the time of flow generation, can also be responsible for the differences observed between the two models and the actual deposits. Perhaps the most important characteristic of a lahar for hazard management is its inherent variability. Lahars often comprise several distinct phases within a single event and consequently flow properties and flood impacts vary considerably in time and space (Procter, 2010; Dumaisnil et al., 2010). This is the primary limitation of Titan2D for modelling lahar hazards – its inability to replicate erosion or deposition, including any variation in topography relating to this and any resulting changes in flow rheology.

Despite the differences outlined above and provided the user understands the limitations of the models, simulations are extremely valuable in understanding flow behaviour, defining flow inundation areas expected on current DEMs and identifying hazard zones. The simulation results of this study have been used to create a lahar inundation map which provides a basis for the assessment of the vulnerability of the city in the event of lahar.

5. Elements at risk: land, building stock and infrastructure in Arequipa

5.1 Introduction

Whilst modelling of the runout and extent of volcanic mass flows is important to identify the areas which could be affected during a future mass flow event, it is equally important to

identify the elements that could be at risk during such an event, such as buildings and infrastructure. It is important to quantify the damage to buildings not only for determining the economical loss, but also for people living in these buildings who could be killed by a collapse. Another tangible effect is the potential damage to infrastructure: such as transportation links (rail, road and air) and lifelines (e.g. the supply and distribution of electricity and water). This information would also lead to the determination of available resources (e.g. shelter, command centre, emergency services) in case of volcanic crisis, in turn these resources might be evaluated according to potential damage if they are located in harms way. Damage to the agricultural industry must also be considered, agriculture plays a vital role in Arequipa's economy and as food supply. This industry is reliant on the irrigation system derived from the Río Chili – a pathway for future lahars. The city of Arequipa is recognised as a UNESCO World Heritage site and every year tourism brings around 1 million visitors to the region. The potential loss of income from dropping tourist numbers would be devastating to the region.

Using methods adapted from Chevillot (2000) and others (e.g. Pomonis et al. 1999; Kelman, 2002; Baxter et al. 2005) to identify elements at risk, a descriptive survey was conducted to characterise the land use patterns, building stock, and key infrastructure present within the two study areas.

5.2 Land-use classification

Land use classification for defining element vulnerability is as crucial as the classification of building and infrastructure construction itself, because the consequence of losses depends on the occupancy of the structures (e.g. private dwellings will usually have less people present than in hotels). By defining the dominant land use, one can easily identify structures whose survival is important and vital during a crisis and which are intended to remain operational during and after a volcanic crisis. These essential facilities can include and are not limited to: medical care centres, power stations and police headquarters. During the survey conducted in Arequipa in 2007 and 2008, twenty different land-use types were identified (Table 4, Fig. 13) varying from non-built intensive agriculture to dense urban areas.

GIS ID	Land use	GIS ID	Land use
1	Urban dwelling	11	Other commercial*
2	Rural dwelling	12	Administration
3	Commercial with dwelling	13	Industry/handicraft
4	Accommodation	14	Service station
5	Medical centre	15	Carpark
6	Police	16	Agriculture
7	Religious establishment	17	Monument
8	Education establishment	18	Abandoned
9	Public area/sports area	19	No construction
10	Restaurant	20	Unknown

*Table 4: Predominant land-use types identified for the areas surveyed in Arequipa. The classification of 'unknown' was assigned to areas which were unseen, and where permission to access the land was not granted. *Other commercial corresponds to commerce does not have dwellings attached, such as supermarkets, larger stores etc.*

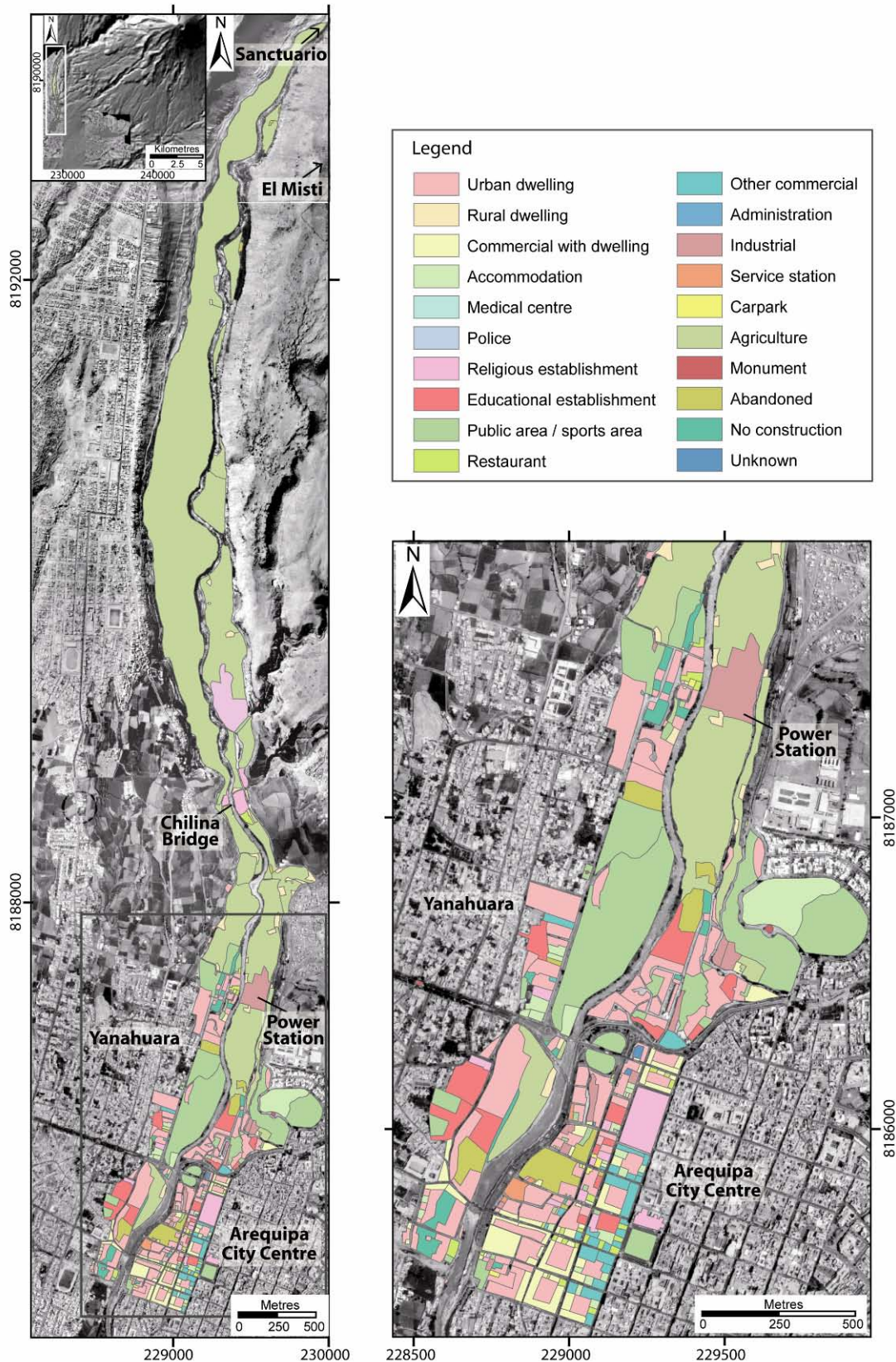


Figure 13: The predominant land use in the Río Chili Valley study area from the Quiñones Bridge to the military school in the upper Río Chili canyon. The southern part of the study area is largely for commercial, industrial and residential use. In contrast, the northern part of the study area is cultivated (valuable arable crops) with very few rural dwellings.

Using methods adapted from the International Building Code (International Code Council, 2006), the Peruvian National Building Code for Earthquake-resistant design (Technical Standard of Building E.030, 2003) and the New Zealand Standard NZS 1170.5:2004 (Standards New Zealand, 2004) the susceptibility of land use in Arequipa was assessed. Coefficients, ranging from 0 (low *importance*) to 1 (high *importance*) were assigned to different categories (such as economic repercussions, population exposure and value) for each land-use type. The land-use types were evaluated against one another to determine the most susceptible land use type present in Arequipa (Table 5).

Land use	Rank	Land use	Rank
1- Dwelling	13	11- Other commercial	12
2- Rural dwelling	11	12- Administration	12
3- Commercial with dwelling	7	13- Industry	4
4- Accommodation	8	14- Service station	9
5- Medical centre	1	15- Carpark	14
6- Police	2	16- Agriculture	6
7-Religious establishment	3	17- Monument	8
8- Educational establishment	5	18- Abandoned	15
9- Public area	12	19- No construction	15
10- Restaurant	10	20- Unknown	16

Table 5: Ranking of the land use susceptibility in Arequipa, where 1 is the most susceptible and 16 is the least. Land-use types were ranked according to to the importance of the particular land use potentially exposed during a crisis, how many of the population will be affected, the value of the land and the economic repercussions during a volcanic crisis.

5.3 Building stock classification

Using methods adapted from Chevillot (2000) and others (Pomonis et al. 1999; Kelman, 2002; Spence et al. 2004a,b, Baxter et al. 2005) building surveys of the two study areas in Arequipa were conducted externally (at street level) and where permitted, within the boundaries of the land-owners property. Initially nine construction types were identified (Table 6, Fig. 14) and defined according to: the dominant building material, number of floors, building reinforcement, roof type and style, opening type and quantity, and overall building structural integrity. The building types were further classified and ranked according to their strength.






Type A		
Structure:	Confined masonry Masonry panels, typically 1-2m in each direction. Wall material generally consists of perforated clay bricks or concrete blocks that are un-reinforced. Cast-in-situ reinforced concrete frames (horizontal and vertical). Generally reinforced with four No.3 (9mm) bars and traverse ties of heavy-gauge wire.	
Height:	1-3 storeys.	
Floor:	Commonly in-situ filler block floors.	
Roof:	Roof is mostly flat or pitched built of reinforced concrete masonry composite slabs.	
Openings:	Large glass windows throughout the building, often with aluminium framing and lower windows secured with steel bars. Doors are generally solid and wooden, with steel security screen/bars.	
Maintenance:	Some covered with stucco which may increase the strength and stiffness. Overall building is well finished with paint, fencing and security. The building and surrounds are well-kept.	
Type B		
Structure:	Confined masonry The same structural components as Type A buildings, however the structure <u>has not been completed</u> (even though occupied). Often the ground storey is lived in but not completed to the same standard as Type A buildings; structure built slowly one storey at a time. With incremental building the vulnerability of the structure increases due to inadequate connections with the existing structure, as well as unsymmetrical configuration.	
Height:	1-3 storeys.	
Floor:	Same as A.	
Roof:	Same as A	
Openings:	Same as A	
Maintenance:	The overall evolution of the structure is positive and the house is well finished with paint, fencing, and security. The building and the surrounds are well-kept.	
Type C		
Structure:	Confined masonry Same structural components as Type A buildings, however the structure <u>has not been completed</u> (even though occupied). Ground floor often painted with subsequent storeys unpainted.	
Height:	2-4 storeys. Vertical extension unfinished and some material that has been used are unstable.	
Floor:	Same as A.	
Roof:	Same as A, however some may be constructed with corrugated iron.	
Openings:	Same as A.	
Maintenance:	Overall long-term evolution will be positive. Environment and building not well kept. Body of building fenced.	
Type D		
Structure:	Confined masonry Same structural components as Type A buildings, however building characteristics similar to Type B with incremental and <u>unfinished</u> construction practices.	
Height:	2-4 storeys. Vertical extension unfinished and some material that has been used are unstable.	
Floor:	+4 storeys.	
Floor:	Same as A	
Roof:	Same as A.	
Openings:	Same as A.	
Maintenance:	The overall evolution of the structure is positive and the house is well finished with paint, fencing, and security. The building and the surrounds are well-kept.	
Type E		
Structure:	Confined masonry Same structural components as Type A buildings, however, building is <u>typically colonial</u> style and constructed from ignimbrite brick and/or adobe.	
Height:	1-2 storeys.	
Floor:	Same as A.	
Roof:	Same as A.	
Openings:	Same as A, however windows tend to be smaller than newer houses constructed in Types A-C.	
Maintenance:	The upkeep of the building is poor and can appear 'shabby'. Parts of the building are likely to be unstable. The overall evolution of the structure is positive and the house is well finished with paint, fencing, and security. The building and the surrounds are well-kept.	

Table 6: Classification of buildings in Arequipa according to the structural components and overall appearance.





Type F		
<i>Structure:</i>	Confined masonry The same structural components as Type A buildings, however the structure is <u>degraded and unstable</u> . The building is often unfinished or constructed poorly, or has been damaged (e.g. earthquake) and not remedied.	
<i>Height:</i>	1-2 storeys.	
<i>Floor:</i>	Same as A.	
<i>Roof:</i>	Roofing is the same as Type A or constructed of corrugated iron. The overall quality is poorer than that of Types A-C. The corrugated iron roofing is often held in place by objects such as rocks and pieces of wood if not nailed in place.	
<i>Openings:</i>	Windows are often small and few with aluminium or wood framing. It is not uncommon for the windows to have no glass or to be boarded up. Security bars not as common as buildings of Types A-C. Doors are constructed of mainly tin/aluminium, and are somewhat flimsy and with or without security.	
<i>Maintenance:</i>	Ground floor and 1st storey constructed from brick with no stucco or paint. Overall long-term evolution of the structure will be negative, and the environment and building are not well kept.	
Type G		
<i>Structure:</i>	Unconfined masonry The building generally comprise of an old base constructed from stones and ignimbrite. The walls are constructed from ignimbrite, brick or adobe and are not confined by either reinforced horizontal or vertical cast-in-situ concrete, and in many cases appear quite unstable.	
<i>Height:</i>	One storey.	
<i>Floor:</i>	Same as A, or no floor.	
<i>Roof:</i>	Typically constructed with corrugated iron placed on wooden rafters and held in place by rocks, bricks, wood etc. In some cases they are nailed into place.	
<i>Openings:</i>	Openings (however it is not uncommon <u>for there to be no windows</u>) are the same as F. Ground floor and 1st storey constructed from brick with no stucco or paint.	
<i>Maintenance:</i>	Overall long-term evolution of the structure will be negative, and the environment and building are not well kept.	
Type H		
<i>Structure:</i>	Make-shift housing Building construction a composition of heterogeneous objects, such as bricks (red, ignimbrite, and adobe), rocks, plastic, wood, straw, iron etc. Little to no structural integrity.	
<i>Height:</i>	One storey.	
<i>Floor:</i>	No constructed floor (ground, plastic etc.).	
<i>Roof:</i>	Roof is constructed out of any material available.	
<i>Openings:</i>	No windows or doors. Often a piece of fabric or plastic as a door.	
<i>Maintenance:</i>	Slum environment with construction mainly by 'illegal squatters'. Overall long-term evolution will be negative. Environment and building not well kept.	
Type I		
<i>Structure:</i>	Unconfined masonry Abandoned and destroyed housing.	
<i>Height:</i>	1-3 storeys.	
<i>Floor:</i>	All types if floor still exists.	
<i>Roof:</i>	Typically mostly flat or pitched built of reinforced concrete masonry composite slabs if roof still exists.	
<i>Openings:</i>	Variable, often with no glass remaining in windows.	
<i>Maintenance:</i>	Some buildings destroyed in the 2001 earthquake and never rebuilt or cleared. Unsafe, unstable, common with squatters.	

Table 6: Continued.

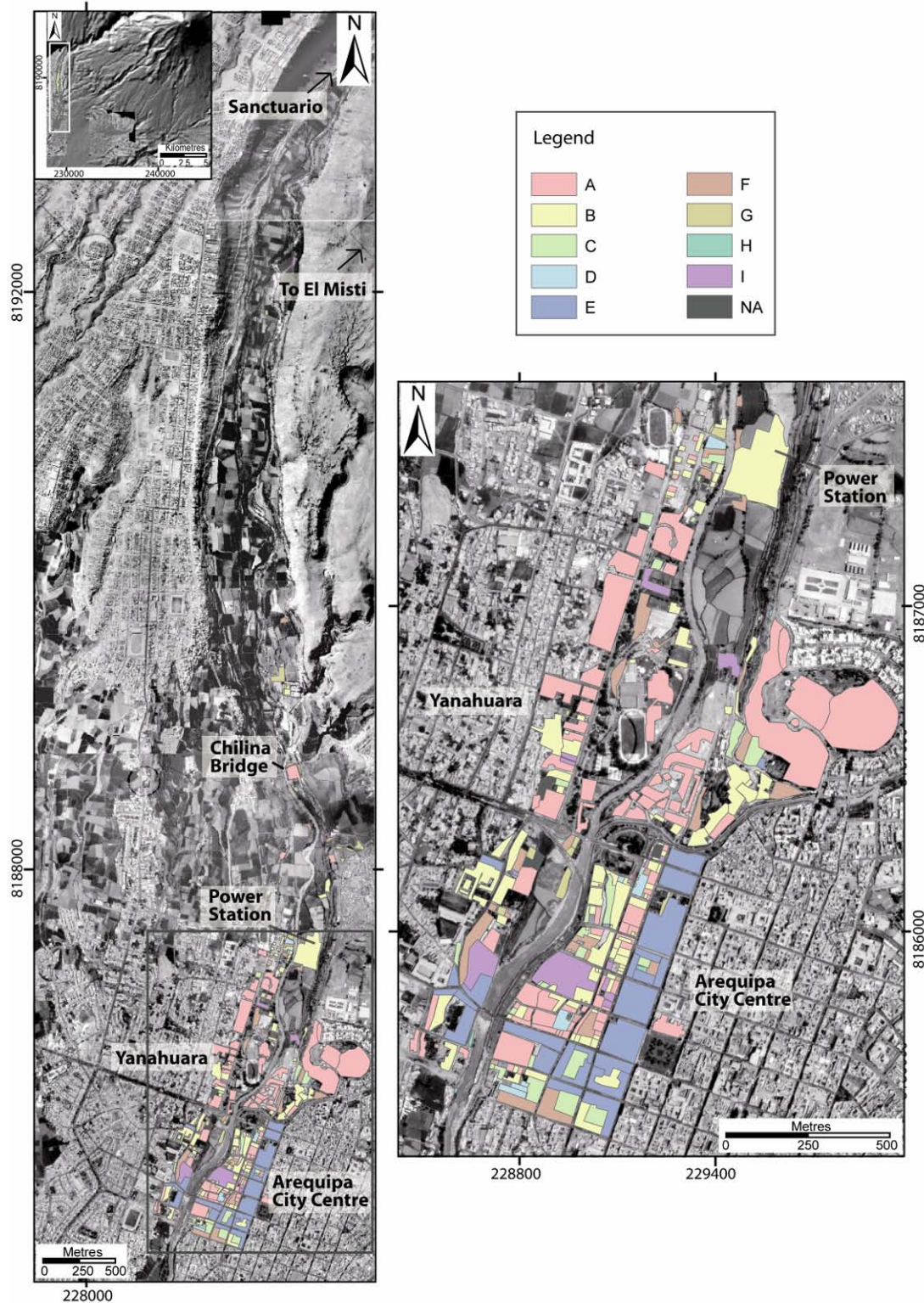


Figure 14: The predominant building types in the Río Chili valley from the Quiñones Bridge up to opening of the canyon. **A:** Close-up map of the study area from the Quiñones Bridge, southern boundary of the city (229410, 8187365), to the entrance of the canyon (232116, 8194785). This valley is heavily cultivated (valuable arable crops) and in close proximity to the EGASA main power station, clubs, factories and some housing. Housing in cultivated areas is usually confined to rural type dwellings. Within this area, the building types are largely for commercial, industrial and residential use. **B:** Close-up map of the predominant building types in the city centre.

Building descriptions in Table 6 are purely based on face value, and building types A to I are not ranked according to structural integrity. The influence of different structural components needs to be taken into consideration in order to determine the most vulnerable building type. Using methods adapted from Vargas et al. (2010b) and others (Prevot, 2009; Palhol, 2008; Pomonis et al. 1999) building types defined in Table 6 were classified and ranked according to frame materials, wall materials, roof types, roof material, storeys, proportion of windows, type of window frames and foundation type. Coefficients, where 0 is not vulnerable/good quality and 1 is very vulnerable/bad quality, were assigned to each building feature, and sub-feature.

Type D buildings came out as the least susceptible building to lahars and floods, followed by Types A, B and C with the same susceptibility index. Type G buildings are the most susceptible, followed closely by type H buildings. Type E buildings are also more susceptible to lahars and flash floods than type F buildings. Confined masonry buildings were the least susceptible (e.g. Type A), whereas unconfined and buildings without mortar were more susceptible. Type H buildings (make-shift) were less susceptible than Type G because there were less structural components in the susceptibility assessment and therefore no coefficients for certain building criteria could be added to the calculation.

5.4 Susceptibility of building types and land use in Arequipa

In order to get one value to determine the vulnerability of the buildings in Arequipa, the land-use susceptibility index was combined with the building susceptibility index to give a single susceptibility value. This value represents the vulnerability of the building combined with the influence of the land use on the vulnerability (Figs. 15 and 16).

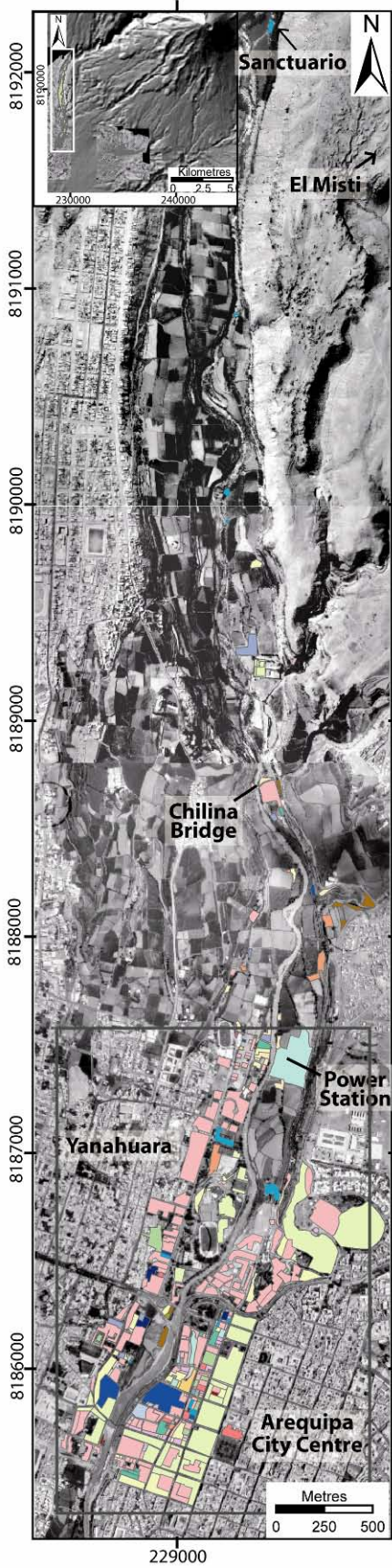
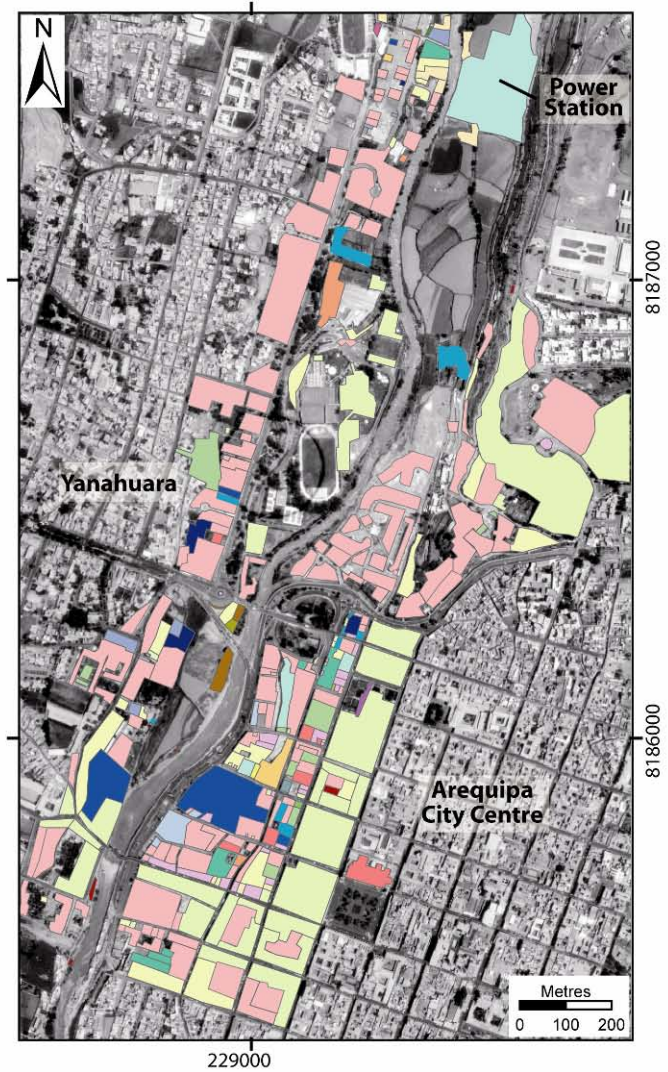
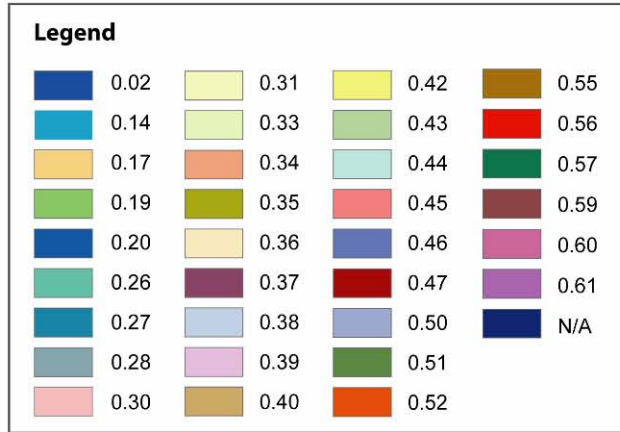


Figure 15: Building and land use susceptibility map for the Río Chili Valley, where 0 is the least susceptible and 1 is the most.



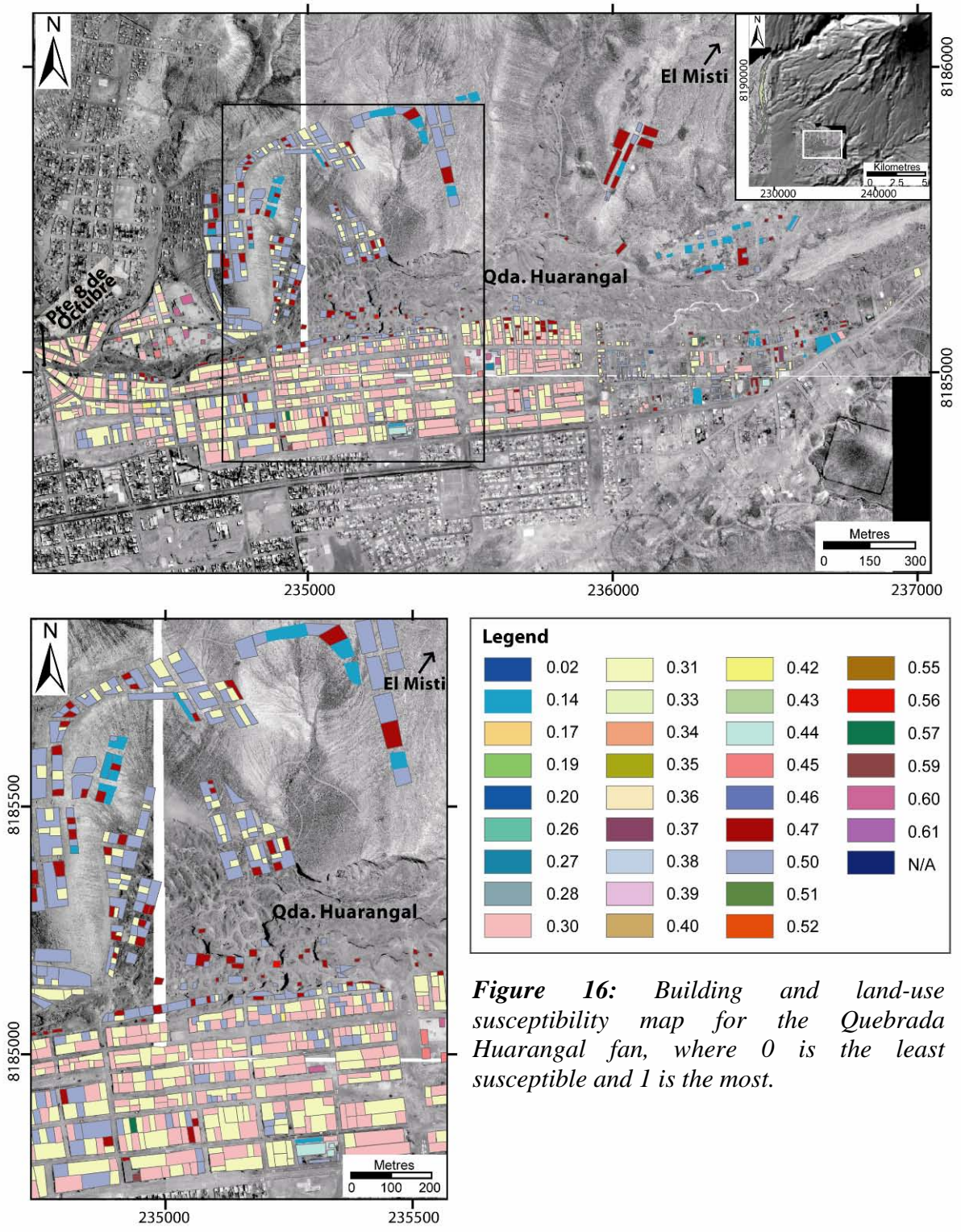


Figure 16: Building and land-use susceptibility map for the Quebrada Huarangal fan, where 0 is the least susceptible and 1 is the most.

The building and land use susceptibility map for the Río Chili Valley shows a region with an overall low susceptibility when compared to the Quebrada Huarangal fan. However, the distribution of susceptibility appears to be more evenly distributed on the Quebrada Huarangal fan where most of the highly susceptible buildings are confined to the north of the study area and within the Quebrada channel, whereas susceptibility in the Río Chili Valley is much more contrasted. It is perturbing that the most vulnerable buildings in the Quebrada Huarangal fan are located within and adjacent to the temporary stream. With regards to a lahar or flood event these buildings, which are already considerably vulnerable due to their

location, are further endangered by their construction type and dominant land use. The results of the building and land-use susceptibility assessment were saved into a GIS database

5.5 Infrastructure classification

As modern urban functions rely on lifeline systems much more heavily than they used to, infrastructure constitutes a major component of the vulnerability of a city if a disaster strikes. Infrastructure can be defined as the basic physical and organisational networks needed for the operation of a society, or the services and facilities necessary for an economy to function. These can include water supply, sewage, gas distribution, power supply and telecommunications network just to name a few. The transportation network, telecommunications, lifelines and emergency services are regarded as essential infrastructure because they need to be operational to cope during and immediately after a disaster. Educational, government and economy services, nutrition and commodities are regarded as important infrastructure/services within a city because while they are important to the city, they are not essential to saving and/or protecting human life during a disaster.

In Arequipa much of the essential infrastructure (e.g. bridges, power lines, water pipes and power stations) are primarily concentrated across and in close proximity to the Río Chili, and also within the city centre. Emergency services and important infrastructure (civil engineering protection works, educational, government and economy services, nutrition and commodities) were addressed in the land use classification; therefore the infrastructure classification will cover transportation networks and lifelines.

Using methods adapted for the analysis of the susceptibility of land-use and buildings in Arequipa, the susceptibility of identified infrastructure was assessed. Coefficients, ranging from 0 (low *importance*) to 1 (high *importance*) were assigned to different categories (such as economic repercussions, population exposure and value) for each infrastructure type (the method and rationale for assigning the coefficients is discussed in chapter 1). These coefficient values were added together and averaged to give a value between 0 and 1 for the *importance* of the particular infrastructure and therefore the susceptibility during a volcanic crisis (Table 7).

Elements		Rank	Elements		Rank	
Roadways	Highway	11	Hydroelectric power stations	Charcani I	10	
	Main road	9		Charcani II	10	
	Minor road	15		Charcani III	10	
	Unsealed road	17		Charcani IV	10	
Bridges	Chilina walking	18		Charcani V	6	
	Chilina	16		Charcani VI	8	
	Grau	1		Hydroelectric dams	14	
	Bajo Grau	5		Other power	Power station	4
	Bolognesi	2		Power poles and lines	Wood	7
	Quinones	3		Concrete	13	
	8 du Octobre	12	Water supply systems	Water canal open	10	
Other transport	Railways	16		Water canal covered	13	
	Airport	11		Irrigation canals	3	
Waste water supply systems	Waste water and sewerage pipes	10		Water treatment plant	15	
Telecommunications	Telecommunication lines	10		Water pipes	13	

The susceptibility analysis of infrastructure indicates that Puente Grau is the most susceptible in Arequipa, followed by Puentes Bolognesi and Quiñones and the irrigation canals. This is not surprising given the relevance of these bridges as major transportation links across the city. In addition Puentes Grau and Bolognesi are the oldest bridges, and perhaps most important with regards to transportation, food supply and tourism in the city. The least vulnerable infrastructure according to the susceptibility analysis are the Chilina walking bridge, unsealed roads, railways and the Chilina bridge. The Chilina walking bridge is situated on private land and is used rarely; the likelihood of people being on the bridge during a mass flow is low and the immediate need for the bridge after a mass flow event is very unlikely. Both the Chilina bridges have very low traffic volumes and are not considered as vital to the transportation network in Arequipa. Similarly unsealed roads have a much lower traffic volume than sealed roads, and despite being often in poorer condition than minor and main roads, they are cheaper and easier to replace after an event. The low susceptibility rating of the railway networks is due to the railway being situated outside of the study area. The railway network in Arequipa is not extensive because other modes of transportation are more utilised.

The irrigation canals are vital to agriculture in Arequipa; in this semi-arid environment crops would not survive without irrigation. Additionally crops will provide nutrition for the community during and after a crisis. The power stations are also very susceptible within the top ten most susceptible infrastructures. The thermal power station is more susceptible than they hydroelectric due to the higher electricity output, larger number of employees and visitors at the station, and also the reliance of the transportation on diesel fuel for power generation. Charcani Quinto is the most vulnerable hydroelectric power station due to its location, the high electricity output and the rebuild cost (i.e. a large tunnel system taking water through the side of the volcano).

5.6 Summary

The most susceptible land, buildings and infrastructure in Arequipa have been identified. The results of the building and infrastructure survey identified a range of construction types, and often within the same city block. The poorest quality houses (and not structurally sound) are often located closest to the river channels with the most vulnerable area identified as within, and adjacent to, the temporary stream of Quebrada Huarangal. Without the susceptibility analysis the buildings are considered vulnerable just due to their location; however the susceptibility analysis confirmed that they are further endangered by their construction type and the dominant land use.

The city is reliant on the Río Chili for power, water and food, and yet if a mass flow event is to occur, these essential services are indeed most vulnerable. Transportation links are vital during a crisis and the analysis of infrastructure highlighted that the bridges, which cross the Río Chili in the city centre are the most vulnerable. If bridges are destroyed, access from one side of the city to the other will be severely limited and in addition water pipes and power and telecommunication lines are often located at bridges, and are thus equally susceptible to damage. Services such as the Egasa power station and the hydro-electric dams are also susceptible, possibly resulting in the severe disruption of power supply to the city, and having a flow-on effect for lifeline services such as hospitals and other emergency services.

6. The risk facing the city of Arequipa

6.1 Introduction

The risk of inundation and/or damage to buildings, land and infrastructure was assessed by combining a number of tools: hazard assessments, flow characteristics and effects, and element vulnerability. The calculations were undertaken in a GIS allowing for the spatial expression of the risk element, which is an attractive method for communicating information to decision makers and the community alike. The following sections give an indication of the buildings, land use and infrastructure risk in the event of a lahar and/or flash floods in Arequipa.

6.2 Building risk

Overall the building risk assessments indicate that the majority of buildings located within the Quebrada Huarangal channel are considered as *high* to *very high* risk from the inundation of lahars and flash floods (Fig. 17). On the other hand, very few buildings are considered as *high* risk in the Río Chili Valley. This could be due to existence of higher ranked buildings in this locality but also due to the placement of buildings – i.e. not within the river channel itself as in the case of Quebrada Huarangal.

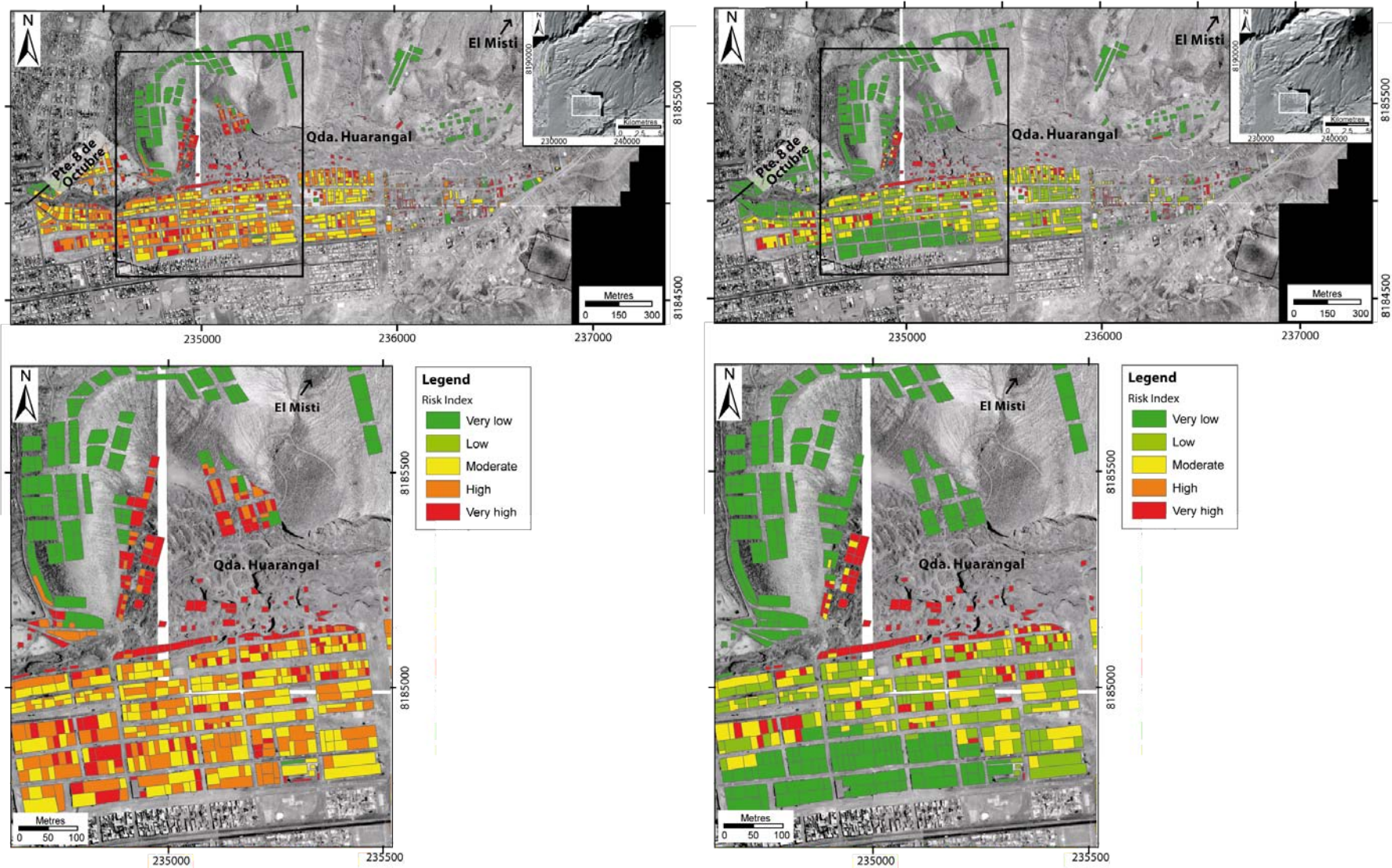


Figure 17: The risk posed to buildings from lahars and flash floods based upon hazard assessment and land use vulnerability functions. The risk calculated from a conventional hazard assessment is presented to the left of the figure, in contrast the Titan2D based risk assessment is presented on the right.

6.3 Land use risk

The level of risk posed to land use in Arequipa from lahars and flash floods is presented in Figure 18. Differences between the two methods of hazard assessment are especially apparent when comparing the Río Chili valley risk maps. In the conventionally derived (i.e. geological mapping) risk map, the majority of land use in this area is of *moderate* risk, whereas the vast majority of land use is identified as *very low* risk with the Titan2D derived risk map. The land use identified as *moderate* risk in the Río Chili valley is not only limited to one or two different types of land use, but covers the spectrum from private dwellings to agriculture. In contrast many businesses and factories (e.g. the brick factories located on the northern bank of the channel) within and adjacent the Quebrada Huarangal channel are considered as *high* to *very high* risk (Fig. 18).

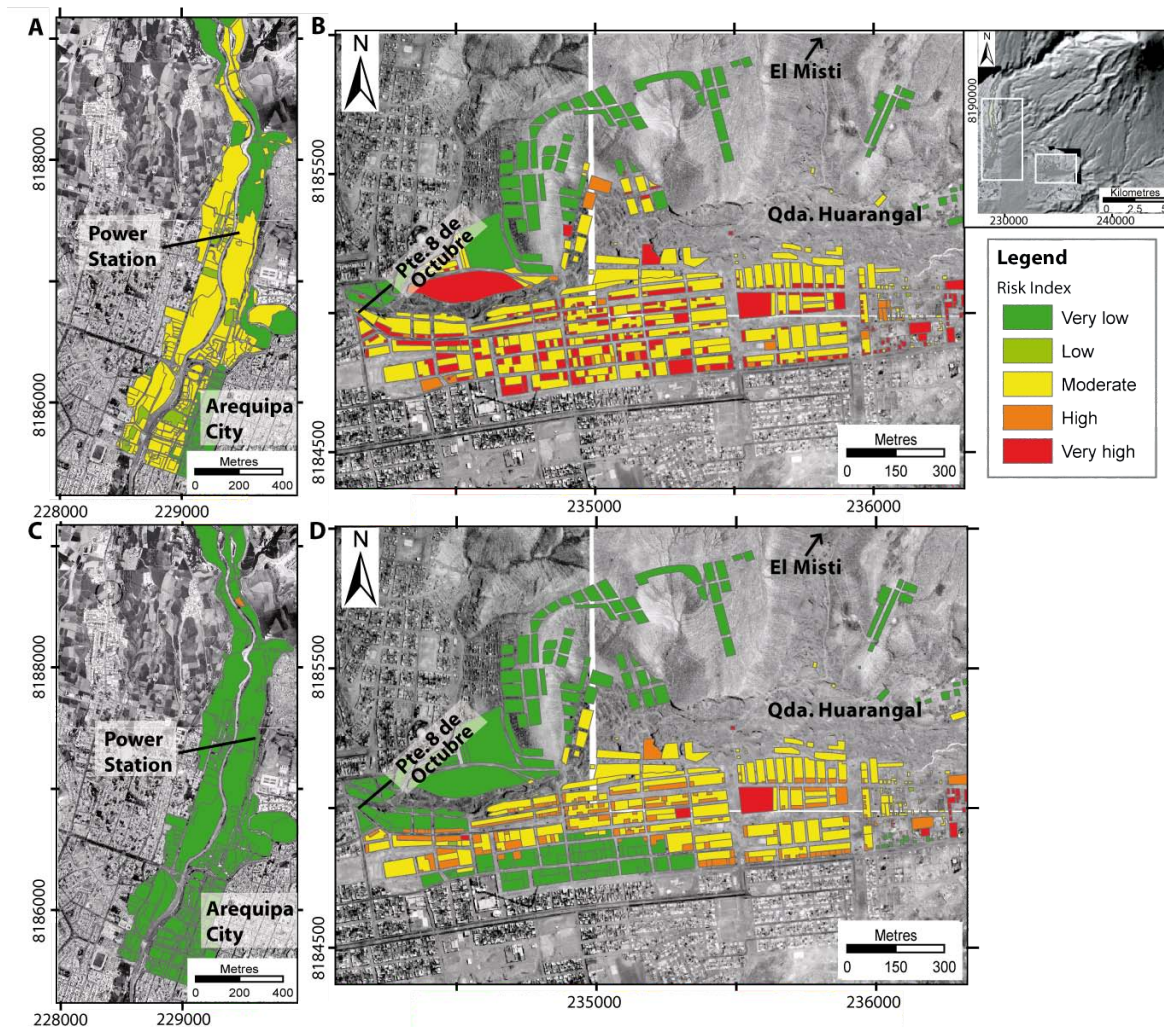


Figure 18: The risk posed to land use from lahars and flash floods based upon a conventionally-derived (A and B) and Titan2D-derived (B and C) hazard assessments and building vulnerability functions. The Río Chili valley is represented by images A and C, and the Quebrada Huarangal fan in images B and D.

Overall the risk assessments indicate that the majority of land use located within the Río Chili valley is considered as at *moderate* risk of inundation and/or damage from lahars and flash floods. On the other hand the main land uses, considered as *high* to *very high* risk, on the Quebrada Huarangal fan are concentrated to small commercial premises and factories.

6.4 Combining building and land use risk

The risk has been determined from the combined building and land use vulnerability and the hazard assessments for each of the reference scenarios. Using the hazard Scenario Three the level of risk to the Río Chili valley from large magnitude ($4.0 \times 10^6 \text{m}^3$ to $>11.0 \times 10^6 \text{m}^3$) but infrequent (100 – 2000 years) lahars and hyperconcentrated flow events are shown in Figure 19. The risk of damage and/or inundation to the majority of the surveyed area, derived from the conventional hazard assessment, is *very low*, *low* and *high* (Fig. 19 A). The entire survey area of the map derived from the Titan2D hazard assessment is of *very low* risk with the exception of the La Choceta restaurant near Chilina (Fig. 19 B) which is a *high* risk property. The extremities of the Titan2D simulated flow at this magnitude was within the vicinity of the restaurant.

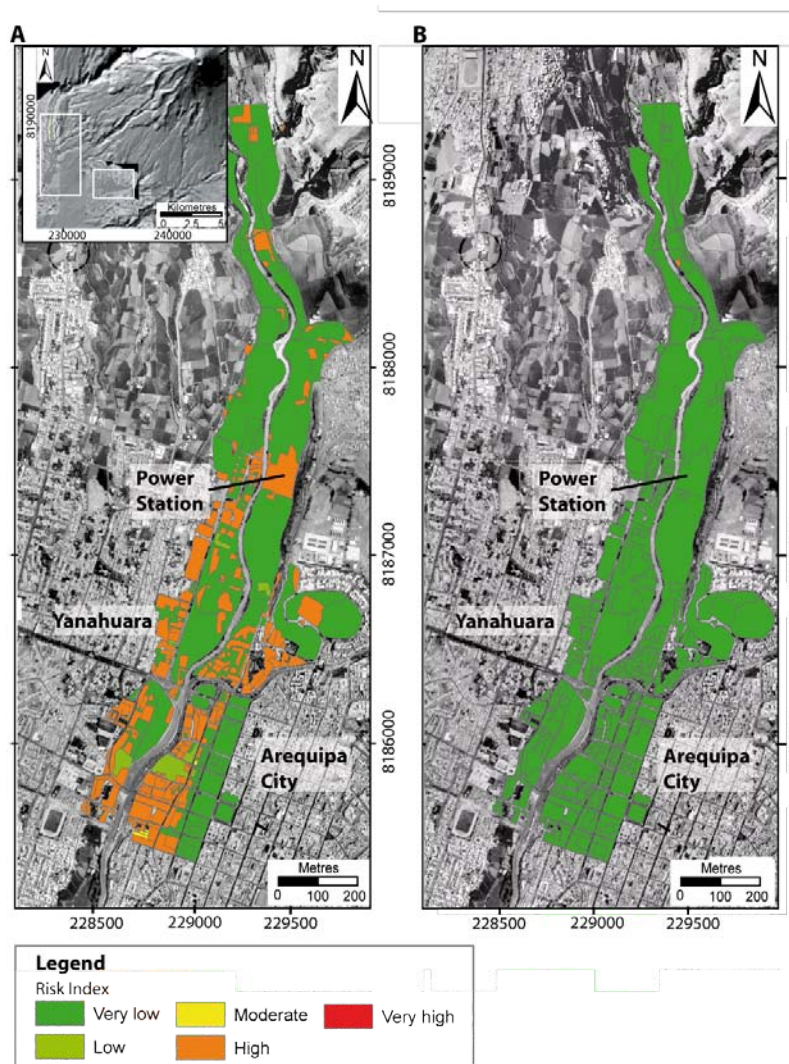


Figure 19: The risk posed to buildings and land use from lahars based upon a conventionally-derived (A) and Titan2D-derived (B) hazard assessments and building and land use vulnerability functions for hazard scenario three. The Río Chili valley is represented in images A and B.

The *very low* risk areas of the map calculated from the conventionally-derived hazard assessment are mostly represented by agricultural land upstream of the city centre. Properties situated on the eastern upper terraces ($>t2'$) on the downstream of the Grau bridge are also *very low* risk (Fig. 19 A). The properties on these upper terraces are of mixed land uses and building types, although they possess considerably better quality than the majority of buildings located on the Quebrada Huarangal fan. As with hazard scenario one, *high* risk

properties are represented by private adobe dwellings located on the western low terraces (t1 to t1') immediately downstream of the Grau Bridge.

Buildings located on the western, lower to middle terraces (t0 to t2) downstream of the Grau Bridge are considered to be of *high* risk. The main land uses are private dwellings, commercial centres and factories which are of a range of building types. More *high* risk properties are located on terraces t1 to t2 just upstream of the confluence of the Río Chili with Quebrada San Lazaro. The properties are private dwellings of building type A and B confined in an upmarket building compound. Many *high* risk properties are also located on the low to moderate terraces (t1 – t2) up to approximately 1.8 km upstream of the Grau Bridge. The properties in close proximity to the Grau Bridge mainly comprise of upmarket hotels and commercial buildings of building types A and B. Much of the constructed property located within Club Internacional is at *high* risk; this however excludes the open areas which are of *very low* risk. As with hazard scenario one, *high* risk properties are identified approximately 500 m upstream of the club on the western low terrace (t1 and t1') and rural properties on either side of the river are also considered as *high* risk. The dwellings and sports fields and arenas of the military camp upstream of the Chilina Bridge are also considered to be at *high* risk during a moderate magnitude and frequency lahar or hyperconcentrated flow event.

On the map constructed from the conventional hazard assessment for the Quebrada Huarangal fan (Fig. 20), the majority of properties located within the channel are considered to be at *high* risk. The buildings are single storey, and represent types F to H comprising of confined and unconfined masonry and make-shift buildings – the lowest ranked. The constructed area of the lower to moderate terraces (t0 - t1'), particularly on the southern side of the channel and on the northern side of the channel immediately after the channel narrows, are of *high* to *high* risk. *Very low* risk properties are located far from the channel. In contrast to the Titan2D derived risk assessments constructed for scenarios one and two, the majority of properties in scenario three are considered at *moderate* to *high* risk (Fig. 20, lower image). This is especially so on the flatter southern channel and terrace where Titan2D simulated flows “overbanked” in this locality. Another area of *moderate* to *high* risk is where simulated flows have not followed the narrowed channel and broken out onto the southern bank. The properties located in the *moderate* to *high* risk zones are heterogeneous and represent a range of building types from Type A to H, and land-use type corresponding to private dwellings, commerce with dwellings, restaurants and industry.

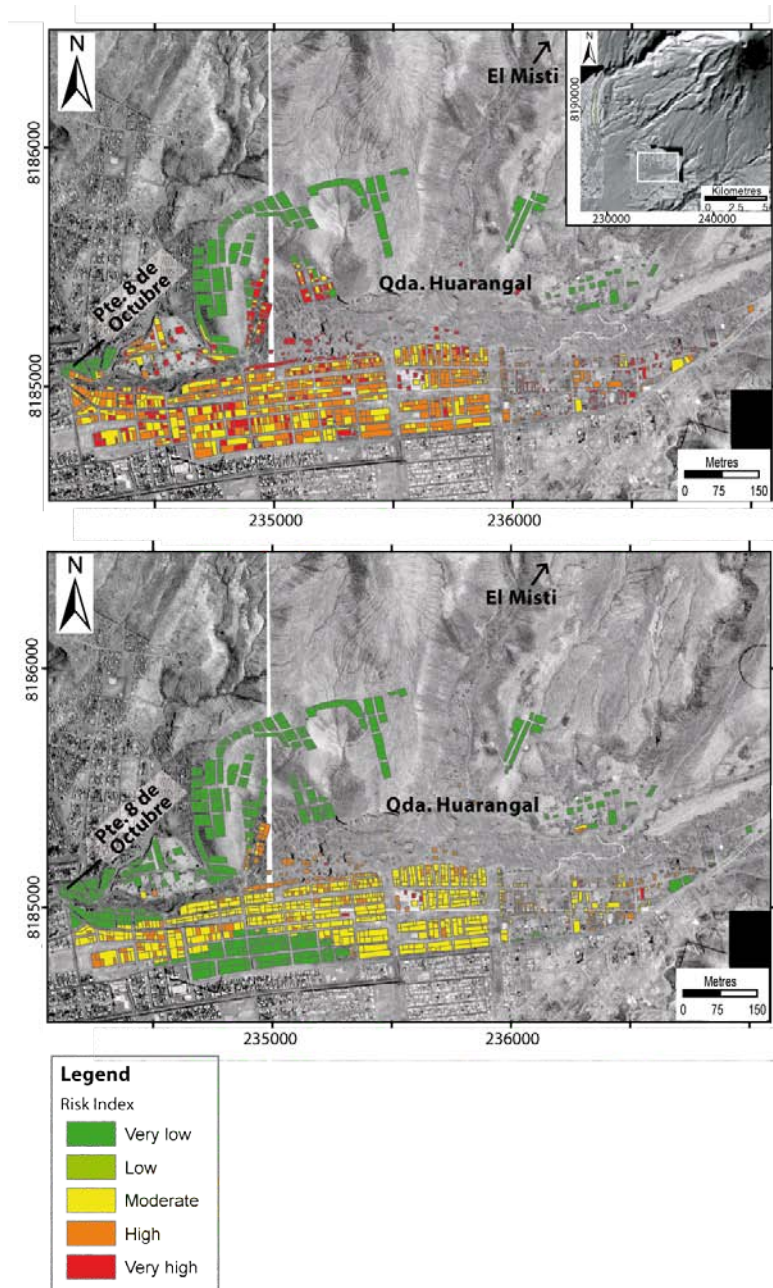


Figure 20: The risk posed to buildings and land use from lahars based upon a conventionally-derived (A) and Titan2D-derived (B) hazard assessments and building and land use vulnerability functions. The Río Chili valley is represented in images A and B.

6.5 Infrastructure risk

Transportation

The level of risk posed to the roadways and bridges in Arequipa from lahars of hazard scenario three is presented in Figure 21. From the map calculated from the conventionally derived hazard map, all bridges are under *moderate* risk from inundation except for Puente Grau which is considered *high* risk (Fig. 21 A). Puente Grau is particularly vulnerable due to its age, construction and importance for the economy – both in terms of transportation and tourism. The road which runs adjacent to Quebrada San Lazaro is considered to be at *very high* risk of inundation. Roadways of the lower to middle terraces (t_0 to t_2') are all considered at *moderate* risk of inundation during a lahar formed during scenario three. Roads on the higher terrace ($>t_3$) possess *very low* risk of inundation. Conversely, the majority of roads and bridges in the Titan2D-derived map are considered at *very low* risk of inundation (Fig. 21 B).

However, the road accessing the military school in the upper Río Chili canyon (Charcani Qunito) is at *high* risk of inundation, as with the Chilina bridge. The Chilina walking bridge has a *moderate* risk of inundation as does a small unsealed rural access road on the eastern bank of the Río Chili, 1.5 km upstream of Chilina. The Titan2D derived risk map is of considerably lower risk than the conventionally derived risk map, due to the Titan2D simulated flows not extend into the city centre.

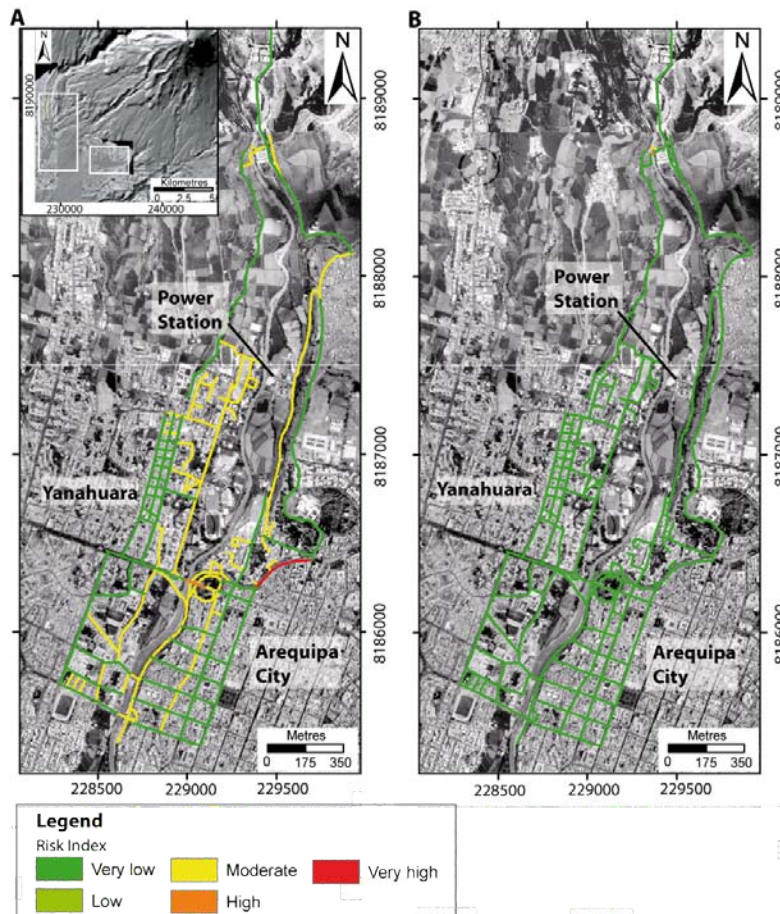


Figure 21: The risk posed to roadways and bridges from lahars based upon a conventionally-derived (A) and Titan2D-derived (B) hazard assessments and building and land use vulnerability functions for hazard scenario three. The Río Chili valley is represented in images A and B.

The majority of the Quebrada Huarangal fan is considered to be of *high* risk of inundation in the risk map derived from conventional hazard assessment (Fig. 22 upper image). The main roads which connect the fan to other parts of Arequipa are at the most risk – *very high*. Roads of *very low* risk are confined to the higher terraces (>t2) on the southern side of the channel and the volcano’s flanks on north of the channel. At risk areas are featured on the Titan2D-derived map include a *very high* risk main road which runs parallel to the channel, a few blocks back from the channel edge (Fig. 22, lower image). *High* risk roads run parallel, north and south, to the *very high* risk road. *Moderate* risk roads are located on the southern portion of the channel bed and lower terraces (t0-t1), and not including the northern roads of the *San Jerinomo* suburb. The majority of roads are of *very low* risk to inundation and/or damage from lahars including the bridge *8 du Octobre*.

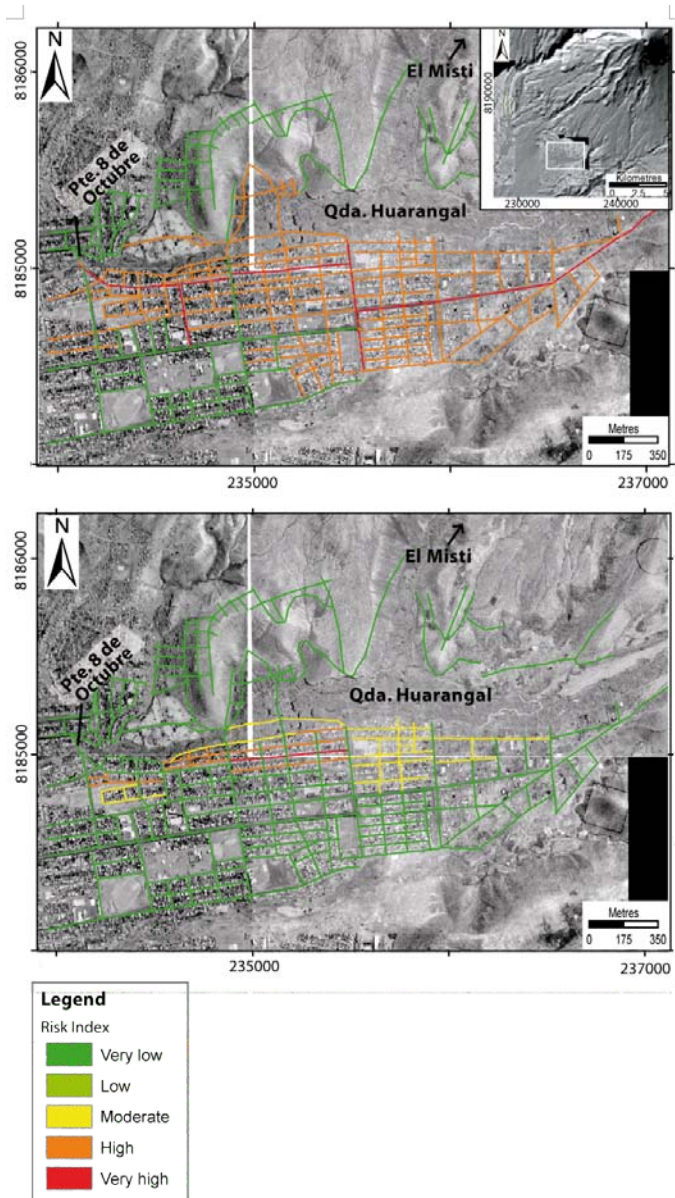


Figure 22: The risk posed to roadways and bridges from lahars based upon a conventionally-derived (A) and Titan2D-derived (B) hazard assessments and building and land use vulnerability functions for hazard scenario three. The Quebrada Huarangal fan is represented in the upper and lower image.

Electricity

The risk to the electricity generation and supply for Arequipa was assessed based upon the hazard scenarios, and land use, building and infrastructure vulnerability. Overall the risk to the dams is the highest for power-related infrastructure due to their location in the river rather than adjacent to. The power stations that are at the most risk are Charcani IV, V, and VI and Chilina due to both their location and importance (i.e. electricity output) to Arequipa. In general the risk posed to dams is the highest for the Titan2D based assessment, followed by Charcani IV and V which are at *high* risk of inundation and/or damage in large but infrequent lahars (i.e. scenario three).

This assessment indicates that even during small magnitude flood events key infrastructure for the generation and supply of electricity to of concern the Arequipa is at risk from inundation and/or damage. Therefore the level of risk posed to this infrastructure in the case of a volcanic crisis (i.e. scenario two and three) is of concern especially when electricity is a vital lifeline both during and after a crisis.

Water

The risk to the water supply for Arequipa was assessed based upon the hazard scenarios, and land use, building and infrastructure vulnerability. The risk to the water treatment plant at the entrance of the Rio Chili canyon is *very high* for scenario three of the conventionally derived risk assessment. This is the point where water from the Rio Chili is taken into the canals for potable water and irrigation. The risk is *moderate to very high* for the open water canals. The risk to the water supply system for Arequipa is negligible with the Titan2D-derived hazard assessment.

Floods and lahars in the Rio Chili may have an effect on the supply and quality of water taken into the canals, even the infrastructure is not inundated. During the floods in February 2011 Arequipa was without potable water for 24 hrs because of high sediment water being drawn into the water canals for purifying at the water treatment plant. The treatment plant clean water that has a high sediment and/or debris content, and the debris can cause blockages and damage to the canals, pipeline and water treatment plant.

This assessment indicates that during small to large floods and lahars, portions of the water canal system and water treatment plant could be affected. The risk map indicated that the highest risk pipelines were located closest the river. Damage to the canals at this point (i.e. close to intake) would compromise the supply to the rest of the canal, affecting not only the potable water supply but the irrigation supply too – essential to agriculture in Arequipa.

6.6 Summary

Depending on the magnitude and frequency of the flood lahar *high* risk properties cover much of the lower (t0 to t2) to middle terraces in the Rio Chili valley area. There exists a mix of land use types from dwellings to commercial centres and factories, and the building types do not vary wildly, reflecting the homogeneous nature of the Rio Chili valley when compared with the Quebrada Huarangal fan. The majority of the Quebrada Huarangal fan (t0 to t2) is of *moderate to very high* risk. There is little pattern to the spread of moderate to very high risk properties, reflecting the heterogeneous nature of the building types in Quebrada Huarangal. Overall the risk posed to properties in the Rio Chili valley is a lot less than for the Quebrada Huarangal fan. This is likely due to the better quality of buildings in the Rio Chili valley, the buildings are in general higher up above the river bed than in Huarangal, and the geomorphology of the channel.

The risk to the Rio Chili valley road network is considered significant in terms of mobility during and after a volcanic crisis – with all bridges considered to have some degree of risk to inundation and/or damage. This has serious implications for providing access from one side of the city to the other – particularly when trying to evacuate people and keep roadways to essential facilities open and clear.

The assessment of the Quebrada Huarangal fan concluded that there is significant risk posed to roads located within the channel of the quebrada, and especially on the southern terraces (t0-t2) due to the overbanking of flows in this locality. For the conventionally derived risk assessment the evacuation of the SE to S portion of the Quebrada Huarangal fan could prove difficult, especially from the east to the west (i.e. towards Arequipa city centre). This is because all the roads on the SE to S portion of the fan are considered *high* risk, with one main road at *very high* risk.

In terms of risk reduction, credible and rehearsed evacuation plans should be put into place, as well as restricting construction within the channel bed of Quebrada Huarangal. In addition, a study should be undertaken into the short- and the long-term effects of disruption and/or damage to the hydroelectric power stations and water supply. Alternative methods of energy and water should be investigated, even if just to supply the city for the first 72 hours (while waiting for government and international aid) after the event occurs.

7. Concluding remarks and application of the research

This research has combined a number of techniques in order to define the physical vulnerability. Vulnerable areas were identified from former and current geological studies; conventional and computer-aided mapping of volcanoclastic and fluvial deposits; numerical flow modelling (Titan2D); field surveys of buildings and infrastructure; statistical analysis including multivariate analysis for the building and infrastructure surveys; GIS; and geotechnical characteristics of building materials (including mechanical tests). The main aim was achieved – combining different methods to establish the physical vulnerability, and risk, of an urban area within close proximity to an active volcano. Also recommendations for reducing risk in these areas, and in particular in Arequipa, have also been achieved.

In terms of the Arequipa case study – this research highlights areas, in particular the Rio Chili valley and quebrada channels, which need to be protected by the Peruvian authorities to ensure the safety of the population in the event of lahars and/or flash floods in Arequipa. Of the utmost importance is the creation, and adherence to, a stringent land-use plan which forbids or limits development in areas of high risk outlined by this study and others (e.g. Vargas et al., 2010). The city limits have been expanding onto the slopes of El Misti and also in, and adjacent to, channels which drain the volcano. While many of the settlements are deemed as “illegal” (i.e. without planning permission) there appears to have been very little management and/or policing to ensure that construction is not continued in at risk areas. However, this year, the City Hall has taken steps to control expansion in to hazardous areas. A law was passed that makes it illegal to build beyond the suburbs on El Misti’s flanks – an area that has been outlined in the 2007 hazard map of El Misti. This is a positive step in reducing the risk to the population.

This study also highlighted the vulnerability of much of the key infrastructure in Arequipa, and alarmingly many of the lifelines (e.g. electricity, water and transportation) are the most vulnerable infrastructure in the case of a lahar and/or flash flood. Strategic risk planning needs to be undertaken by local authorities to identify the limitations on infrastructure and lifelines in case of a crisis, and contingency plans need to be put in to place to deal with a serious loss of the main infrastructure. For example, should the water become contaminated, is there an alternative water source available to supply potable water to the city? If the bridges crossing the Rio Chili are damaged, is there a way to transport the potable water from one side of the city to the other? What will be the effects of no potable water supply on emergency services? Another example is the loss of power; how long would power be lost to the city? How long would it take to repair, keeping in mind that the hydroelectric power stations are located within the high-hazard zones close to El Misti and across the Rio Chili canyon? How long would the hospitals be able to run on a backup generator? Could fuel be delivered to the hospital if transportation routes are severely damaged? Could patients be evacuated? Many questions need to be answered so that the risk to the population from lahars and/or flash

floods is reduced to an acceptable level for the population of Arequipa. A comprehensive risk analysis of the entire infrastructure is recommended to identify and highlight obstacles or weak points in case of a volcanic crisis. For example, in terms of emergency management, it is imperative to have an operational road network for co-ordinating relief efforts and reaching those people in need.

Some resistance measures (e.g. building a bund or deflection structure) could be employed to minimise the impact of lahars and flash floods directly affecting buildings and giving occupants more time to relocate. Avoidance measures include not building in lahar and/or flash flood risk areas where possible, raising the ground or floor level of buildings, and the construction of local bunds to protect groups of buildings from inundation. Future bridges could be built with larger spans and higher free boards to help in cases where a large volume of debris is anticipated.

Public education and awareness is paramount. During the 2008 field campaign discussions with residents of the San Jerinomo suburb, located within the channel of Quebrada Huarangal, revealed that they were unaware of the level of risk posed from lahars and flash floods in their area. Furthermore, the residents of the dwellings and businesses situated within the Quebrada Huarangal channel were under the impression (from the authorities) that the risk of flooding was non-existent to very low. It would have come as a surprise then, when flash floods swept through the suburb flooding 22 homes on 11 February 2011. The public and local authorities need to be educated on the risk posed to Arequipa from lahars and/or flash floods (e.g. evacuation simulation in 2010, Luisa Macedo). In addition, the education needs to be consistent, correct and verified by scientists and other professionals in order to ensure that everyone receives the same information and are well informed.

Finally, emergency shelters and evacuation routes need to be clearly identified, communicated and ensured during a crisis – such as the contingency plans developed for the Ubinas crisis (Rivera et al., 2010). Vargas et al. (2010) suggested that the evacuation route towards the SW be improved to allow for four lanes of traffic to join the Panamericana highway, rather than the two lanes which currently exist. The paved route towards Cerro the Verde Mine south of Arequipa could be used alternatively. In addition the road to the SE should be improved all the way to the Rio Tambo, 30 km SSE of Arequipa, and linked to the Panamericana road towards Moquegua. An advantage of establishing an adequate and reliable SE evacuation route is that it would allow the evacuation of people into an area where there is no direct evidence of erupted deposits from El Misti in this area (Vargas et al., 2010). Vargas et al. (2010) also suggested that shelters should be built near the villages of Yarabamba and Quequeña at the SE end of the depression, (in addition towards the west beyond the town of Yura.).

The majority of recommendations can be also be applied to other volcanoes world-wide – proper land-use planning, risk analysis of the infrastructure (paying particular attention to lifelines), public education and awareness and the establishment of evacuation routes and procedures are paramount in reducing the risk to cities under the threat of an active volcano.

Using a GIS in the field of volcanic hazard, vulnerability and risk assessment has shown its capabilities in terms of preparation of maps and information requests from a solid database. The capabilities and limitations of diagnostic tools such as GIS and Titan2D were tested in the application to the assessment of volcanic hazards, vulnerability and risk. A georeferenced database on the El Misti region, including Arequipa city, has been compiled by the acquisition

of information layers. New layers of information have been included, such as optimised lahar and flood-hazard scenarios eruptions; building, land use and infrastructure susceptibility maps, etc. The calculations were undertaken in a GIS allowing for the spatial expression of the risk element, which is an attractive method for communicating information to decision makers and the community alike. Another advantage of using a GIS is that databases can be readily updated when new information becomes available, thus allowing for the analysis of data in quasi real-time.

The GIS database created in this research project will be reviewed and verified, and made available for the Peruvian authorities. The maps and information layers can be interactive and would be a valuable addition for government authorities. With the popularity of computers, a learning tool which encompasses technology would prove to be very effective for educating members of the public. The introduction of this research project in interactive form to younger members of the community (i.e. through schools, sports clubs etc.) would be a top priority. Overall, this study has shown that the use of dedicated GIS analysis of volcanic hazards and risks is an extremely powerful tool to manage a study of a preventive nature in volcanic hazards, vulnerability and risk.

References

- Baxter, P. J., Baubron, J. C., and Coutinho, R. 1999. *Health hazard and disaster potential of ground gas emissions at Furnas volcano, São Miguel, Azores*. Journal of Volcanology and Geothermal Research. 92: 95-106.
- Baxter, P. J., Boyle, R., Cole, P., Neri, A., Spence, R. J. S., Zuccaro, G. 2005. *The impacts of pyroclastic surges on buildings at the eruption of the Soufrière Hills volcano, Montserrat*. Bulletin of Volcanology 67: 292-313
- Baxter, P.J., Aspinall, W.P., Neri, A., Zuccaro, G., Spence, R.S., Cioni, R. and Woo, G. 2008. *Emergency planning and mitigation at Vesuvius: A new evidence-based approach*. Journal of Volcanology and Geothermal Research 178: 454-473.
- Blaikie, P., Cannon, T., Davis, I., and Wisner, B., 1994. *At Risk: Natural Hazards, People's Vulnerability, and Disasters*. London: Routledge
- Blong, R. 1984. *Volcanic Hazards: A Sourcebook on the Effects of Eruptions*. Academic Press, London.
- Blong, R. 2000. *Volcanic hazards and risk management*. In: Sigurdsson, H., Houghton, B., McNutt, S.R., Rymer, H., Stix, J. (Eds.). *Encyclopedia of Volcanoes*. Academic Press, San Diego. Pp. 1215-1227.
- Blong, R. 2003. *Building damage in Rabaul, Papua New Guinea*. Bulletin of Volcanology 65: 43-54.
- Chester, D., Degg, M., Duncan, A.M., Guest, J.E. 2001. *The Increasing Exposure of Cities to the Effects of Volcanic Eruptions: A Global Survey*. Global Environmental Change Part B: Environmental Hazards 2: 89-103.
- Chevillot B. 2000. *Rapport de mission a Arequipa (sud Pérou) 26 juillet - 15 août 2000. Objet: mise en oeuvre d'un S.I.G. appliqué aux risques hydrologiques et volcaniques*. Rapport., Lab. De traitement de données géographiques ENITA de Clermont-Ferrand, Pp. 44.
- Cobeñas, G., Thouret, J.-C., Bonadonna C., Boivin P., 2011. The c.2030 yr. BP-old Plinian eruption of El Misti, Peru: characteristics of the fallout and pyroclastic flows, and eruption dynamics. *Submitted to J. Volcanology Geothermal Research, 30 October 2011*.
- Delaite, G. 2003. *Méthodes pour le Diagnostic des Risques Volcaniques Fondées sur les Systèmes d'Information Géographique et le Code de Simulation LAHARZ* (M.Sc. thesis): Clermont-Ferrand, Laboratoire Magmas et Volcans, Department of Geology, Université Blaise-Pascal. Pp. 55.

- Delaite, G., Thouret, J.-C., Sheridan, M. F., Stinton, A., Labazuy, P., Souriot, T., and van Westen, C., 2005. *Assessment of volcanic hazards of El Misti and in the city of Arequipa, Peru, based on GIS and simulations, with emphasis on lahars*. *Zeitschrift für Geomorphology N.F.*, suppl.140: 209-231.
- Dumaisnil, C., Thouret, J.-C., Chambon, G., Doyle, E.E., Cronin, S.J., Surono. 2010. *Hydraulic, physical and rheological characteristics of rain-triggered lahars at Semeru volcano, Indonesia*. *Earth Surface Processes and Landforms*, 35: 1573-1590.
- Hayashi, J.N., Self, S., 1992. A comparison of pyroclastic flow and debris avalanche mobility. *Journal of Geophysical Research* 97: 9063– 9071.
- International Code Council (ICC). 2006. *International building code*. Falls Church, Virginia, USA. Pp. 637.
- Iverson, R. M. 1997. *The physics of debris flows*. *Reviews of Geophysics* 35: 245-296.
- Johnston, D.M. 1998. *Modelling ash distribution for Auckland scenarios*. Institute of Geological and Nuclear Sciences Client Report 71770D.10A. Institute of Geological and Nuclear Sciences, Lower Hutt, New Zealand. Pp 1-12
- Kelman, I. 2002. *Physical Flood Vulnerability of Residential Properties in Coastal, Eastern England*. PhD Thesis, University of Cambridge, UK. Available from: <<http://www.ilankelman.org/phd.html>>.
- Kelman, I. and Spence, R. 2004. *An Overview of Flood Actions on Buildings*. *Engineering Geology*. 73: 297-309.
- Leger, P., Tremblay, R. 2009. *Earthquake Ground Motions for Seismic Damage Assessment and Re-Evaluation of Existing Buildings and Critical Facilities. Damage Assessment and Reconstruction after War or Natural Disaster*. NATO Science for Peace and Security Series I: 193-219
- Magill, C., Blong, R., 2005a. *Volcanic risk ranking for Auckland, New Zealand. I: Methodology and hazard investigation*. *Bulletin of Volcanology* 67: 331-339.
- Magill, C., Blong, R., 2005b. *Volcanic risk ranking for Auckland, New Zealand: II. Hazard consequences and risk calculation*. *Bulletin of Volcanology* 67: 340-349.
- Nagata, M. 1999. *Una introduccion a las inundaciones en el area urbana de Arequipa, Informe sobre las Tormentas en Arequipa* INDECI-IGP-ORSTOM. Pp. 99
- Neri, A., Aspinall, W.P., Cioni, R., Bertagnini, A., Baxter, P.J., Zuccaro, G., Andronico, D., Barsotti, S., Cole, P.D., Esposti Ongaro, T., Hincks, T.K., Macedonio, G., Papale, P., Rosi, M., Santacroce, R., Woo, G. 2008. *Developing an event tree for probabilistic hazard and risk assessment at Vesuvius*. *Journal of Volcanology and Geothermal Research* 178: 397-415.
- Newnham, R.M., Lowe, D.J., Alloway, B.V. 1999. *Volcanic hazards in Auckland, New Zealand: a preliminary assessment of the threat posed by central North Island silicic volcanism based on the Quaternary tephrostratigraphical record*. In: Firth, C.R., McGuire, W.J. (eds). *Volcanoes in the Quaternary*. Special Publication 161, Geological Society Publishing House: Bath; 27-45.
- Palhol, H. 2008. *Méthodes d'étude de l'endommagement induit par les effets des lahars au bâti ; le cas de la ville d'Arequipa, Pérou*. Master 1: Rapport du Travail d'Etude et de Recherche. Laboratoire Magmas et Volcans, Université Blaise Pascal, France. Pp. 24.
- Patra, A.K., Bauer, A.C., Nichita, C.C., Pitman, E.B., Sheridan, M.F., Bursik, M., Rupp, B., Webber, A., Stinton, A.J., Namikawa, L.M., Renschler, C.S. 2005. *Parallel adaptive simulation of dry avalanches over natural terrain*. *Journal of Volcanology and Geothermal Research* 139: 1–22
- Pierson, T.C. 2005. *Hyperconcentrated flow; transitional process between water flow and debris flow*. In: Jakob, M., Hungr, O. (Eds). *Debris-flow hazards and related phenomena*. Springer. Berlin, Federal Republic of Germany.

- Pierson, T.C., Costa, J.E., 1987. *A rheologic classification of subaerial sediment-water flows*. In: Costa J.E., Wiczorek G.F. (Eds). *Debris flows/ avalanches; process, recognition, and mitigation*. Reviews in Engineering Geology. Geological Society of America (GSA), Boulder, CO, United States. Pp. 1-12.
- Pitman, E.B., Patra, A.K., Bauer, A., Sheridan, M.F., Bursik, M.I. 2003. *Computing debris flows and landslides*. *Physics of Fluids* 15: 3638–3646
- Pitman, E.B., Le L. 2005. *A two-fluid model for avalanche and debris flows*. *Philosophical Transactions of the Royal Society A: Mathematical, Physical and Engineering Sciences*. 363: 1471-2962
- Permanent Technical Committee of Earthquake-Resistant Design. 2003. *Technical Standard of Building E. 030 earthquake resistant design*. Lima, Peru. Accessed 27 July 2007:
http://iisee.kenken.go.jp/net/seismic_design_code/peru/NTE-030-PERU.pdf
- Pomonis, A., Spence, R.J.S., Baxter, P.J. 1999. *Risk assessment of residential buildings for an eruption of Furnas Volcano, São Miguel, the Azores*. *Journal of Volcanology and Geothermal Research* 92: 107-131.
- Prevot, T. 2009. *Lahars de la Soufrière (Basse-Terre, Guadeloupe) : étude des impacts potentiels sur le bâti. Master 1: Rapport du Travail d'Etude et de Recherche*. Laboratoire Magmas et Volcans, Université Blaise Pascal, France. Pp. 29.
- Procter, J.N., Cronin, S.J., Zernack, A.V. 2009. *Landscape and sedimentary response to catastrophic debris avalanches, western Taranaki, New Zealand*. *Sedimentary Geology* 220: 271-287
- Procter, J.N. 2010. *Towards Improving Volcanic Mass Flow Hazard Assessment at New Zealand Stratovolcanoes*. PhD thesis, Massey University, Palmerston North, New Zealand.
- Procter, J.N., Cronin, S.J., Fuller, I.C., Sheridan, M.F., Neall, V.E., Keys, H. 2010a. *Lahar hazard assessment using Titan2D for an alluvial fan with rapidly changing geomorphology: Whangaehu River, Mt. Ruapehu*, *Geomorphology*, Volume 116: 162-174
- Reese, S., Markau, H.-J., 2002. *Risk handling and natural hazards, new strategies in coastal defense-a case study from Schleswig-Holstein, Germany*. In: *Proceedings of the Solutions to Coastal Disasters Conference*, American Society for Civil Engineers (ASCE), San Diego, California, pp. 498-510 24-27 February 2002.
- Rodolfo, K.S. 2000. *The hazard from lahars and Jökulhlaups*. In: Sigurdsson, H (Ed). *Encyclopedia of Volcanoes*, Academic Press, San Diego, CA. Pp. 973-996.
- Saucedo, R., Macías, J.L., Sheridan, M.F., Bursik, M.I., Komorowski, J.C. 2005. *Modeling of pyroclastic flows of Colima Volcano, Mexico: implications for hazard assessment*. *Journal of Volcanology and Geothermal Research* 139:103–115
- Schilling, S.P. 1998. *LAHARZ: GIS programs for automated delineation of lahar-hazard zones*. US Geological Survey, Open-file Report 98–638. Pp. 84
- Scott, K.M. 1989. *Magnitude and Frequency of Lahars and Lahar-Runout Flows in the Toutle-Cowlitz River System*. US Geological Survey Professional Paper 1447-B
- Sheridan, M. F., Stinton, A. J., Patra, A., Pitman, E. B., Bauer, A., Nichita, C. C. 2005. *Evaluating Titan2D mass-flow model using the 1963 Little Tahoma Peak avalanches, Mount Rainier, Washington*. *Journal of Volcanology and Geothermal Research* 139: 89- 102.
- Small, C., Naumann, T. 2001. *The global distribution of human population and recent volcanism*. *Global Environmental Change Part B: Environmental Hazards* 3: 93-109.
- Spence, R.J.S., Baxter, P.J., Zuccaro, G. 2004a. *Building vulnerability and human casualty estimation for a pyroclastic flow: a model and its application to Vesuvius*. *Journal of Volcanology and Geothermal Research* 133: 321-343

- Spence, R.J.S., Zuccaro, G., Petrazzuoli, S., Baxter, P.J. 2004b. *The resistance of buildings to pyroclastic flows: analytical and experimental studies and their application to Vesuvius*. *Natural Hazards Review* 5: 48-59.
- Standards New Zealand. 2004. *NZS 1170.5:2004 Structural Design Actions Part 5: Earthquake actions – New Zealand*. Wellington, New Zealand. Pp. 50.
- Stevens, N.F., Manville, V., Heron, D.W., 2003. *The sensitivity of a volcanic flow model to digital elevation model accuracy: experiments with digitised map contours and interferometric SAR at Ruapehu and Taranaki volcanoes, New Zealand*. *Journal of Volcanology and Geothermal Research* 119, 89–105.
- Stinton, A., Delaite, G., Burkett, B., Sheridan, M., Thouret, J.-C., and Patra, A.. 2004a. *Titan2D simulated debris flow hazards: Arequipa, Peru*: Abstracts, International Symposium on Environmental Software Systems (ISESS), U.S.A.
- Thouret, J.-C., Davila, J. and Eissen, J.-P., 1999a. *Largest explosive eruption in historical times in the Andes at Huaynaputina volcano, A.D. 1600, southern Peru*. *Geology* 27: 435-438.
- Thouret, J.-C., Lavigne, F., Kelfoun, K., Bronto, S. 2000. *Toward a revised hazard assessment at Merapi volcano, Central Java*. *Journal of Volcanology and Geothermal Research* 100: 479-502.
- Thierry, P., Stieltjes, L., Kouokam, E., Ngueya, P., Salley, P. M. 2007. *Multi-hazard risk mapping and assessment on an active volcano: the GRINP project at Mount Cameroon*. *Natural Hazards* 45: 429-456.
- Thouret, J.C., Finizola, A., Fornari, M., Legeley-Padovani, A., Suni, J. Frechen, M. 2001. *Geology of El Misti volcano near the city of Arequipa, Peru*. *Geological Society of America Bulletin* 113: 1593-1610.
- Tilling, R. I. 2005. *Volcano Hazards*. In: Martí, J. and Ernst, G. J. E. (eds). *Volcanoes and the Environment*. Cambridge University Press, Cambridge, U.K., p. 55-89.
- Toyos, G.T., 2000, *GIS modelling the risks to debris flow for Arequipa, Southern Peru*, Master PhD, University of Cambridge.
- Van Gorp, S., 2002, *Systèmes d'Information Géographique et Risques volcaniques: Approche méthodologique et application au cas du volcan Misti et de la zone urbanisée d'Arequipa (sud du Pérou)*, TER, Université Blaise-Pascal, Clermont-Ferrand.
- Vargas Franco, R.D., Thouret, J.-C., Delaite, G., van Westen, C., Sheridan, M.F., Siebe, C., Mariño, J., Souriot, T., Stinton, A. 2010a. *Mapping and assessing volcanic and flood hazards and risks, with emphasis on lahars, in Arequipa, Peru*: 265-280. In: Gropelli, G, Viereck-Goette, L (eds.) *Stratigraphy and Geology of Volcanic Areas*. Geological Society of America Special Papers 464. pp. 293.
- Vargas Franco, R.D., Thouret, J.-C., Martelli, K.M. 2010b. *Physical Vulnerability and Quantitative Risk Assessment of Housing and Infrastructure from The Potential Impacts of Volcanic Mass Flows in Arequipa, Peru*. CoV6/2.1/P/15. *Cities on Volcanoes 6 Conference Abstract Volume*. *Cities on Volcanoes 6 Conference*, Tenerife, Spain. May 31 - June 4, 2010.
- Voight, B. 1990. *The 1985 Nevado del Ruiz volcano catastrophe: anatomy and retrospection*. *Journal of Volcanology and Geothermal Research* 44: 349-386.
- Westgate, K. and P. O'Keefe. 1976. *Natural Disasters: An Intermediate Text*. Bradford Disaster Research Unit, University of Bradford, Bradford, U.K.,
- Williams, R., Stinton, A.J., Sheridan, M.F. 2008. *Evaluation of the Titan2D two-phase flow model using an actual event: Case study of the 2005 Vazcún Valley Lahar*. *Journal of Volcanology and Geothermal Research*, 177: 760-766.
- Wilson, C.J.N., and Stirling, M.W. 2002. *Towards a probabilistic volcano hazard analysis model for New Zealand*. In: Johnston, D.M., Tilyard, D. (eds) *Proc 5th Natural Hazards Management Conf*. Te Papa, Wellington, 14-15 August 2002. Institute of Geological and Nuclear Sciences, Lower Hutt, New Zealand, Pp 73-81

Witham, C.S. 2005. *Volcanic disasters and incidents: A new database*. Journal of Volcanology and Geothermal Research 148: 191-233.